Feasibility study for crossing Sognefjorden

Submerged Floating Tunnel

REINERTSEN Dr. techn. Olav Olsen

Document title:
Feasibility study for crossing the Sognefjord
Submerged Floating Tunnel

Document no.:
11744-ROO-R-001

Client file no.:
2011145371

Date:
28.11.2012

Revision:
01

Prepared by:
Anette Fjeld

Checked by:
Tore H. Søreide

Approved by:
Stein Atle Haugerud

Table of Contents

1 Summary

The present design of a Submerged Floating Tunnel (SFT) for crossing of Sognefjorden at Lavik/Oppedal is conceived for Norwegian Public Road Administration (Road Administration) by the Reinertsen Olav Olsen Group.

The main scope of this project is to establish the technical feasibility of the arched SFT crossing concept for the 3.7 km wide Sognefjord and similar crossing sites on the western coast of Norway, hence providing the Road Administration with a basis for comparison with other crossing alternatives.

The main SFT configuration and dimensions are shown in Figure 3-2, and principal tunnel data are given in Sec.3.2.

An arched Submerged Floating Tunnel has shown to be a safe and sound concept well suited to fulfill its intended functions during its planned life time. The design process has demonstrated the feasibility of the SFT, for Sognefjorden in particular, and for similar fjord crossings in general. The structure is designed to withstand all functional and environmental loads with ample margins. Motions set up by wind, waves and currents are moderate and will not cause driving discomfort or traffic disruption. A high level risk analysis (HAZID) concluded the structure to have an adequate robustness to withstand all relevant accidental and unforeseen actions.

Construction time is estimated to 7 – 9 years. Duration of the planning/design phase is estimated to two years. Cost estimate has not been part of the present work scope.

Main features of the concept:

Traffic is guided through two arch shaped concrete tubes, where each tube has sufficient diameter to accommodate two road lanes in each direction. Only one of these lanes is used for traffic, whereas the other is used for emergency stops, maintenance works etc., thus avoiding accidental traffic disruption.

A rigid connection between the two tubes is achieved by diagonal bracings. Some bracings with regular spacing will be adopted to secure escape routes, control rooms and other facilities.

Elevation of the tubes is set below the reach of ship keels; direct ramming form ships is therefore not possible.

The tunnels are designed to be neutral in water for a mean load situation, but are stabilized in the vertical direction by pontoons connected to the main tubes by steel

shafts, this to absorb the load variations. The pontoons are exposed to ship collisions, and the shafts are therefore provided with a weak link solution to prevent the largest collisions to transferee the most extreme forces, and cause damage to the traffic tubes. A weak link design of the pontoon/tunnel connection provides adequate safety against damage on the traffic tubes, and the structure is therefore designed to resist ramming of large ships with a displacement of 100 000 t and 20kts speed. For large collisions with a return period higher than 100 years the pontoons will hence be knocked off, but due to substantial redundancy in bearing capacity, road traffic can proceed unhindered.

The proposed SFT concept has shown to meet all requirements laid down by the Road Authorities and in present Norwegian design codes (Eurocodes). Marine issues not covered by these codes are designed to satisfy NORSOK codes and DNV recommended practice for offshore structures.

The SFT has reserve strength and is rather insensitive to changes in the functional requirements. It is designed to withstand environmental loads from tides, wind driven waves, swell, 2nd order wave effects, slide generated waves, internal waves, currents, wind, snow and ice.

Approach tunnels and landfalls are established by recognized and well proven methods. 15 SFT elements, about 250 - 300 m long, will be constructed in an existing graving dock such as Hanøytangen, 150 km north of the bridge site. The elements will be launched and towed to a tranquil site in proximity to the bridge for assembly and installation. Here the elements will be joined together to three main segments, and then connected to a string about 3 800 m long. The assembled tunnel will then be towed in place, and each end will be mounted separately to the preinstalled landfall elements. All joints will be completed by methods which have been successfully applied, without significant leaks, for several immersed tunnels. Previously mentioned marine operations will be completed by facilities and procedures well proven from North Sea activities.

In the next phases of design and planning the present feasibility study will be supplemented by more detailed analyses, mock-up tests and operation simulations for optimization and refining the submerged floating tunnel concept.

2 Introduction

2.1 Project development team

Concept development is performed by a consortium named "Reinertsen Olav Olsen Group" which consists of the two companies Reinertsen (Trondheim) and Dr.techn. Olav Olsen (Oslo). The consortium has strengthened the team with several relevant experts as follows:

- Arup (Netherland) – World leading design company, responsible for operation and maintenance and contributes on risk assessment and geology
- BergerABAM (USA) – Design company, responsible for Washington lake pontoon bridges
- NTNU , Prof. Odd M Faltinsen (Trondheim) – Leading hydrodynamic expert
- Per Johansson (Oslo) – Naval architect, experience from advanced marine operations
- Snøhetta (Oslo) – Recognized architects

2.2 Project description

'Ferjefri E39' is a project by Norwegian Public Roads Administration that aims to design a road without ferry connections from Kristiansand S to Trondheim. One of the major tasks is to design a 3.7 km long crossing over Sognefjorden from Lavik to Oppedal, see Figure 2-1. Presently this is the world longest fjord crossing concept. The water depth is about 1 250 m at the site location. Several crossing alternatives have been investigated in the feasibility phase, and this report presents the concept of submerged floating tunnel.

Figure 2-1, Location of the Sognefjord crossing

2.3 Objective

The ultimate goal for this project is to demonstrate technical feasibility for a fixed link crossing the Sognefjord. Optimization of the concept is expected to be carried out in later project phases.

2.4 Scope of feasibility study

Reinertsen Olav Olsen group have studied the concept submerged floating tunnel, concept number ROO4 from the dialogue phase. Design methods have been defined and presented in a separate Design Brief. Essential features are also mentioned in this report. Key assumptions for the feasibility study are listed in Design Basis.

The study should provide documentation that supports the Client decision on the feasibility and the level of documentation should be leading towards '*Teknisk delgodkjenning*' as defined in HB185, ref. (1). '*Teknisk delgodkjenning*' implies documentation of safety, technical integrity and cost. Relevant key points to be delivered for '*teknisk delgodkjenning*' are:

- Design Basis (Loads, materials, CP approach, Geotechnical report)
- Ownership and O&M responsibility
- Design input and possible additional surveys
- General arrangement drawings
- Drawings to show typical details:
  - Substructures/Superstructure
  - Accidental (Collision) forces on structural members
  - Erosion
  - Construction execution relevant for the functionality of the bridge
- For post/pre tensioned structural members, the location of all tension lines including anchoring, the whole cable length should be defined
- Selected design calculations including assumptions, load effects and dimensions including the actual capacity in typical cross-sections. Together with drawings, this should define the bridge.
- Selected wearing course and wet insulation
- Guardrail type
- Technical part of the tender documents with assumptions and description of the bridge construction and operation.
- Design of cross sections and bearing systems for steel structures, most important nodes should be designed
- Form drawing with measures of all main structural parts

- Reinforcement drawings of the most stressed structural parts (cross-sections)
- Drawings to show guardrail solutions, bearings and joints, lightning, drain and drainage systems
- List of drawings

As the main focus of this project has been to solve all technical details that would jeopardize technical feasibility, not all elements necessary for *'Teknisk delgodkjenning'* have been designed. Adjustment to the concept will definitely be made in an optimization phase, and to go to deep into all the details would be a waste of resources. This report presents all documentation necessary to demonstrate technical feasibility.

3 Crossing concept

3.1 Configuration

3.1.1 General

The envisaged crossing concept is described by an arched SFT consisting of two parallel concrete tubes anchored to pontoons on the sea surface. The horizontal alignment follows a circular arch with a radius of 2 682 m and a rise of 740 m with the cavity/intrados to the west. The bridge center line length is 4 083 m. The vertical alignment is adapted to the ship clearance requirement having a slightly curved, symmetric trajectory with a draft of 20 m within the 400 m navigational channel. At the landfalls the tunnel is located 12 m below mean sea level giving ample keel clearance to avoid direct ship impact. The land tunnel rises inside the rock with 5 % slope up to free air.

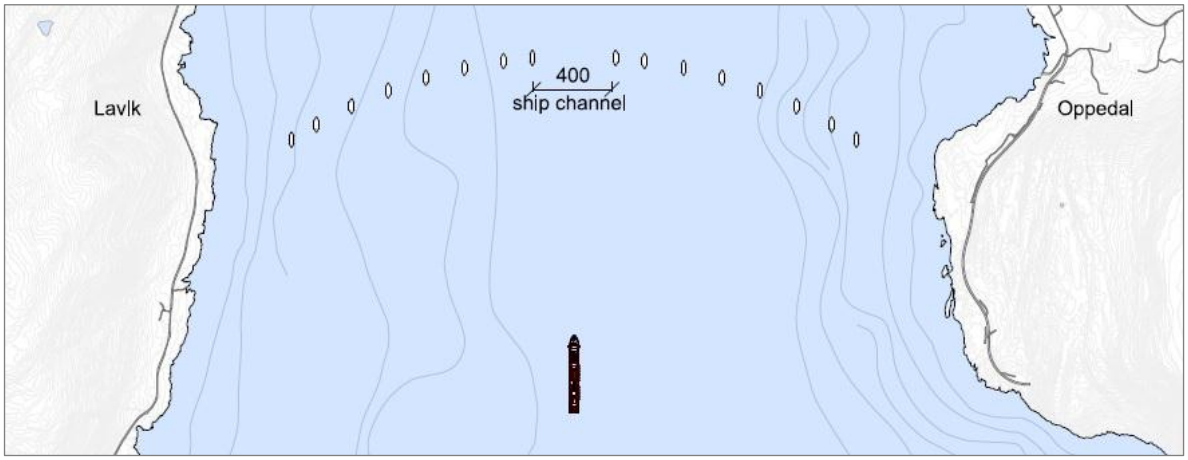

Figure 3-1: Overview arched SFT

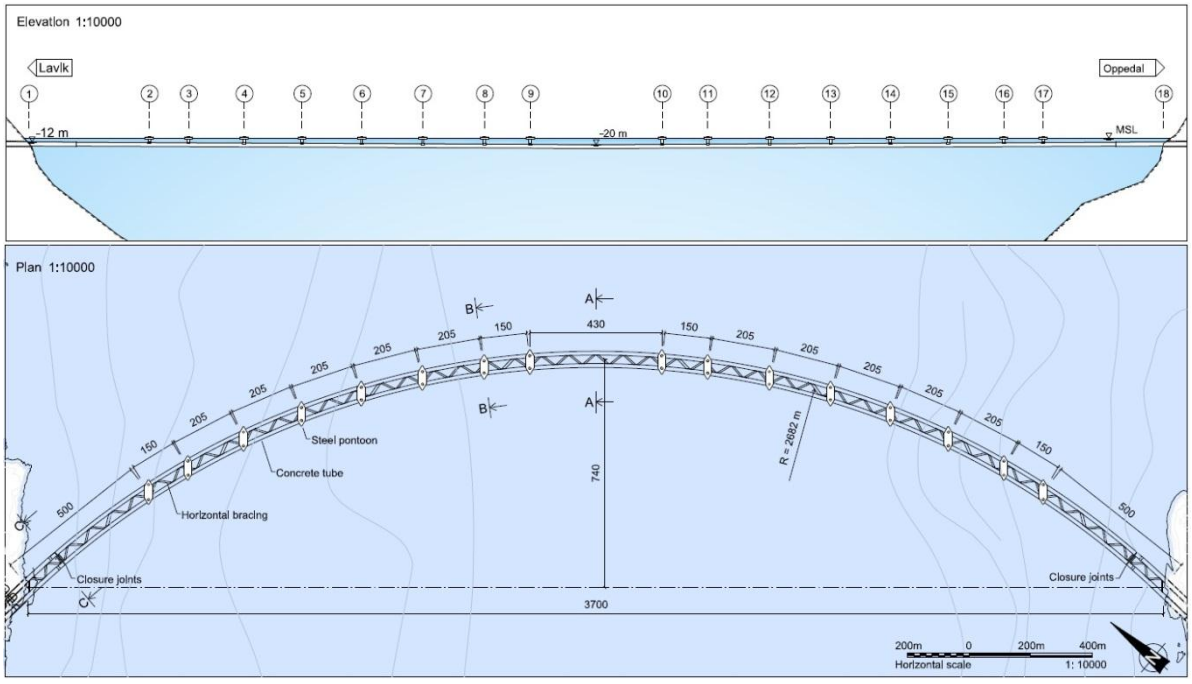

Figure 3-2: Elevation and plan

The vertical position and motions of the tubes are controlled by pontoons. The SFT is designed to float as neutral as possible in the water, and the pontoon draught will vary depending on the loading condition. The general distance between the pontoons is approximately 205 m. At the main fair lead the net distance between the pontoons is 400 m in compliance with the ship clearance requirements in the addition to HB185, ref. (2). To support the fairway span closer pontoon spacing (~150 m) is required for the adjacent spans. The length of the end span (~500 m) is chosen as to minimize the vertical supporting moments at the pontoons next to the landfalls. The tunnel is designed to be clamped in the bedrock at the landfalls assuming firm rock conditions.

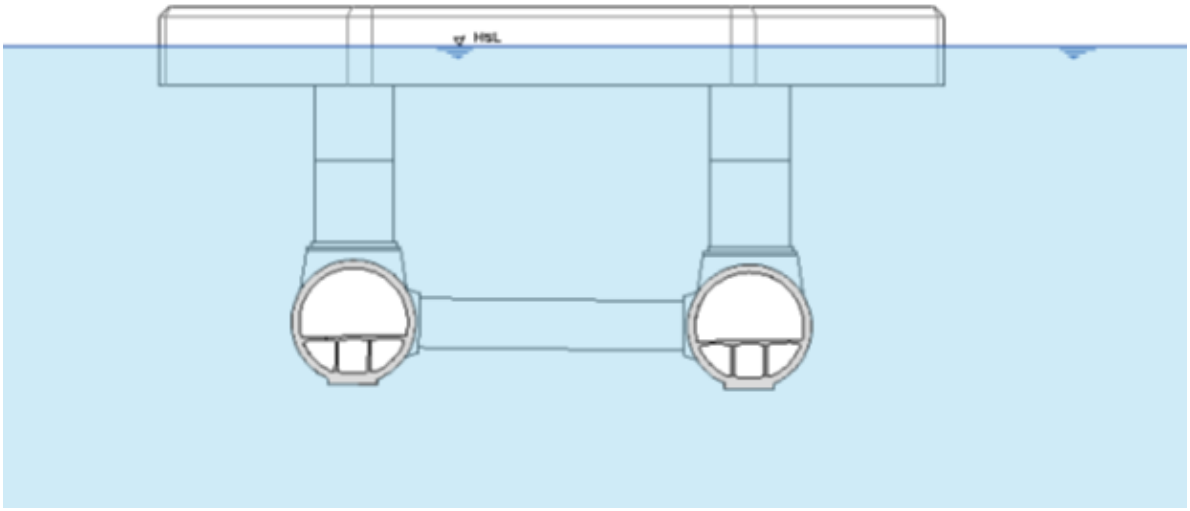

Figure 3-3: General section

The main traffic tubes are coupled by large diameter diagonal truss elements, bracing, to enhance the horizontal stability of the arch. Approximately every 500 m the bracing facilitates escape ways and room for technical installations. The twin arch configuration is found effective in resisting asymmetric current loading as well as suppressing long-period resonances. The center distance between the tubes was in the dialogue phase assumed to 40 m, and as no new results suggested otherwise, the distance remains the same. In a future project phase, it would be valuable to do a parametric study on the center distance with model experiments in order to enhance dynamic behavior and constructability of the tunnel.

The tunnel configuration is mainly determined by the section required to accommodate the two-lane highway tunnel profile T9.5. The circular tubes have an outer diameter of 12.6 and the inner diameter is 11.0 m. In each tube there will be two driving lanes of 3.5 m, one sidewalk of 1.25 m and sidewalk of 2.0 m where there is access to the ballasting system. The height of the driving lanes is 4.8 m. One way traffic is assumed in each tube. Lanes for pedestrians and bicycles may be arranged underneath the main traffic compartment. The demand for such access is however assumed to be limited, and would require an increase in the tube diameter. In order to minimize unnecessary puncture of the main tubes, only the cross tunnels utilized for escape routes are operated dry.

The pontoons are made of steel and composed of an upper rectangular basin with triangular ends with a tentative water plane area of 1 600 m^2 (26 x 80 m). They are connected to the concrete tubes by circular cylindrical shafts with diameter 8 m. The pontoons are exposed to ship impact. A ship impact mechanism, i.e. a weak link, is introduced in the shafts to prevent overloading of the tunnel structure.

3.1.2 Concrete tubes

The concrete tubes have an outer diameter of 12.6 m and a general wall thickness of 0.8 m. Inside, the tube is divided by a concrete slab to provide an upper main compartment for car traffic. The space above the free room for cars may be used for ventilation ducts, traffic signals and sign boards. Below the traffic deck the section is compartmentalized into three non-communicative compartments. The central compartment is designated for waster ballast. The other compartments are used for piping and solid ballast (concrete slurry). The maximum amount of solid and fluid ballast is estimated to occupy a cross-section of about 10 m^2.

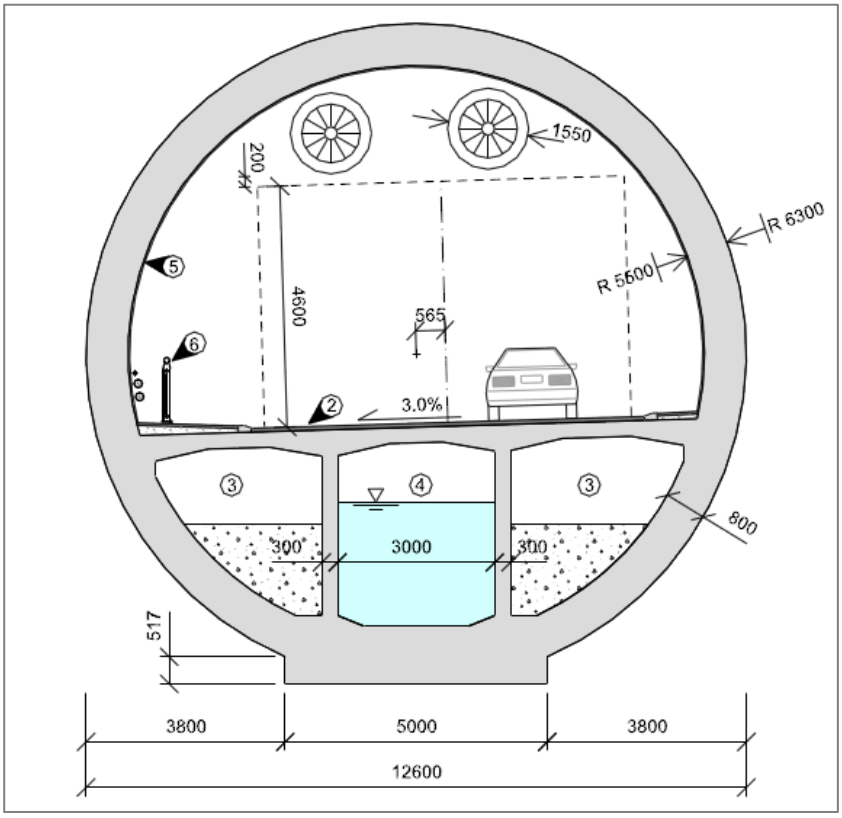

Figure 3-4, Tube layout

The concrete grade B55 M40 is suggested for the tubes. Plastic fibers will be added to the mix in the cast of the inner face of the soffit to avoid spalling and improve the fire resistance of the tunnel. The tube is post-tensioned by longitudinal tendons to achieve water tightness when exposed to bending moments. Hoop post-tensioning is provided to withstand an accidental inner explosion pressure and to warrant water-tightness.

Due to large reaction forces in the landfalls of the SFT, the cross-section will have to be increased in these regions. At the landfalls adequate axial- and bending resistance is obtained by increasing the outer diameter to 14 m and the wall thickness to 1.0 m.

If the detailed design or Client's requirements call for a larger tube cross-section, such increase may easily be provided. If so, the increase should concern the full tube length.

3.1.3 Horizontal bracing

A concrete truss is used to mobilize composite action between the two tubes. The horizontal bracing of the tubes consists of diagonals with a constant inclination of about 40°. The bracing elements are foreseen as circular concrete tubes having an outer diameter of 5 m and 0.5 m wall thickness. Approximately every 500 m the bracing diameter is increased to 8 m to accommodate escape ways and technical installations. All other diagonals are water filled. As main pipe punctures should be kept at a minimum, the bracing members except escape ways do not communicate with the tubes.

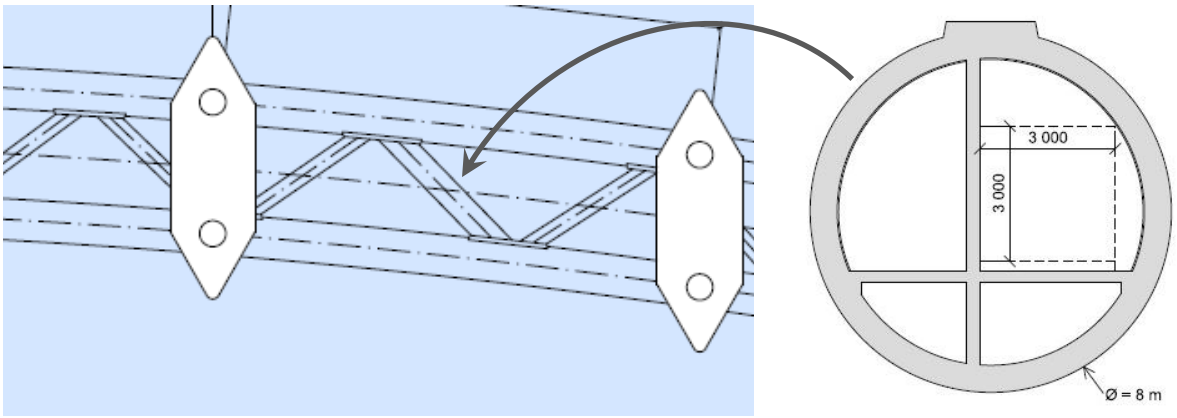

Figure 3-5: Bracing configuration and escape way section

3.1.4 Landfalls

The tubes are guided horizontally into the entrance of the land tunnel with its apex beneath elevation -12 m. The land tunnel rises inside the rock with 5 % inclination up to free air. The tube arches are designed to be clamped in the bedrock at the landfalls. There will be peaked restraining moments due to loads caused by;

- Tides
- Distributed vertical loads
- Wave loads

The effect of tidal variation may be relieved by adjustable water ballasting of the pontoons closest to shore. This will require and active ballasting scheme, thus ballasting for tidal effects have been considered not to be beneficial to the SFT due to operation and maintenance conditions. As mentioned earlier the outer diameter is increased to 14 m and

the wall thickness to 1.0 m at the landfalls. Figure 3-6 and Figure 3-7 show the landfall elevation and some relevant sections.

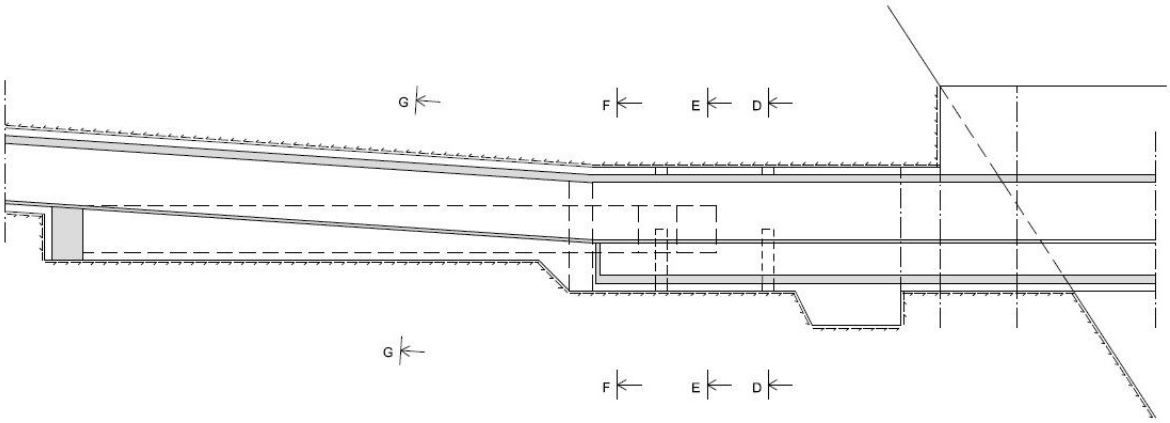

Figure 3-6: Landfall elevation

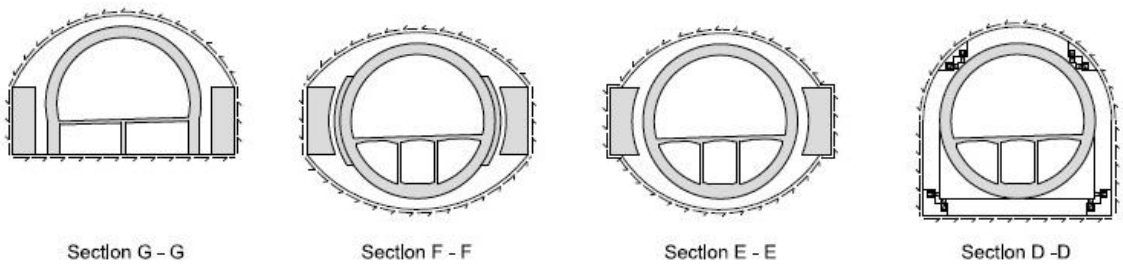

Figure 3-7: Landfall sections

3.1.5 Pontoons

The pontoon is composed of an upper rectangular basin with triangular ends with a tentative water plane area of 1 600 m^2 (26 × 80 m) connected to the concrete tube by a lower circular cylindrical shaft with diameter about 8 m. Steel pontoons are preferred from a construction and installation point of view. Ultimately, the pontoon design will be governed by the adopted ship impact strategy.

The pontoons are exposed to ship collision. The following preventive measures are implemented to assure full structural integrity of the tunnel in case of an accidental ship impact:

- The tunnel is designed to tolerate loss of one pontoon without losing its structural integrity or suffering other structural damage.
- The pontoons are designed to have two-compartment damage stability, i.e. to have adequate residual stability after damage and flooding of up to two adjacent compartments. Apart from compartmentalization, infill of buoyant material in the outmost chambers is considered.
- A ship impact mechanism, “weak link”, is introduced between in the shaft to prevent overstressing of the tunnel structure.

- Introduction of energy absorbing capability, a sliding fender is suggested in the feasibility study. The reason for adding such a fender is to protect the medium size vessels, if The Norwegian Coastal Administration wishes to do so.

The ship impact mechanism between the pontoons and the tunnel is justified by the fact that the accidental (ALS) ship impact forces are significantly higher than the ordinary lateral loads acting on the pontoons which the tunnel has to resist. A principle solution for a weak impact link has been worked out and is shown in Figure 3-8. The failure mechanism is based on shear failure in shear plinth in the middle of the shaft. Axial forces and bending moments have been isolated from the shear bearing plinth by the use of tendon strands in the shaft wall. In order to avoid the ship ramming the shafts, the weak link is located with ample keel clearance, in this study suggested at elevation MSL -12 m.

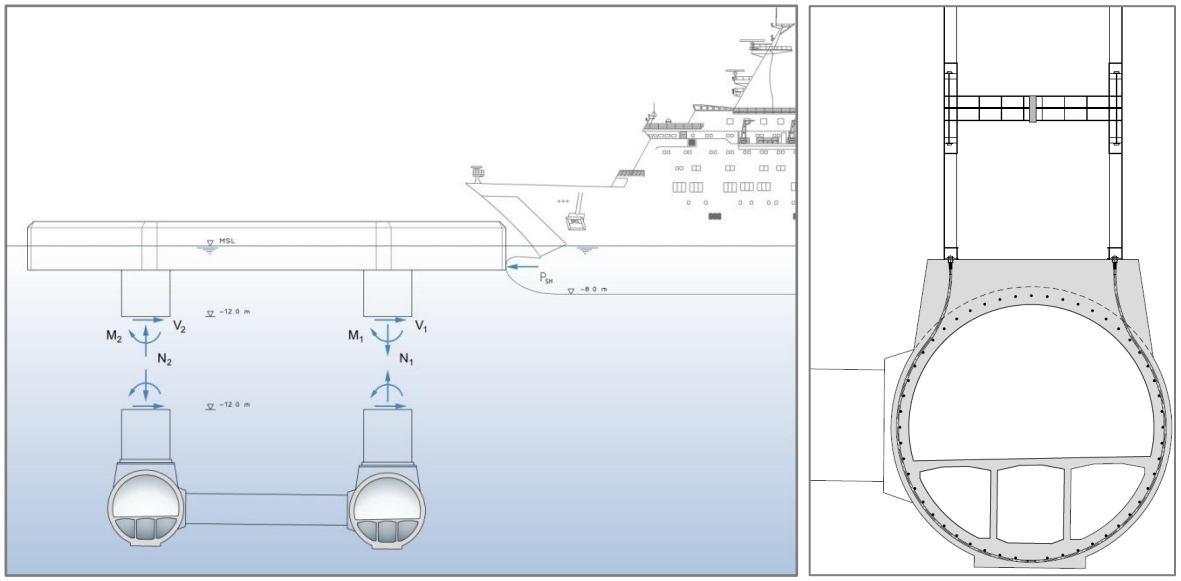

Figure 3-8: Ship impact mechanism

The steel shaft will be permanently water filled, but possible to drain for inspections. The pontoon will be designed as stiff, but will be equipped with fenders to prevent critical hull damage on smaller vessels. Preventive measures to avoid larges ship 'climbing' onto the pontoon and overload the tunnel vertically comprise a generous camber on upper pontoon edge and a weak link in the vertical connection between the shafts and the pontoon.

3.1.6 Pedestrian access

If required the central compartment in the tubes can be used as a pedestrian and bicycle lane. This will lead to an increase in tube diameter to have sufficient space for solid ballast and water ballast in the side compartments. An increase in diameter is not a problem from a structural view, rather the opposite, but it will of course increase the concrete volumes and steel quantities.

3.2 Key figures

Crossing

– Length of crossing	:	3 700	m
– Total length of tunnel	:	4 083	m
– Number of spans	:	17	nos
– Horizontal alignment	:	R = 2 682	m
– Vertical alignment	:	R = ∞	
– Gradient	:	0.4	‰
– Maximum water depth	:	1 300	m
– Clearance (above tunnel)	:	12 - 20	m (MSL)
– Total concrete volume	:	398 800	m^3
– Total mass, reinforcement	:	89 201	tonnes
– Total mass, tendons	:	24 432	tonnes
– Total steel weight	:	61 488	tonnes
– Concrete ballast	:	25 859	m^3

Tunnel

– Span length	:	150 – 500	m
– Number of tubes	:	2	nos
– Tube spacing	:	40.0	m
– Tube outer / inner radius	:	6.30 / 5.50	m
– Concrete volume	:	349 144	m^3

Pontoons

– Number of pontoons	:	16	nos
– Dimensions	:	26 × 80 × 8	m
– Height of pontoons	:	8.0	m

Shafts

– Number of permanent shafts	:	32	nos
– Number of temporary shafts	:	28	nos
– Outer diameter of shafts	:	8.0	m
– Max. height of shafts	:	25.5	m

Landfalls

– Abutment length	:	88	m
– Tube outer radius	:	7.00	m
– Concrete volume	:	49 668	m^3

3.3 Technical drawings

A number of technical drawings have been prepared in the feasibility study. An overview of the drawings is given in Table 3-1.

Table 3-1: Drawing list

Drw. #	Title
A101	Front page
A102	Drawing list
B101	Sognefjord SFT crossing - Overview
B102	Sognefjord SFT crossing - Navigation channel
F101	Normal profiles - Submerged floating tunnel - Typical sections
F102	Normal profiles - Landfalls - Typical sections
K101	Submerged floating tunnnel - General plan and elevation
K102	Submerged floating tunnnel - Typical sections
K111	Submerged floating tunnnel - Mid span
K112	Submerged floating tunnnel - Landfall Lavik
K113	Submerged floating tunnnel - Landfall Lavik - Elevation and sections
K121	Concrete tubes - Form - Typical sections
K131	Concrete tubes - Reinforcement layout - Typical sections
K132	Concrete tubes - Reinforcement layout - Landfall section
K141	Concrete tubes – Post-tensioning - Typical sections
K142	Concrete tubes – Post-tensioning - Landfall section
K143	Concrete tubes – Post-tensioning - Element joints
K201	Submerged floating tunnel - Element key plan
K202	Submerged floating tunnel - Landfall element Lavik - Isometric view
K203	Submerged floating tunnel - Tunnel element nº 1 - Isometric view
K211	Submerged floating tunnel - Floating sequences
Y101	Construction sequence - Jointing of elements - Jetty and outrigger support
Y102	Construction sequences - Jointing of elements 1
Y103	Construction sequences - Jointing of elements 2
Y104	Construction sequences - Towing of tunnel
Y105	Construction sequences – Pontoon installation

4 Loads

4.1 Self-weight

Two contributions to self-weight need to be considered:

- G_1 : permanent self-weight including structure and equipment
- G_2 : variable self-weight due to marine growth and water absorbed by structure and permanent ballast

The permanent self-weight G_1 of tunnels includes:

- calculated weight of tunnel β_1
- calculated weight of structural elements in tunnel β_2
- weight of permanent and relocatable ballast β_3
- weight of permanent pavement (asphalt coating) β_4
- weight of permanent equipment β_5

The variable self-weight G2 is intended to cover:

- weight of marine growth β_7
- weight of water absorbed by concrete structure β_8
- weight of water absorbed by solid ballast β_9

A fraction of relocatable ballast $\Delta\beta_3$ is related to expected weight increase (weight of marine growth and weight of water absorbed by structure and permanent ballast). The initial weight of relocatable ballast $\Delta\beta_3$ shall be 150% of the expected weight increase G_2, and the minimum amount in operation 75% of the expected weight increase G_2.

In order to cover tolerances in permanent weight and buoyancy of the floating tunnel, a "free self-weight" ΔG in the order of ±3% of the permanent self-weight G_1 shall be assumed in each section of the tunnel according to HB 185 (1). As the SFT is designed to float as neutral as possible and rigorous weight control will be executed to ensure that, a modified calculation of ΔG is used in this feasibility study. When the construction of an element is finished the dry dock will be filled with water and the freeboard measured. The element weight is then adjusted with ballast. The tolerances in Table 4-1 are suggested.

Table 4-1, Contributions to the free self-weight ΔG

G_1	ΔG contribution	Comment
β_1, weight of tunnel	ΔH=30 mm	The main uncertainty for calculation of the weight out of dock is the freeboard measurement.
β_2, weight of structural elements in tunnel	3%	The prescribed variation from HB185
β_3, weight of permanent and relocatable ballast	3%	The prescribed variation from HB185
β_4, weight of permanent pavement (asphalt coating)	50%	Wide tolerance to ensure robustness and flexibility in operating the SFT
β_5, weight of permanent equipment	3%	The prescribed variation from HB185

Weight from the structural elements and permanent equipment in the tunnel has not been calculated, but is included in the weight budget as a rough estimate. The exact value is not necessary for the feasibility study due to great possibilities for adjustment of both ballast and concrete cross-section.

The long-term effect of water absorption is to be considered in the estimation of the specific weight of concrete. In the absence of precise data, a weight increase of 1.0 % of the initial concrete weight is assumed for permanently submerged concrete.

Buoyancy is determined on the basis of MSL water level and the most unfavorable value for the specific weight of water. Buoyancy calculations are based on net structural dimensions without marine growth.

The weight of reinforced concrete is 26.5 kN/m^3.

Table 4-2, Weight calculation

			Per tube [kN/m]	ΔG	Comment
G1	$\beta_{1,1}$	Calculated weight of tube	967	3.0	30 mm draught tolerance
	$\beta_{1,2}$	Calculated weight of bracing	126		
	β_2	Calculated weight of structural elements in tunnel	20	0.6	3 %
	$\beta_{3,1}$	Weight of permanent (solid) ballast	76		Tolerance included in β1
	$\beta_{3,2}$	Weight of relocatable (water) ballast	70	2.1	3 %
	β_4	Weight of permanent pavement (asphalt)	19	9.5	50 %
	β_5	Weight of permanent equipment	20	0.6	3 %
	∑		1 298		
G2	β_6	Weight of marin growth	8		
	β_7	Weight of water absorbed by concrete structure	11		
	β_8	Weight of water absorbed by solid ballast	1		
	∑		20		
ΔG				16	
G,max		G1+G2+ΔG	1 334		
G,min		G1-ΔG	1 282		
Buoyancy, B,min			1 299		
Buoyancy, B,max			1 325		

The solid ballast and water ballast in Table 4-2 have been chosen to balance the maximum and minimum self-weight, see Table 4-3. Equal maximum and minimum self-weight gives the lowest response and as the response from wave loading is symmetrical, it is beneficial to have self-weight and traffic as symmetrical load cases as well.

Table 4-3, Self-weight loads applied in the analysis

Maximum downwards		Maximum upwards	
G, max	1 334	G, min	1 282
T, max	10.2	T, min	0
B, min	-1 299	B, max	-1 325
Net weight	45.3	Net weight	-42.6
Selfweight max	35.2	Selfweight min	-42.6

4.2 Traffic

Global effects from traffic loads are calculated according to the 2009-edition of HB 185. This gives the following loads:

Table 4-4, Traffic loads

Two lanes with full traffic loading, HB185, sec. 3.3.1 [kN/m]	18
One lane with pedestrian loading, HB185, sec. 3.4.1 [kN/m]	2
Two lanes with axial loading, HB185 sec. 3.3.1 [kN]	1260
Distributed load per tube [kN/m]	10
Joint load, one per tube [kN]	630

4.3 Tide

In the absence of more precise data, water levels from Ålesund are used to calculate the sea level variation. The highest/lowest levels measured since 1993 estimates a 100 year return period.

Table 4-5, Water levels

Lowest astronomical tide (LAT)	0.00 m
Mean Sea Level (MSL)	+1.20 m
Highest astronomical tide (HAT)	+2.39 m

Return period [years]	Highest sea level [m]	Lowest sea level [m]
1	+2.61	-0.10
10	+2.88	-0.27
20	+2.97	-0.32
*	+3.05	-0.38

*Highest/lowest measured since 1993

High tide:

$$\Delta Z = 3.05m - 1.20m = 1.85m$$

Low tide:

$$\Delta Z = -0.38m - 1.20m = -1.58m$$

4.4 Current

4.4.1 Drag forces

Drag forces from current are calculated as follows

Pontoon point load:

$$F_D = \frac{1}{2}\,\rho_w\,C_D\,A\,U_\infty^2$$

First tube distributed load:

$$F_D = \frac{1}{2}\,\rho_w\,C_D\,D\,U_\infty^2$$

Shadow effect on second tube calculated by Schlichting's wake formula using Blevins approach with virtual origin 6 diameters in front of the first cylinder Ref. (3):

$$\frac{u^2}{U_\infty^2} \approx \left(1 - 2 \cdot 0.95 \cdot \sqrt{\frac{C_D \cdot D}{CDBT + 6D}}\right) = 0.46$$

where CDBT is the Center Distance Between Tunnels

Second tube distributed load (shadow effect accounted for):

$$F_D = \frac{1}{2}\,\rho_w\,C_D\,D\,u^2 = \frac{1}{2}\,\rho_w\,C_D\,D \cdot 0.46 U_\infty^2$$

A drag coefficient of C_D=0.75, which is highly conservative at this Reynolds number, is assumed and the current drag forces are show in Table 4-6.

Table 4-6, Drag forces

		U_{IN}	U_{OUT}	$\lvert U_{DIM} \rvert$
Current velocity	0-10m	0.77	-0.56	1.27
	26.3 m*	0.33	-0.35	0.60
	30m	0.23	-0.3	0.55
Drag force	Pontoon [kN]	23.5	12.4	63.8
	First tube [kN/m]	0.5	0.6	1.7
	Second tube [kN/m]	0.3	0.3	0.9

*Assuming linear distribution between 10 and 30 m

Three current scenarios have been described in the amendment to HB185 (2):

1) Constant current acting symmetrically over the full width of the fjord
2) Constant current acting over the mid half of the fjord
3) Constant current acting asymmetrically about the fjord mid axis

4.4.2 Vortex Induced Vibrations (VIV)

Vortex shedding occurs because the flow is unable to follow along the surface of the structure and separates from the surface, as shown in Figure 4-1. This flow separation creates a vortex which causes a local increase in rotational velocity. Higher flow velocity yields a reduction in dynamic pressure, which creates an attraction force by the vortex on the structure.

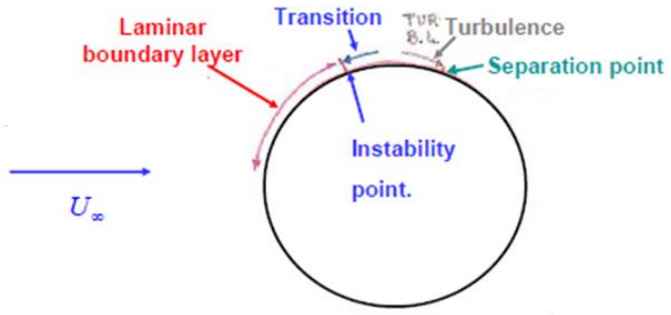

Figure 4-1: Flow around a circular cylinder

The position of the separation point alternates between the top and bottom of the cylinder, and creates a vortex street, as illustrated in Figure 4-2. These vortexes create a force fluctuation due to the previously mentioned pressure changes. Due to the spatial properties of the problem the forces inline flow direction will have a period half of the shedding period, while the forces in cross flow will have a period identical to the shedding period. The vortex shedding period may be determined for a fixed cylinder from equation (1).

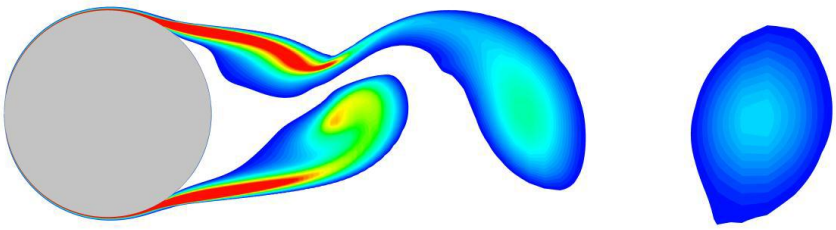

Figure 4-2: Vortex street behind a circular cylinder

$$T_{Sp} = \frac{D}{St \cdot U_\infty} \tag{1}$$

Where D is the structural diameter ($D = 12.6m$), St is the Strouhal number which, for a cross section with two cylinders in tandem arrangement, is $St = 0.125$ Ref. (4) (p. 1007) and a design current velocity at a depth 25m of $U_\infty = 0.60m/s$ (linearly interpolated from data given in (5)). The vortex shedding period for a fixed cylinder T_{Sp} is then:

$$T_{Sp} = \frac{D}{St \cdot U_\infty} = \frac{12.6m}{0.125 \cdot 0.60m/s} = 168\ s$$

The high vortex shedding period for a fixed cylinder suggests that only motion in the first deflection modes in heave (cross flow motion) and sway (inline motion) will be induced. For a fixed cylinder the correlation length, in span direction, of the vortex shedding is only about 1-3 D, and will therefore not produce resonance issues. When the structure is free to oscillate however, the vortex shedding frequency will change towards the natural frequency of the structure and create a lock-in effect between the motion of the structure and the vortex shedding. This lock-in will increase the correlation length significantly, and a resonance effect will occur. The phenomenon of lock-in may only appear when the vortex shedding frequency is sufficiently close to the natural frequency of the structure.

For a fixed cylinder the correlation length, in span direction, of the vortex shedding is only 1-3 D, and will therefore not produce resonance issues. When the structure is free to oscillate however, the vortex shedding frequency will change towards the natural frequency of the structure and create a lock-in effect between the structure motion and the vortex shedding. This lock-in will increase the correlation length significantly, and resonance will occur. The phenomenon of lock-in may only appear when the vortex shedding frequency is sufficiently close to the natural frequency of the structure. When these frequencies are sufficiently close are in most guideline discussed by the use of the reduced velocity factor (V_R).

$$V_R = \frac{U_\infty}{f_n \cdot D} \tag{2}$$

where;

U_∞: is current velocity
f_n: is the Eigen frequency of the first mode of motion
D: is the outer diameter of pipe

The most relevant design guideline is DNV-RP-F105 Ref. (6) for subsea pipelines, where values for reduced velocities where lock-in may occur are given for one cylinder. To be able to use this guide line for the present concept, one has to adjust for the difference in vortex shedding period for one cylinder versus two cylinders in tandem. By adjusting the reduced velocity by a factor of:

$$\frac{\text{Vortex shedding period for one cylinder}}{\text{Vortex shedding period for two cylinders}},$$

By using eq. (1) this relation can be expressed as:

$$\frac{St_{two\ cylinders}}{St_{one\ cylinder}} \tag{3}$$

The Strouhal number used in the guidelines for one cylinder is $St = 0.20$, while experiments of Zdravkovich Ref. (4) p 1007 have shown a $St = 0.125$ for the combined cross section. Figure 4-3 illustrates the cross flow motion amplitude as function of reduced velocity and shows that cross flow motion has an onset at $V_R = 2$, and inline response has

an onset of $V_R = 1$. The reduced velocity for the SFT in cross flow motion is decided by the highest Eigen frequency in a vertical mode
$(f_n = \frac{1}{22s} = 0.045s^{-1})$, using eq. (2)and the correction factor in (3) it yields:

$$V_{R.cr} = \frac{U_\infty}{f_n \cdot D} \cdot \frac{St_{two\ cylinders}}{St_{one\ cylinder}} = \frac{\frac{0.60m}{s}}{0.045s^{-1} \cdot 12.6m} \cdot \frac{0.125}{0.20} = 0.66$$

Figure 4-3 suggests that a reduced velocity of $V_R = 0.66$ will not cause cross flow motion induced by vortex shedding.
Figure 4-4 illustrates the inline motion amplitude as function of reduced velocity, and for several values of the stability parameter K_S, representing the damping of the system for a given mode shape:

$$K_s = \frac{4\pi \cdot m_e \zeta_T}{\rho D^2} \quad (4)$$

where ζ_T is the total damping ratio, and m_e is the effective mass.
The inline reduced velocity for the SFT is decided by the highest Eigen frequency in a vertical horizontal mode $(f_n = \frac{1}{54.9s} = 0.018s^{-1})$, which using eq. (2) and (3) yields:

$$V_{R.Il} = \frac{U_\infty}{f_n \cdot D} \cdot \frac{St_{two\ cylinders}}{St_{one\ cylinder}} = \frac{0.60m/s}{0.018s^{-1} \cdot 12.6m} \cdot \frac{0.125}{0.20} = 1.65$$

The K_s is estimated to be 0.68, where ζ_T contain contributions from structural damping $\zeta_{structure} = 0.008$ (HB185 (1)), viscous damping from shafts, bracing and pontoons $\zeta_{viscous} = 0.011$ and a damping contribution caused by the fact that the current velocity close to shore is too low to obtain a reduced velocity (Ref. (5))a bow the onset at $V_R = 1$. Therefore, 20% of the width of the fjord are assumed to be outside locks in area, and will therefore contribute to the damping $\zeta_{uncorrelated} = 0.01$, and $\zeta_T = 0.029$

Figure 4-4 suggests that for $Ks = 0.68$ and a reduced velocity of $V_R = 1.65$ the motion amplitude is approximately:

Inline motion amplitude: $A_{inline} = 0.04 \cdot D = 0.50m$

Which results in a cross sectional moment of:

$$M_{VIV} = 0.04 \cdot D \cdot \left(\frac{2\pi}{L\left(1 - \frac{0.33}{2}\right)} \right)^2 \cdot EI_z = 1.27GNm$$

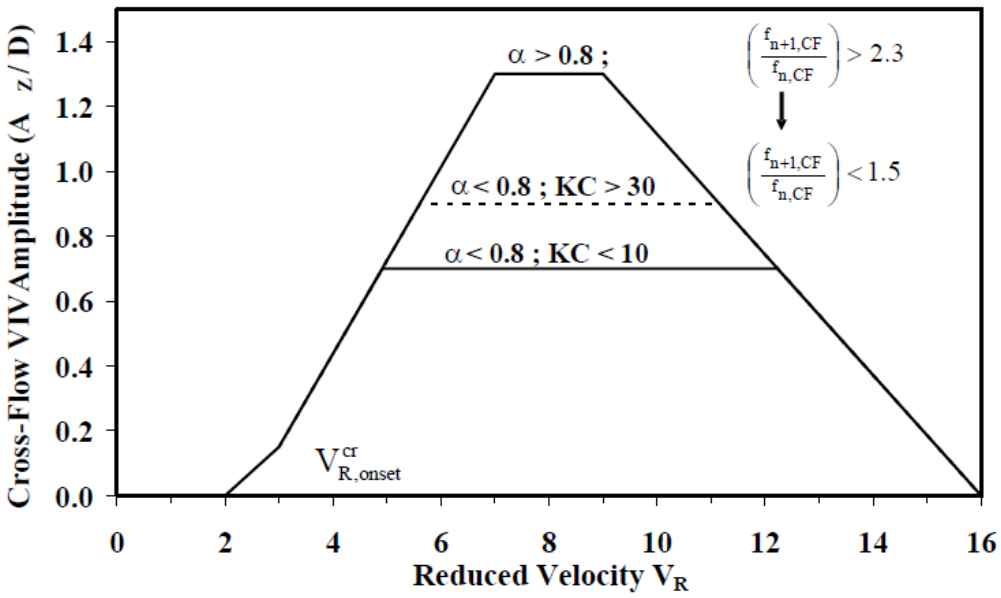

Figure 4-3: Basic cross-flow response model (DNV-RP-F105 (6))

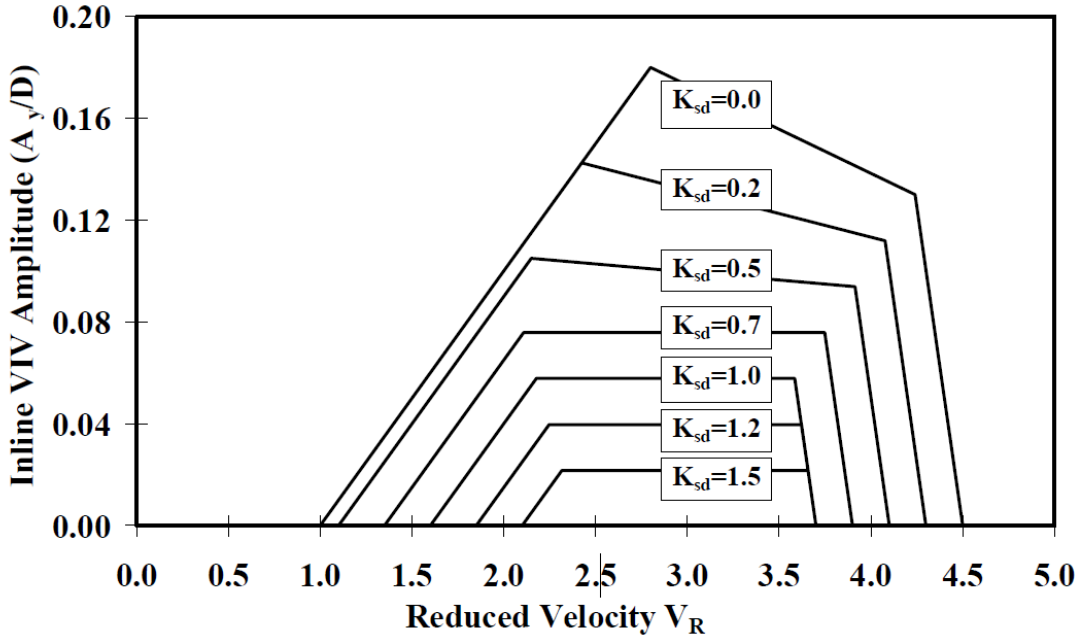

Figure 4-4: Illustration of the in-line VIV Response Amplitude versus $V_R$and K_S (DNV-RP-F105 (6))

One may presume that there will be no pure vortex induced cross flow motion, but an inline motion may occur for high current velocities.

Since no relevant experiments have been conducted at correct Reynolds number, experiments should be conducted at an accurate Reynolds number before a final verification can be made.

4.4.3 Wake induced vibrations

Motion induced vibration can normally not occur for circular cross sections; however when a cylinder is placed in the wake of another such effects may take place due to changes in lift and drag.

Motion induced vibrations can be described by a change in the drag (C_D) and lift (C_L) coefficients with respect to the angle of attack of the resultant flow velocity on the structure.

The angle of attack of the resultant flow velocity is a function of the rotational motion of the structure as shown in Figure 4-5, where a rotation of the bridge (φ) changes the angle the incident flow hits the cross section. In addition, the cross flow motion of the bridge adds a velocity component which contributes to the total flow velocity and the angle of attack on the cross-section (α), as illustrated in Figure 4-6

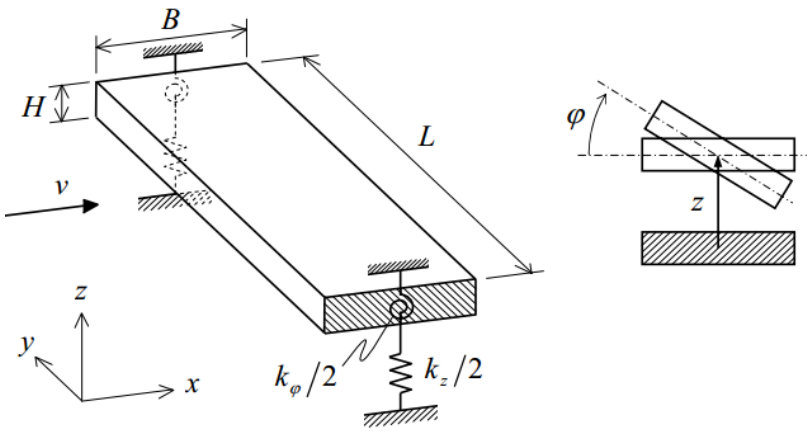

Figure 4-5: Visualization of the flutter effect

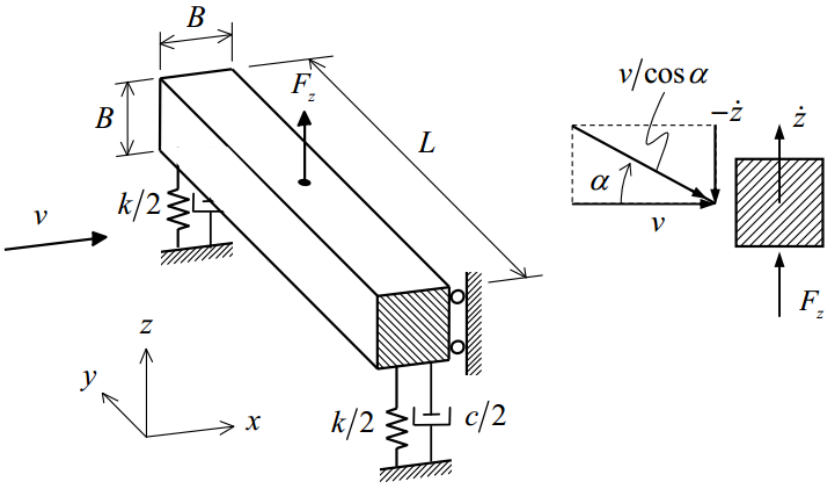

Figure 4-6: Visualization of the galloping effect

The angle of attack of the current on the SFT determines the second cylinders position in the wake behind the first cylinder. An offset of the second cylinders position in the wake

causes a variation in shadow effect on the upper half of the cylinder compared to the bottom half, which results in changes in the dynamic pressure caused by the variation in flow velocity. It is the forces resulting from these pressure differences which causes the previous mentioned change in drag and lift coefficient with respect to the angle of attack of the current $[C_D(\alpha+\varphi),\ C_L(\alpha+\varphi)]$.
By assuming uncoupled motions and the use of a quasi-static approach it can be shown that the motion of the structure imposes a negative damping in the vertical direction:

Reduced vertical damping:
$$-\frac{\rho_w}{2}U_\infty D\left(\left(\frac{\delta C_L}{\delta\alpha}\right)_{\alpha=0}+C_D(0)\right) \quad (5)$$

And a negative contribution to the damping and stiffness of the angular motion:

Reduced angular damping:
$$-\frac{\rho_w}{2}U_\infty D\cdot CDBT^2\cdot\left(\frac{\delta C_L}{\delta\varphi}\right)_{\varphi=0} \quad (6)$$

Reduced angular stiffness:
$$-\frac{\rho_w}{2}U_\infty^2 D\cdot CDBT\cdot\left(\frac{\delta C_L}{\delta\varphi}\right)_{\varphi=0}$$

Where ρ_w is the water density and CDTB is the Center Distance Between Tunnels.
It is important to understand that motion induced vibration is directly affected by the wake behaviour behind the first cylinder, which is vastly influenced by vortex shedding. This causes the vortex lock in effect and the motion induced vibration to be highly interdependent effects.

Relevant experimental investigations on such effects have been conducted by Assi, G.R.S. et al. Ref. (7), which have conducted experiments on flow past two circular cylinders. Some of their results on cross flow motion are shown in Figure 4-7.

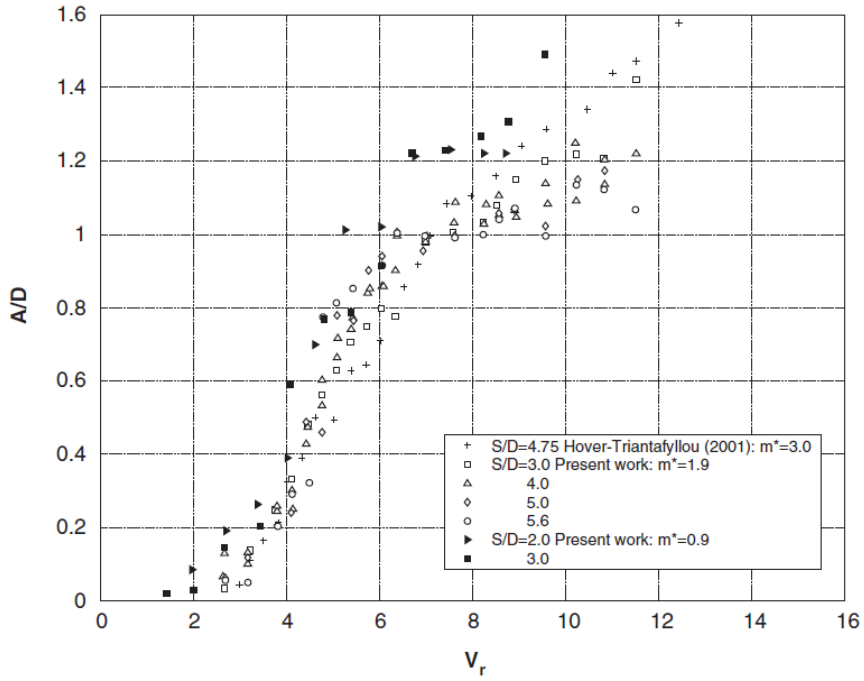

Figure 4-7: Variation of the reduced amplitude A/D versus reduced velocity V_r for the trailing cylinder of a pair in tandem arrangement. (7)

The present cross section holds a distance between cylinders close to 3.2D, and a relation between weight and buoyancy m^* close to 0.9. The highest reduced velocity for a vertical mode is given by:

$$V_R = \frac{U_\infty}{f_n \cdot D} = \frac{0.6m/s}{0.045s^{-1} \cdot 12.6m} = 1.05 \quad (7)$$

From Figure 4-7 one can extract that the results of Assi, G.R.S et al. (7) suggests that one may expect the motion amplitude for the combined effect of vortex and motion induce vibration to be very little, and because this occurs only for the first mode of motion such amplitude results in a neglect able cross sectional forces and accelerations.

Since no relevant experiments have been conducted at correct Reynolds number, experiments should be conducted at an accurate Reynolds number before a final verification can be made.

4.5 Wave induced loading

4.5.1 Describing the sea state

Wave data for the crossing site have been provided by SINTEF in (5), where the sea state is described by a JONSWAP power spectrum with a maximum significant wave height of 2.14 m and wave period of 4.8 s for a fifty year return period. Note that the bridge is not sensitive to wave direction due to the geometry of the structure.
The swells at the crossing site are due to the ocean waves coming into the Lavik-Opedal area, which will have a highly reduced energy due to topography along the fjord. SINTEF in (5) have estimated around 1% of the ocean wave height to reach the crossing site, coming up with maximum significant wave height of 0.1 m. The maximum single wave height during a storm may then be set to H_{max} = 0.2 m. The period follows the ocean waves and lies with peak period of 14 seconds. The JONSWAP spectra is strictly speaking not valid for such low wave heights, but are still used to describe the swell contribution to the sea state on the basis that the origin of the waves, the ocean waves, are very well described by the JONSWAP spectrum.
To obtain a two dimensional description of the sea state, a directionality function given in DNV RP 205 Ref. (8) is utilized:

$$D(\theta, n) = \frac{\Gamma\left(1+\frac{n}{2}\right)}{\sqrt{\pi} \cdot \Gamma\left(\frac{1}{2}+\frac{n}{2}\right)} \cos(\theta)^n \quad for \quad |\theta| \geq \frac{\pi}{2} \quad (8)$$

Here θ is the wave direction, Γ is the gamma function and n is a steepness value which states the density of the wave directions around the mean value. Some direction functions are plotted in Figure 4-8 for different values of n. Recommended practice from DNV for

regular sea stated is n = 2 – 4 for wind generated sea, and n = 6 for swells. The present problem is related to the sea state in a fjord, and a more uniformed direction is to be expect, the values of n is therefore presumed to be n = 6 for wind generated sea, and n = 8 for swells

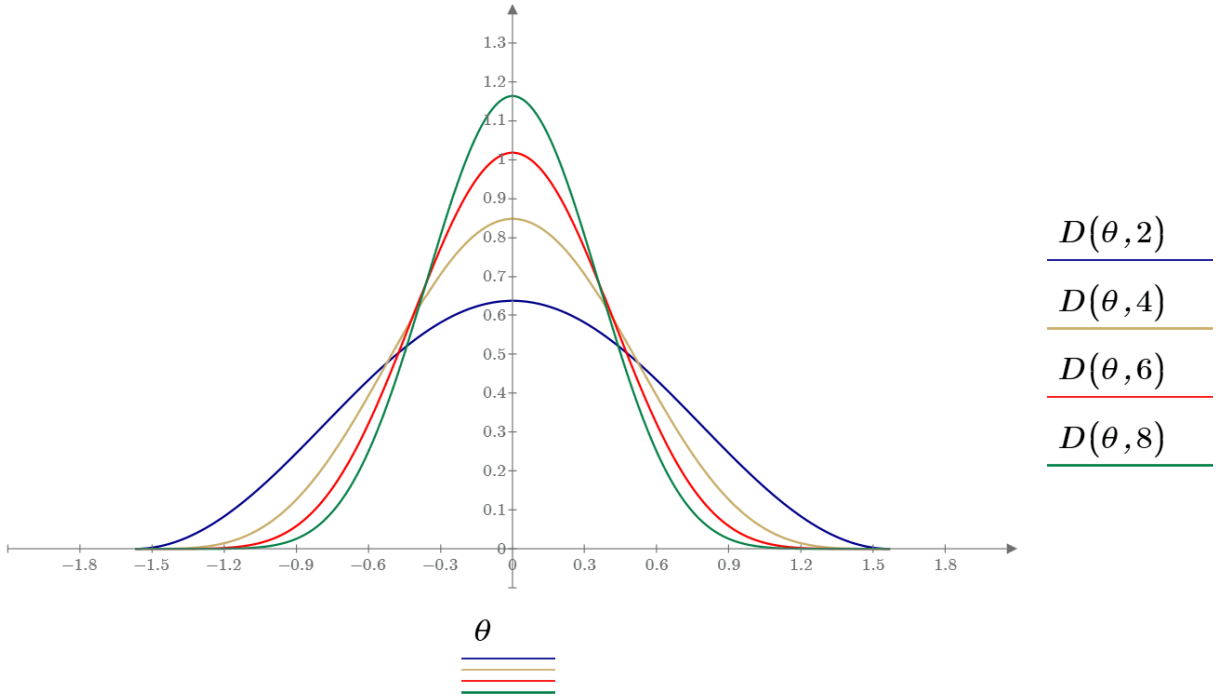

Figure 4-8: Direction function for n = 2, 4, 6, 8

The relation between the cross sectional dimensions and the wave dimension (height and length) are as such that the forces caused by the waves are highly dominated by mass forces, meaning that the resulting forces can be expressed in the term of the acceleration of the wave. This implies that the Froude-Kriloff and the diffraction wave potential can be expressed based on the acceleration terms only. The wave radiation potential of the tunnels is very small due to the depth of their location, but the pontoons have a significant wave radiation potential, which have to be accounted for. It should also be noted that the energy, and acceleration, of the wind generated waves at a depth of 20 m is less than 2 % of that at the surface.

4.5.2 Second order load effects

The Froude-Kriloff and diffraction potentials only take linear terms in to account, an evaluation of the higher order effects is therefore necessary. This has been provided by Prof. O. M. Faltinsen:

We assume that the incident waves are long-crested and in deep water. The wave spectrum is denoted $S(\omega)$. We neglect the interactions with the pontoons, tubular bracing, shafts, cross-tunnels and land fall details.

Traffic tunnels

We will consider slowly varying forces due to second order effects in the incident waves. We can write the spectral density of the slowly varying force in the lateral (j=2) and vertical (j=3) directions as

$$S_{Fj}(\mu)=\frac{2\left(\rho A_c L+A_{jj}\right)^2}{g^2}\exp\left(-2\frac{\mu^2 d}{g}\right)\mu^4\int_0^\infty S(\omega)S(\omega+\mu)(\omega+\mu)^2(2\omega+\mu)^2\exp\left(-4\frac{\mu\omega d}{g}\right)d\omega$$

The explanations are

$\rho=$ water density

L= considered length of the tunnel

$A_c L=$ displaced volume of water

$A_{jj}=$ added mass in direction j

g=acceleration of gravity

d=vertical distance between mean free surface and the centre of a tunnel

If we neglect hydrodynamic interactions between the tunnels and free-surface effects, we can approximately write $A_{jj}=2\rho\pi(D/2)^2 L$ with D as outer diameter of each tunnel.

Pontoons

The low-frequency force spectral density in the longitudinal (j=1) and vertical (j=3) directions of the pontoons are expressed as

$$S_{Fj}(\mu)=8\int_0^\infty S(\omega)S(\omega+\mu)\left[\bar{F}_j(\omega+0.5\mu)/\zeta_a^2\right]^2 d\omega$$

Here $\bar{F}_j(\omega+0.5\mu)$ is the mean wave force on the pontoon in direction j=1 and 3 in regular waves with frequency $\omega+0.5\mu$ and wave amplitude ζ_a. Depending on the frequency content in the wave spectrum we may approximate $\bar{F}_1(\omega+0.5\mu)$ with the high-frequency asymptotic value Ref. (9). For an accurate expression for the slowly varying effects in the vertical directions on the pontoons $\bar{F}_3(\omega+0.5\mu)$ needs to be calculated by a wave diffraction program such as WAMIT. However, the contributions to reactions in the SFT from the slowly varying vertical forces on the pontoons have been estimated to be so small that they have been deemed not to be essential within the present scope. Slowly varying forces on the tubes and the horizontal directed forces on the pontoons are taken in to account.

4.5.3 Slide generated wave

SINTEF in their wave estimates in Ref. (5).have considered slide generated waves created in Flåm at the inner part of Sognefjorden as governing. The waves then travel over a distance of 140 km out to the site of Lavik – Opedal, and the amplitude reached the bridge would be in the range of 0.2 m. The wave period is estimated by SINTEF to around 85 seconds, which is so far from any response periods that the structure response is less than for regular waves.

4.5.4 Internal wave

The most probable type of internal wave is the dispersive waves as generated by ship traffic. Via Prof. Faltinsen we have been in contact with Prof. John Grue UiO. In summer time a 4 m layer of fresh water with density 1 may be overlaying sea water with density 1.026. The so called internal reference velocity is then close to c_0 = 1 m/s. Wave pattern introduces a fluid velocity in upper layer close to 10% of c_0, 0.1 m/s, and in lower layer about 5%, descending towards bottom. Period is 10 times upper layer divided by c_0, ending up in 40 seconds based on above data. With a low probability of occurrence in combination with a loading period outside the area of the response periods, this effect has been estimated to be of no interest within this scope.

4.6 Wind

DNV-RP-C205, Environmental conditions and environmental loads, are used to calculate the wind forces on the pontoons.

$$F_w = C\ q\ S\ sin\alpha$$

Where C is the shape coefficient, q is the basic wind pressure or suction, S is the projected area normal to the direction of the surface and α is the angle between the direction of the wind and the axis of the exposed member or surface. According to table 5.5 in RP-C205, C is 1.1 for wind acting towards the long side of the pontoon and 0.7 for wind acting towards the short side.

$$q = \frac{1}{2}\rho_a\ U_{T,z}^2 = \frac{1}{2} \cdot 1.226 \frac{kg}{m^3} \cdot \left(28 \frac{m}{s}\right)^2 = 481 \frac{N}{m^2}$$

DNV-OS-C101, sec.3 E703, states that the pressure acting on external bulkheads exposed to wind shall not be taken less than 2.5 kN/m^2 unless otherwise documented. This standard is intended for North Sea conditions, but to be conservative a pressure of 2.5 kN/m^2 is used in the further calculations.

The total wind forces acting on the short side of a pontoon is thereby:

$$F_w = C\ q\ S\ sin\alpha = 0.7 \cdot 2.5\ \frac{kN}{m^2} \cdot 26\ m \cdot 4\ m = 182\ kN$$

And on the long side:

$$F_w = C\ q\ S\ sin\alpha = 1.1 \cdot 2.5\ \frac{kN}{m^2} \cdot 80\ m \cdot 4\ m = 880\ kN$$

The wind forces acting on the pontoons are negligible compared to the other loads and excluded in the design combinations.

4.7 Snow and ice

The characteristic snow load on ground for the crossing site is 2.5 kN/m^2 and ice caused by rain/snow according to NORSOK N-003, ref. (10), is 0.9 kN/m^2. These load cases are regarded not to act simultaneously. NORSOK in addition describes icing on horizontal surfaces more than 5 m above the sea level, but this is not relevant as the pontoon height is below that level.

2.5 kN/m^2 equals a displacement of the pontoons:

$$\Delta Z = \frac{2500\ \frac{N}{m^2}}{1015\ \frac{kg}{m^3} \cdot 9.81 \frac{m}{s^2}} = 0.25\ m$$

It is assumed that the snow load is the same for all pontoons, and thereby only imposes deformations in the SFT from the landfall to the first pontoon. This load case will give the same response mode as the low tide. The difference in magnitude between high tide and low tide is 0.27 m, which is more than the effect of snow load. Snow loads are therefore neglected in the dimensioning load combinations.

4.8 Ship impact

As discussed in the concept description, chapter 3, loading from ship collisions are handled by a weak link which is designed to break before causing severe damage on the tubes. It is therefore essential to design the weak link in such a manner that it will break before damage is caused to the tubes, but not make it so weak that it breaks so easily that the return period for such an event is too low. Rambøll have therefore performed a detailed probability analysis, ref. (11), which yielded a design load of 2MNm with a return period of 50 years. To display the robustness of the concept a return period of 100 years have been chosen as a design criteria for the weak link. A hundred year return period imposes a design collision energy load of 51 MNm. For design purposes this implies an ULS load on the tubes of 51 MNm, and a criterion for the weak link to fail for any load above 51 MNm.

The weak link has to be designed for any ship collision larger than the failure criterion. A ship collision will act as an impulse. To describe the impulse, the maximum force and the introduction period needs to be determined. Investigations have therefore been made to evaluate types of ship collisions that can occur based on the range of ships sailing in the Sognefjord. Figure 4-9 a) illustrates the array of hull properties that can be expected, and Figure 4-9 b) gives a combined load-indentation curve for both ship and pontoon. Figure 4-10 shows the collision sequence in the form of the speed for the colliding vessel for both the scenario with a rigid pontoon, and with a deformation of the pontoon.

Table 4-7 and Table 4-8 contain the input data from the various ship classes, and resulting deformation, collision time and maximum forces.

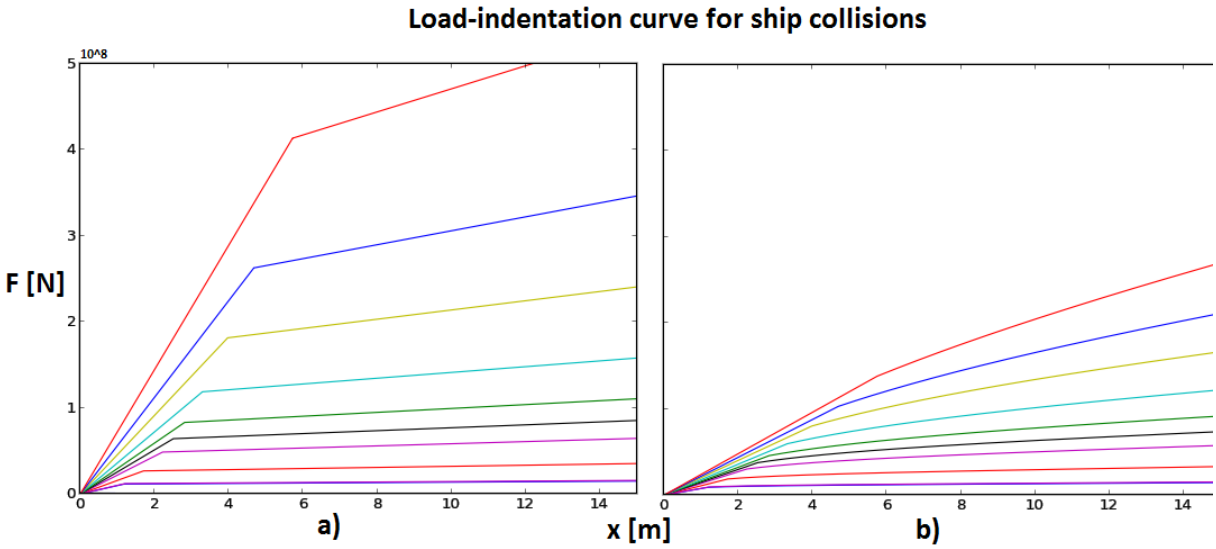

Figure 4-9: Force displacement curve for ship hulls (a), and ship hull and pontoon deformation (b) for all GT classes

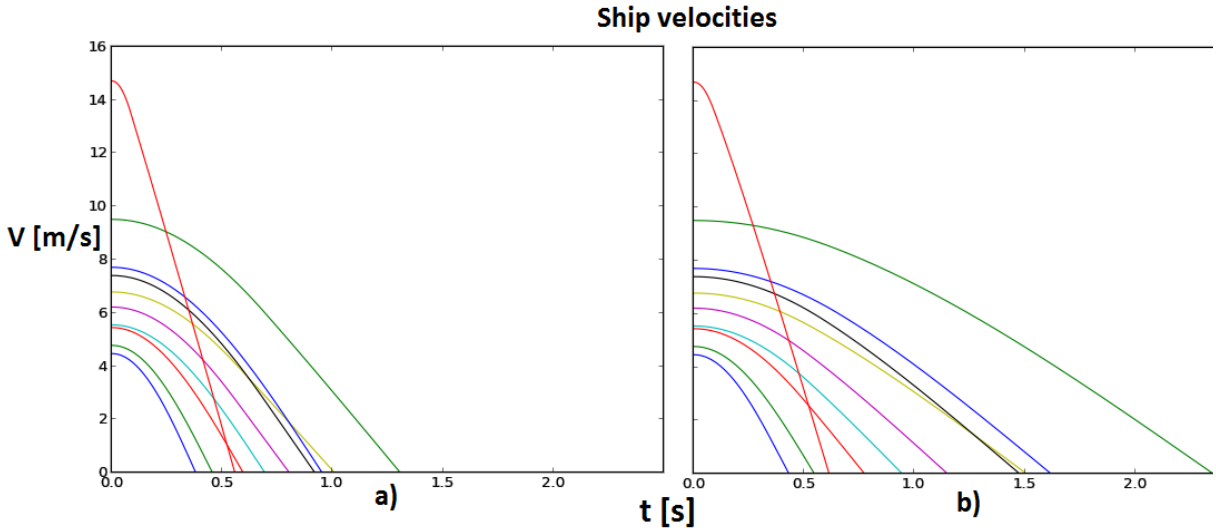

Figure 4-10: Ship velocities , a) for scenario with rigid pontoon, and b) scenario with deformations in the pontoon

Table 4-7: Collision scenarios with rigid pontoon

GT class	1	2	3	4	5	6	7	8	9	10
Mass [Ton]	580	1300	3200	5000	7500	13000	15000	21000	44000	440
Velocity [m/s]	4.5	4.8	5.5	5.6	6.2	6.8	7.4	7.7	9.5	1.5
Length [m]	35	56	78	91	110	130	160	200	260	36
Energy [MNm]	6.1	16	49	81	150	320	440	650	2100	50
Deformation [m]	1.1	1.4	2.1	2.5	3.2	4.3	4.4	4.8	7.8	4.6
Time [s]	0.38	0.45	0.50	0.69	0.8	1.0	0.92	0.95	1.3	0.56
Fmax [MN]	11	23	47	64	84	120	180	260	440	13

Table 4-8: Collision scenarios with deformations in the pontoon

GT class	1	2	3	4	5	6	7	8	9	10
Mass [Ton]	580	1300	3200	5000	7500	13000	15000	21000	44000	440
Velocity [m/s]	4.5	4.8	5.5	5.6	6.2	6.8	7.4	7.7	9.5	1.5
Length [m]	35	56	78	91	110	130	160	200	260	36
Energy [MNm]	6.1	16	49	81	150	320	440	650	2100	50
Deformation [m]	1.3	1.7	2.7	3.4	4.5	6.4	6.9	7.9	14	5.2
Time [s]	0.43	0.55	0.77	0.94	1.1	1.5	1.5	1.6	2.4	0.61
Fmax [MN]	9.2	19	33	43	57	83	110	140	260	12

4.9 Forces generated by a passing ship

A moving ship is displacing water due to the forward motion, this cause a time varying flow on the SFT. Due to the size and velocity of the ships sailing in the Sognefjord, these effects must be investigated. Prof. O. M. Faltinsen has derived the forces caused by a passing ship based on potential theory and source sink method:

We consider a ship of length L_1 and speed U_1 passing transversally the two tubes of the submerged floating bridge. The distance between the centres of the two tubes is denoted *S* and the submergence of a tube centre is *h*. The submerged cross-sectional areas of the ship are denoted S_1. Coordinate systems are shown in Figure 4-11. The Froude number $U_1/\sqrt{L_1 g}$ is assumed lower than approximately 0.2 so that waves generated by the ship are secondary and we can use a rigid free-surface condition. The latter fact allows us to make a mirror image of the ship with respect to the mean free surface so that we can consider the flow caused by the submerged part of the ship and its mirror image in infinite fluid.

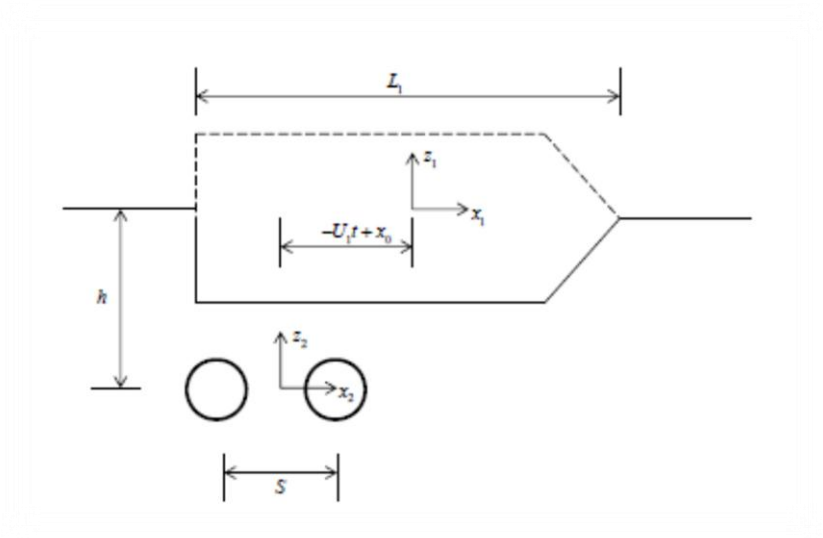

Figure 4-11: Coordinate systems and definitions of parameters. Dashed lines symbolize the mirror image of the submerged part of the ship.

We neglect first the presence of the tubes and assume a slender ship which implies that the ship ends should not be too blunt. The far-field velocity potential due to the ship plus the image ship can be represented as a line distribution of infinite-fluid sources and sinks, i e.

$$\varphi_1 = \frac{U_1}{2\pi}\int_{L_1}\frac{S_1'(x)dx}{\sqrt{(x_1-x)^2+y_1^2+z_1^2}} \tag{9}$$

We assume the tubes are in the far-field of the ship which is only an approximation in reality. However, the latter assumption provides us with simple estimates of the loads on the tubes. The estimates are expected to be non-conservative. We may, for instance, underestimate the forces by 30% based on experience with interacting forces between ships. A more correct procedure based on potential flow theory is described by Xiang and Faltinsen Ref. (12). In lack of data for representative ships we may assume semi-circular cross-sections with radii given by

$$r(x) = R\left[1-\left(\frac{2x}{L_1}\right)^2\right]^{\alpha}, \qquad S_1(x) = 0.5\pi r^2 \tag{10}$$

Here α may be 0 in one case and 0.5 in another case.
The incident vertical velocity on the tubes can be expressed as

$$W = \frac{U_1 h}{2\pi}\int_{L_1}\frac{S_1'(x)dx}{[(x_1-x)^2+y_1^2+h^2]^{3/2}} \tag{11}$$

$$x_1 = -U_1 t \pm \frac{S}{2} + x_0, \qquad t \geq 0$$

Here x_0 is the initial x_1-coordinate of the centre of the two tubes sufficiently ahead of the ship so that the interacting forces are negligible. Different x_0-values can be tried out in practice. The vertical force per unit length on one of tubes is by neglecting hydrodynamic interaction between the tubes equal to

$$df_3 = \rho 0.5\pi D^2 \cdot \frac{\partial W}{\partial t} \tag{12}$$

Here x_1 is calculated according to eq. (11) dependent on which tube is considered. Further D is exterior tube diameter and ρ is mass density of water. We can similarly analyze the transverse force by differentiating eq. (9) with respect to x_1 and find the transverse inflow velocity as

$$W = -\frac{U_1}{2\pi}\int_{L_1} \frac{(x_1 - x)S_1'(x)dx}{[(x_1 - x)^2 + y_1^2 + h^2]^{3/2}}, \tag{13}$$

$$x_1 = -U_1 t \pm \frac{S}{2} + x_0, \qquad t \geq 0$$

The transverse force per unit length on one of tubes is by neglecting hydrodynamic interaction between the tubes equal to

$$df_1 = \rho 0.5\pi D^2 \cdot \frac{\partial U}{\partial t} \tag{14}$$

We assume a tube diameter *D*=12.6m and a distance *S* between the tube centres equal to 40m. The submergence *h* of the tube centre is 25m. An academic ship with semi-circular cross-sections with maximum radius *R*=15m. Further $\alpha = 0.5$ in eq. (10). The ship length L_1=300m and the ship speed U_1 is 10m/s. Results for time dependant vertical and transverse force per unit length at y1=0 are presented in Figure 4-12 and Figure 4-13. The results have independently been verified by Andreas Saur Brandtsegg at Dr. Techn. Olav Olsen.

The predicted magnitude of the force can be related to the vertical and transverse force due to swell which will be approximated as a regular wave with period 15s and wave amplitude 0.1m. The transverse and vertical swell force amplitude per unit length is 2840N/m, i.e. the force per unit length due to the passing ship can be clearly larger in magnitude. However, the longitudinal distribution of the forces along the tube is obviously different. The latter is illustrated in Figure 4-14 for the vertical force per unit length due to the passing ship. In order to judge the importance of the loads due to the passing ship we have to apply the loads in a transient dynamic analysis of the tubes. If the response is important, more realistic ship forms have to be considered.

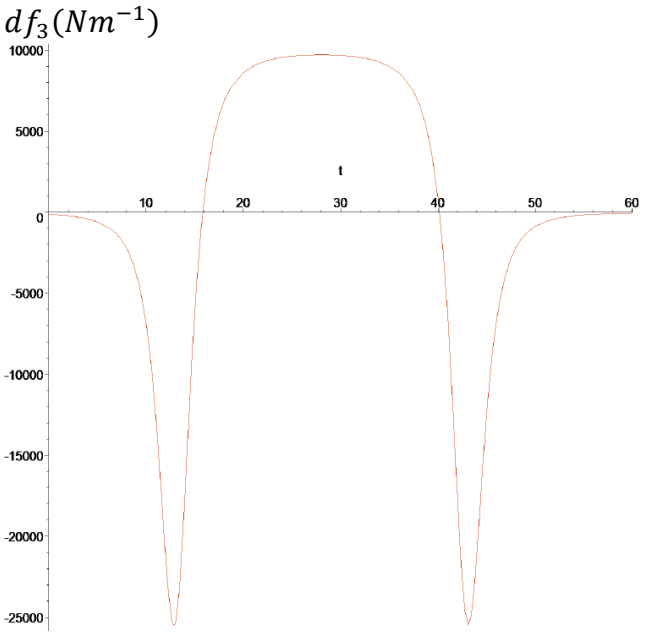

Figure 4-12: Vertical force per unit length at y1=0 for tube situated at $x_1 = -U_1 t \pm \frac{S}{2} + 300$ as a function of time

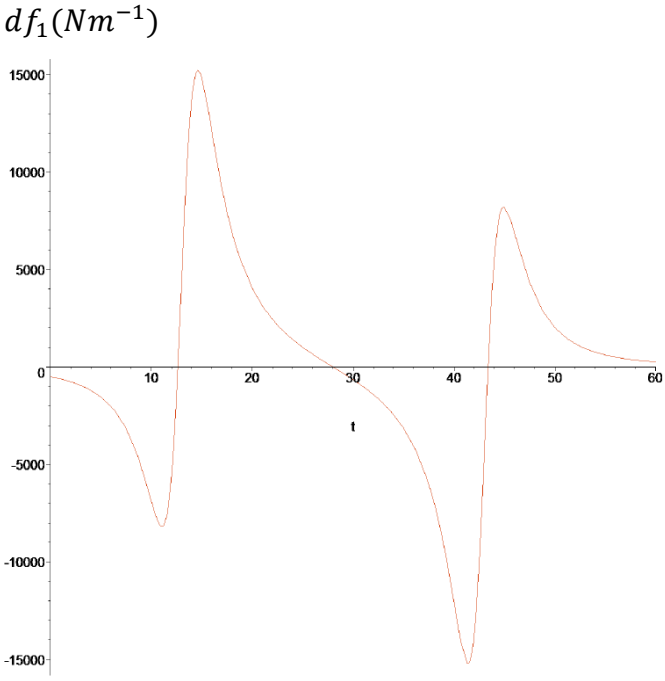

Figure 4-13 Transverse force per unit length at y_1=0 for tube situated at $x_1 = -U_1 t \pm \frac{S}{2} + 300$ as a function of time

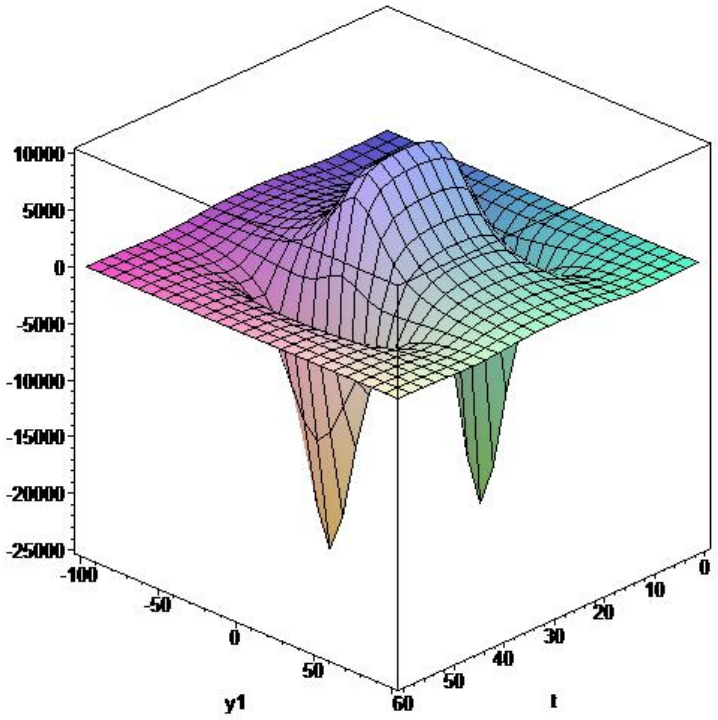

Figure 4-14: Vertical force per unit length with dimension N/m for tube situated at $x_1 = -U_1 t \pm \frac{S}{2} + 300$ as a function of time in seconds and y_1 in meters.

4.10 Compartment flooding

In case a valve from the ballast pipelines to the water ballast chamber fails one compartment of 50 meters length can be flooded. The compartment is approximately 10 m^2 so this area holds 100 kN/m when filled. In the weight configuration water ballast of 70 kN/m is assumed. The variable self-weight contribution from marine growth and water absorption in the concrete is 20 kN/m, and if the water ballast is reduced to adjust for these elements over time, then the maximum added load from compartment flooding is:

$$q_{flooding} = 100\frac{kN}{m} - \left(70\frac{kN}{m} - 20\frac{kN}{m}\right) = 50\frac{kN}{m}$$

For the 50 meter compartment this yields a resulting load of 2500 kN, which is insignificant in an ALS load combination, and omitted in the feasibility study.

4.11 Deformation loads

The effects of imposed deformations due to temperature, creep, shrinkage and post-tensioning are considered in the design.

4.11.1 Creep and shrinkage

Creep and shrinkage of the concrete tunnel depend on the concrete mix, maturity, effective wall thickness and the ambient humidity. The environmental conditions considered when calculating the creep and shrinkage deformations are:

- During construction in dry dock the relative humidity *RH* is assumed to 70 % for both outside and inside of the tunnel element.
- In operation and temporary floating phases the relative humidity inside the tunnel is taken as 70 % while the outside condition corresponds to 100 % *RH*.

Until the tunnel is set afloat, creep- and shrinkage-induced deformations will be similar for both faces as the outside and inside perimeters are almost equal. In submerged condition the tunnel will be exposed to drying on the inside and swelling on the outside. Since the drying / swelling perimeter is reduced by ~ 50 %, the equivalent thickness h_0 is doubled.

Creep

Creep deformations result from long-term loading in the tunnel longitudinal axis. Relevant loads are longitudinal post-tensioning and 'built-in' water pressure. The time-dependent creep deformations are predicted according to NS-EN 1992-1-1 B.1, ref. (13), and are converted to equivalent temperature deformations.

The creep coefficient $\varphi(t,t_0)$ is calculated from:

$$\varphi(t,t_0) = \varphi_0 \cdot \beta_c(t,t_0)$$

where the notional creep coefficient is estimated from:

$$\varphi_0 = \varphi_{RH} \cdot \beta(f_{cm}) \cdot \beta(t_0)$$

The influence of the relative humidity on the creep coefficient is defined by the φ_{RH} factor as:

$$\varphi_{RH} = \left[1 + \frac{1-RH/100}{0.1 \cdot \sqrt[3]{h_0}} \cdot \left(\frac{35}{f_{cm}}\right)^{0.7}\right] \cdot \left(\frac{35}{f_{cm}}\right)^{0.2}$$

The influence of the concrete strength and age is accounted for by:

$$\beta(f_{cm}) = \frac{16.8}{\sqrt{f_{cm}}} = \frac{16.8}{\sqrt{63}} = 2.12$$

$$\beta(t_0) = \frac{1}{(0.1+t_0^{0.2})}$$

The creep development over time is estimated by the following expression:

$$\beta_c(t,t_0) = \left[\frac{(t-t_0)}{(\beta_H+t-t_0)}\right]^{0.3}$$

with:

$$\beta_H = 1.5[1+(0.012RH)^{18}]h_0 + 250\left(\frac{35}{f_{cm}}\right)^{0.5}$$

The effect of reduced temperature on the maturity of concrete is accounted for by adjusting the concrete age:

$$t_t = \sum_{i=1}^{n} \Delta t_i \cdot e^{-(4000/[273+T(\Delta t_i)])}$$

Creep coefficients are determined for three load stages / intervals for;

- Longitudinal prestress applied in dry dock at a concrete age t_0 of 90 days (average).
- External water pressure (on end caps) applied at sea launch at an average concrete age t_0 of 180 days.
- Long-term loads applied in installed position. Average concrete age t_0 taken as 3 years.

Table 4-9: Creep coefficients.

Load stage		*In dock*	*Submerged*	*Inplace*
		1	2	3
t_0	[days]	90	180	1 600
t	[days]	180	35 600	35 600
RH	[%]	70 / 70	70 / 100	70 / 100
h_0	[mm]	800	1 600	1 600
φ_{RH}	[ ]	1.08	0.97	0.97
$\beta(f_{cm})$	[ ]	2.12	2.12	2.12
$\beta(t_0)$	[ ]	0.39	0.34	0.24
φ_0	[ ]	0.89	0.70	0.49
β_H	[ ]	1 118	1 118	1 118
$\beta_c(t,t_0)$	[ ]	0.30	0.98	0.98
$\varphi(t,t_0)$	[ ]	**0.269**	**0.686**	**0.485**

Shrinkage

The free drying shrinkage depends on the ambient humidity, duration of the drying/swelling and the notional thickness h_0. The basic unrestrained drying shrinkage strain $\varepsilon_{cd}(t)$ is predicted according to NS-EN 1992-1-1 B.2 (13)from:

$$\varepsilon_{cd}(t) = \beta_{ds}(t,t_s) \cdot k_h \cdot \varepsilon_{cd,0}$$

where:

$$\beta_{ds}(t,t_s) = \frac{(t-t_s)}{(t-t_s)+0.04\sqrt{h_0^3}}$$

$$\varepsilon_{cd,0} = 0.85\left[(220+110\cdot\alpha_{ds1})\cdot exp\left(\alpha_{ds2}\frac{f_{cm}}{f_{cmo}}\right)\right]\cdot 10^{-6}\cdot\beta_{RH}$$

$$\beta_{RH} = 1.55\left[1-\left(\frac{RH}{RH_0}\right)^3\right]$$

Table 4-10: Free drying shrinkage strain.

Load stage		*Drying two sides*	*Drying one side*	*Swelling one side*
		$\varepsilon_{cd,d2}$	$\varepsilon_{cd,d1}$	$\varepsilon_{cd,s1}$
t_0	[days]	0	0	0
t	[days]	100 × 356	100 × 356	100 × 356
RH	[%]	70	70 / 100	70 / 100
h_0	[mm]	800	1 600	1 600
β_{RH}	[ ]	1.02	0.60	0.60
$\beta_s(t,t_0)$	[ ]	0.98	0.93	0.93
$\varepsilon_{cd,0}$	[‰]	-0.27	-0.16	0.10
$\varepsilon_{cd}(t)$	[‰]	-0.18	-0.10	0.07

For the final value of drying shrinkage, ⅔ drying of the air face and ⅓ swelling from the submerged face is assumed.

$$\varepsilon_{cd}(0,100\cdot 356) = {}^2/_3\cdot\varepsilon_{cd,d1\infty} + {}^1/_3\cdot\varepsilon_{cd,s1\infty} = -{}^2/_3\cdot 0.10 + {}^1/_3\cdot 0.07 = 0.04‰$$

The time-dependent shrinkage deformation corresponds to a temperature decrease of 4 °C.

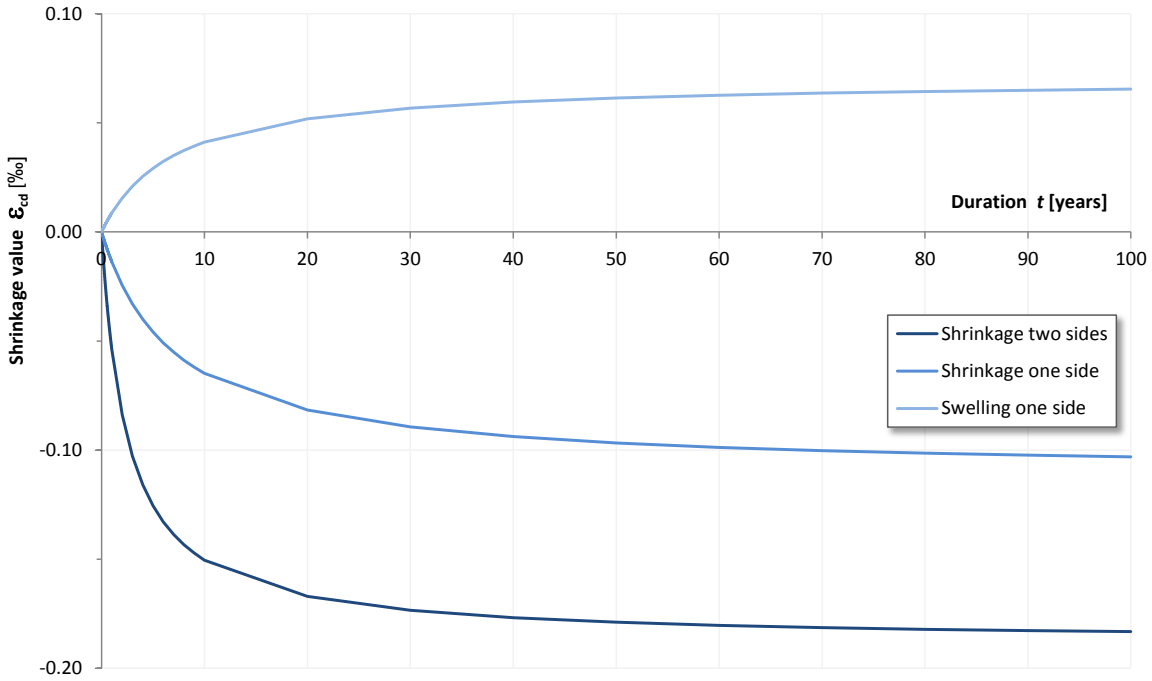

Figure 4-15: Development of unrestrained drying shrinkage.

4.11.2 Post-tensioning

The tunnel elements will be post-tension in both longitudinal and hoop direction. The calculation of post-tensioning losses includes immediate losses due to friction and anchorage slip and long-term losses due to creep and shrinkage.

Friction losses resulting from angular deviation θ and unintended wobbling β is estimated from the Coulomb's formula:

$$\Delta P_\mu(x) = P_0\left[1 - e^{-\mu(\theta+\beta\cdot x)}\right]$$

where;

μ : Friction coefficient
θ : Accumulated angular deviation (rad)
β : Wobble coefficient (rad/m)

The friction coefficient μ is taken to 0.20 and the wobbling factor β to 0.005 for the relevant tendon sizes, both values in agreement with relevant ETAs (e.g. ETA-06).

Besides friction losses an anchorage slip corresponding to 6 mm wedge draw-in at lock-off and 50 % elastic deformation of the concrete (successive stressing) is considered in prediction of the immediate losses. The time dependent losses are calculated based on an average concrete age t_0 of 90 days at stressing and 180 days at the time of sea launch.

Tunnel longitudinal cables:
The calculation of the effective long-term prestressing force distribution in the longitudinal cables (type 6-31) is based on an average cable length of L = 100 m and stressing at one end only. Due to the marginal loss from angular deviation, an average radius of 2 682 m (i.e. tunnel CL) is assumed for the cable curvature in both tubes. The prestressing level is determined to approximately 10 MPa. The obtained distribution of the relative prestressing force is shown in Figure 4-16 for t_0 and t_∞.

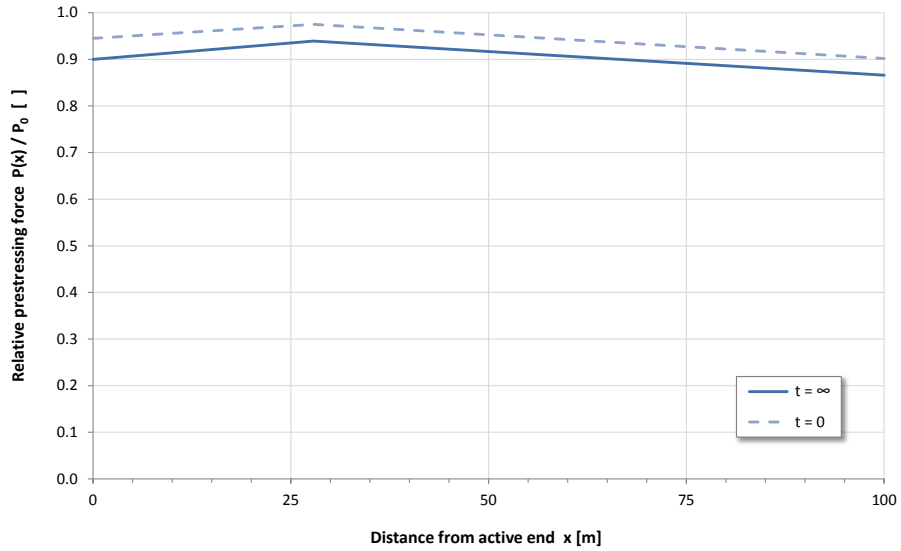

Figure 4-16: Prestressing distribution in tunnel longitudinal direction.

Based on Figure 4-16 and accounting for the positive effect of anchor staggering a mean prestressing force after time-dependent losses of 0.9 P_0 is used in the design.

Tunnel hoop cables:
The effective long-term prestressing force distribution in the hoop cables (type 6-19) assumes stressing of both ends to compensate for the significant friction losses. The cable length is taken to the circumferential length of the wall center line; 2 πR_m (37.07 m). The level of hoop prestress $p_{h,\infty}$ is generally, that is outside areas with high transverse shear, chosen to counter-balance the net internal over-pressure from explosion $p_{Ed,i}$;

$$P_{hoop,\infty} = \frac{p_{Ed,i} \cdot R_i - p_w \cdot R_o}{\gamma_p} = \frac{700 \cdot 5.50 - 9.86 \cdot 18.3 \cdot 6.30}{1.0} = 2\,713\ kN/m$$

The obtained distribution of the relative prestressing force is shown in Figure 4-17 for t_0 and t_∞. The mean prestressing force after time-dependent losses is found to 0.7 P_0.

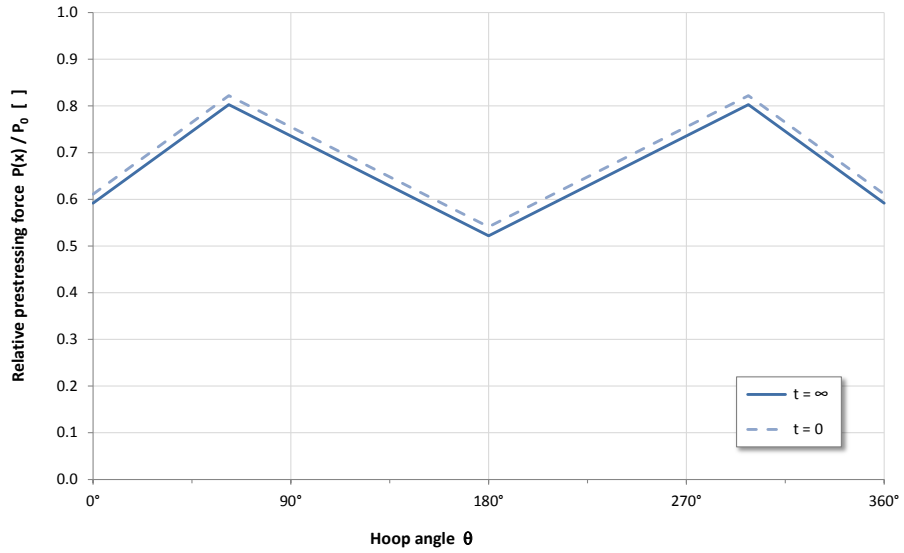

Figure 4-17: Prestressing distribution in tunnel hoop direction.

4.11.3 Temperature loads

In the absence of accurate data, a temperature variation of sea water temperature at 20 m water depth of ±5°C is assumed.

5 Structural analysis and design

5.1 General

The submerged floating tunnel (SFT) is modeled by a static global space frame model in STAAD. In this model, all static and quasi-static action effects are represented, and also ship impact modeled as an impulse load. Hydrodynamic calculations were performed separately, and response from load cases like 1st order wave, swells etc were calculated and combined with the other load cases.

First, a simple model was created to decide the pontoon configuration. In this model the double tube cross-section and the interconnecting truss structure was replaced by a beam element with geometry and stiffnesses simulating the full cross-section.

The following sections describe the final STAAD model with full tunnel geometry and translational and rotational springs to simulate the pontoons.

A hydrodynamic analysis in Wadam was performed to calculate response from wave loads during the tow from Bergen to Sognefjorden.

5.2 Analysis model

5.2.1 Model generation

To make the geometry highly regular, one simplification is made; the pontoons are placed in the radial direction rather than in the longitudinal direction of the fjord (y-direction). Then, nodes for the two tubes were generated by polar coordinates partitioned by a fixed angular distance. To obtain an angle of approximately 40 degrees between the tubes and the interconnecting bracing, 93 nodes where chosen and every other node is a bracing connection point. The angular increment between the nodes is thereby

$$\theta_{tot} = \frac{4083 \cdot 360}{2 \cdot \pi \cdot 2682} = 87.22$$

$$\Delta\theta = \frac{87.22}{92} = 0.948$$

From the pontoon configuration study, a distance of 500 m between the landfall and first pontoon seems to give the best balance between tidal load effects and distributed weight effects. The second pontoon should be approximately 150 m from the first to ensure a manageable span in case of an ALS ship impact in the first pontoon. This philosophy also applies for the pontoons next to the navigation channel. The remaining pontoons are

distributed evenly. Table 5-1 show the angle used in STAAD for placement of the pontoons.

Table 5-1, Landfall and pontoon nodes

Node	θ	L
1/94	46.39	0
12/105	56.82	488
15/108	59.66	621
19/112	63.45	799
24/117	68.19	1021
29/122	72.93	1243
34/127	77.67	1464
39/132	82.41	1686
42/135	85.26	1819
52/145	94.74	2263
55/148	97.58	2396
60/153	102.32	2618
65/158	107.06	2840
70/163	111.80	3062
75/168	116.54	3284
79/172	120.34	3461
82/175	123.18	3595
93/186	133.59	4082

Figure 5-1 shows the structural elements in the analysis. The shafts are connected by a rigid pontoon, and the springs are applied to the center node.

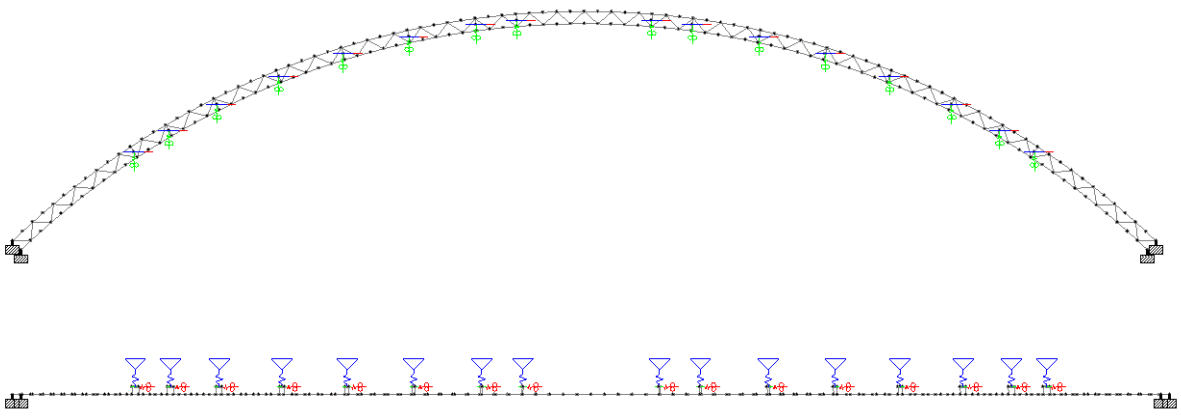

Figure 5-1, Plan view (xy) and vertical alignment of the STAAD model

5.2.2 Member properties

Pontoon spring stiffnesses, global coordinate system:

$$K_{FZ} = \rho_w g A = 1015\ \frac{kg}{m^3} \cdot 9.81\ \frac{m}{s^2} \cdot 1600\ m^2 \cdot 10^{-3} = 1.5931 \cdot 10^4\ \frac{kN}{m}$$

$$K_{MX} = \int_{-L/2}^{L/2} x^2 \rho_w g dx B = 2 \cdot \left[\frac{1}{3} \cdot 40^3 \cdot 1015 \cdot 9.81\right] \cdot 20 \cdot 10^{-3} = 8.497 \cdot 10^6\ \frac{kN}{rad}$$

$$K_{MY} = \int_{-B/2}^{B/2} x^2 \rho_w g dx L = 2 \cdot \left[\frac{1}{3} \cdot 10^3 \cdot 1015 \cdot 9.81\right] \cdot 80 \cdot 10^{-3} = 5.310 \cdot 10^5\ \frac{kN}{rad}$$

The spring stiffnesses are calculated from a simplified pontoon footprint, a 20x80 m rectangle. Free surfaces inside pontoons are deemed small and thereby neglected. The accuracy is sufficient at this stage, as the pontoons can be designed a prescribed stiffness.

5.3 Structural response

5.3.1 Modal analysis

A modal analysis has been carried out, and the calculated eigenperiods show good agreement with the analytical model used for the wave calculations. The first eigenperiod in sway (horizontal translation) is 55 seconds and the first period in heave (vertical translation) is 23 seconds. Table 5-2 shows the 30 first eigenperiods and the corresponding participating mass. The 10 first modes are shown in Figure 5-2 to Figure 5-11.

Table 5-2, Eigenperiods with participation factors

MODE	FREQUENCY	PERIOD	X	Y	Z	SUMM-X	SUMM-Y	SUMM-Z
1	0.018	54.9	28.90	0.00	0.00	28.90	0.00	0.00
2	0.034	29.5	0.00	2.26	0.00	28.90	2.26	0.00
3	0.044	22.6	0.00	0.00	13.24	28.90	2.26	13.24
4	0.055	18.1	0.00	0.00	0.00	28.90	2.26	13.24
5	0.055	18.1	0.00	0.00	49.95	28.90	2.26	63.19
6	0.057	17.6	0.00	0.00	6.25	28.90	2.26	69.44
7	0.057	17.6	0.00	0.00	23.54	28.91	2.26	92.98
8	0.06	16.5	10.29	0.00	0.00	39.20	2.26	92.98
9	0.061	16.5	0.07	0.00	0.00	39.27	2.26	92.98
10	0.062	16.1	0.00	0.00	1.38	39.27	2.26	94.37
11	0.073	13.8	0.00	0.00	0.00	39.27	2.26	94.37
12	0.079	12.7	0.00	0.00	0.81	39.27	2.26	95.17
13	0.081	12.3	0.00	28.76	0.00	39.27	31.03	95.17
14	0.091	10.9	0.00	0.00	0.00	39.27	31.03	95.17
15	0.103	9.7	0.00	0.01	0.53	39.27	31.04	95.70
16	0.104	9.6	0.00	48.30	0.00	39.27	79.34	95.70
17	0.118	8.5	0.00	0.00	0.00	39.27	79.34	95.70
18	0.124	8.1	6.03	0.00	0.00	45.30	79.34	95.70
19	0.134	7.5	0.00	0.00	0.09	45.30	79.34	95.79
20	0.151	6.6	0.01	0.00	0.00	45.30	79.34	95.79
21	0.167	6.0	0.00	3.03	0.00	45.30	82.37	95.79
22	0.17	5.9	0.00	0.00	0.68	45.30	82.37	96.48
23	0.191	5.2	0.01	0.00	0.00	45.31	82.37	96.48
24	0.201	5.0	13.99	0.00	0.00	59.30	82.37	96.48
25	0.214	4.7	0.00	0.00	0.40	59.30	82.37	96.87
26	0.228	4.4	18.13	0.00	0.00	77.43	82.37	96.87
27	0.234	4.3	0.01	0.00	0.00	77.44	82.37	96.87
28	0.235	4.3	0.00	0.15	0.00	77.44	82.53	96.87
29	0.239	4.2	11.27	0.00	0.00	88.70	82.53	96.87
30	0.254	3.9	0.00	0.97	0.00	88.70	83.50	96.87

Horizontal modes

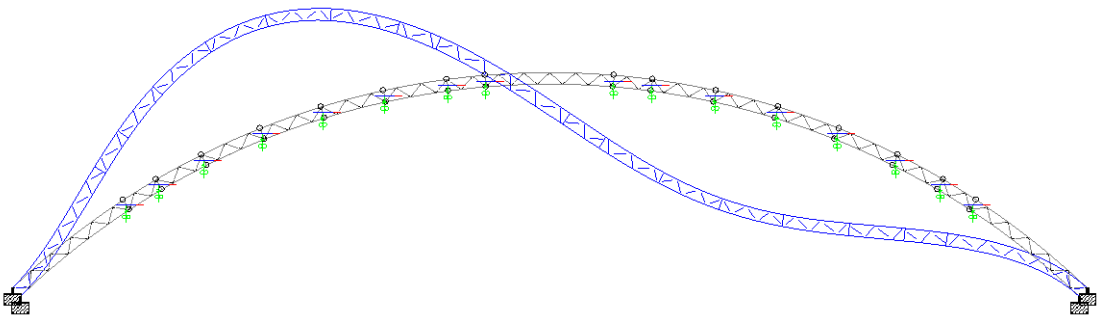

Figure 5-2: Mode 1, T=54.9s

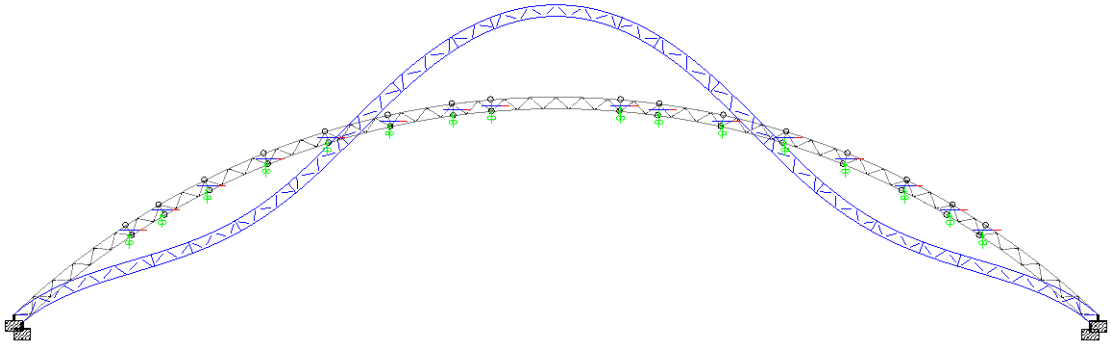

Figure 5-3: Mode 2, T=29.5s

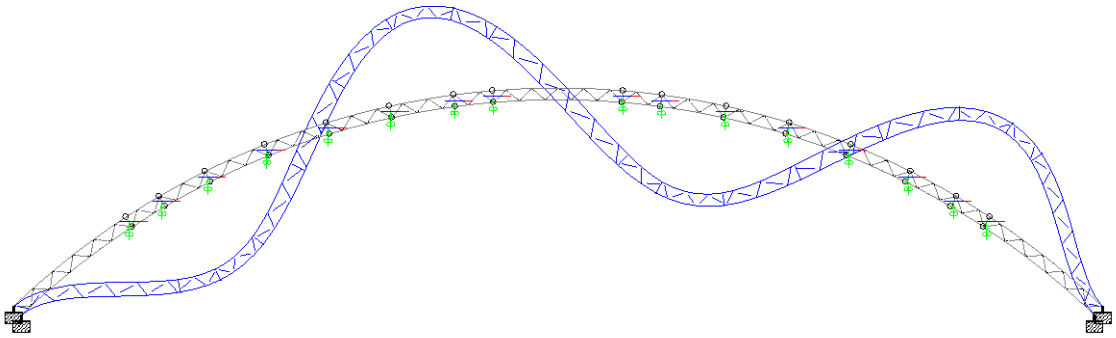

Figure 5-4: Mode 8, T=16.5s

Vertical modes

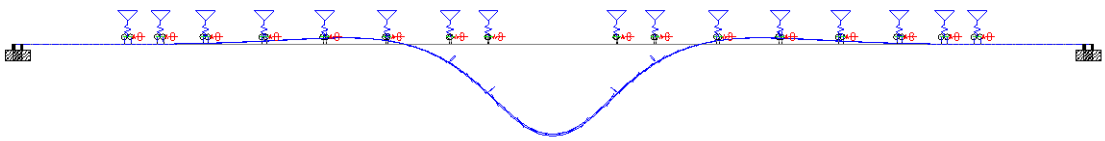

Figure 5-5: Mode 3, T=22.6s

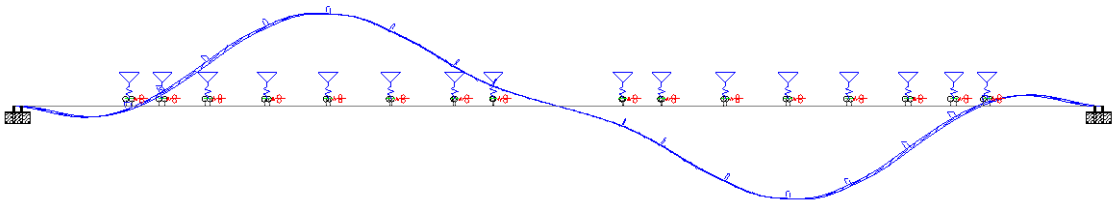

Figure 5-6: Mode 4, T=18.1s

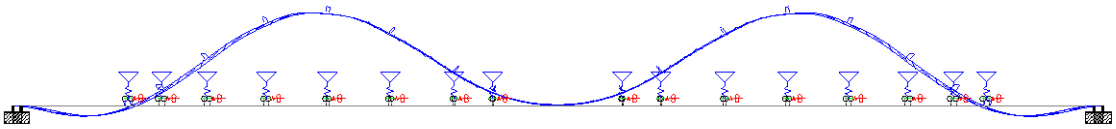

Figure 5-7: Mode 5, T=18.1s

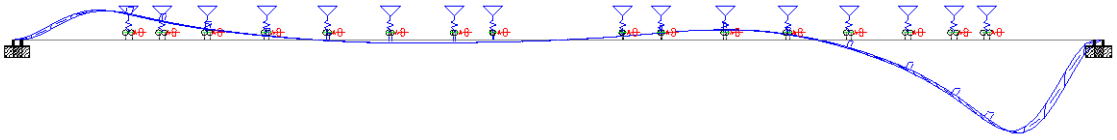

Figure 5-8: Mode 6, T=17.6s

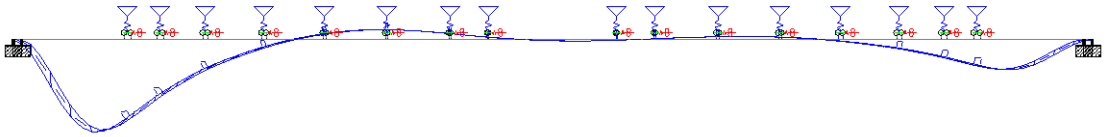

Figure 5-9: Mode 7, T=17.6s

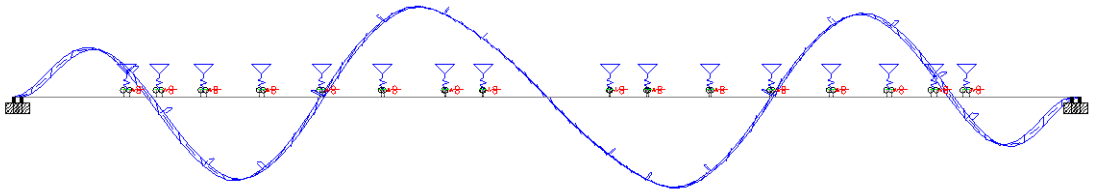

Figure 5-10: Mode 9, T=16.5s

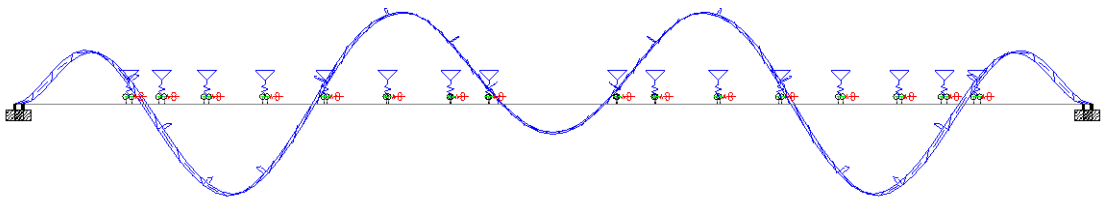

Figure 5-11: Mode 10, T=16.1s

5.3.2 Self-weight

Figure 5-12 and Figure 5-13 shows the moment- and shear distribution for the maximum self-weight load case. The shear forces are in general moderate; the large moments are caused by long spans.

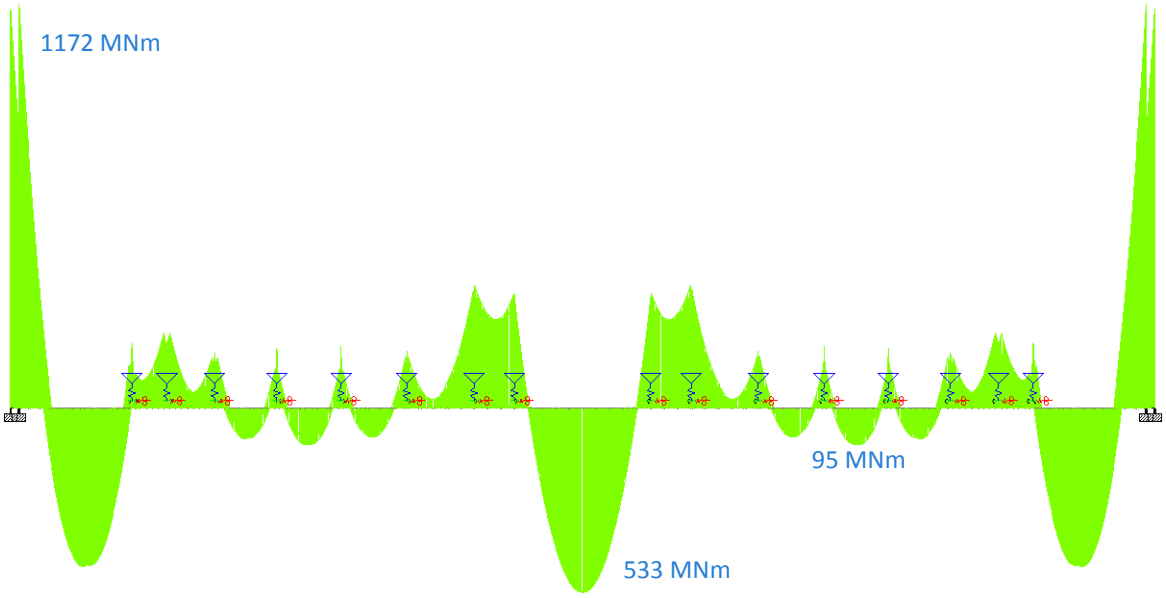

Figure 5-12, Moment distribution, M_y, from maximum self-weight

Figure 5-13, Shear distribution, V_z, from maximum self-weight

5.3.3 Traffic

Traffic loads give the same response as the maximum self-weight. Figure 5-14 and Figure 5-15 show the moment- and shear distribution from traffic loads with the joint load placed in the middle of the navigation channel.

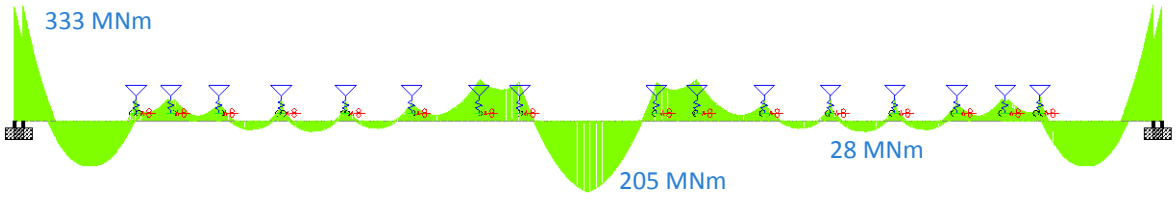

Figure 5-14, Moment distribution, M_y, from traffic

Figure 5-15, Shear distribution, V_z, from traffic

5.3.4 Tide

Tidal variations are modeled as joint loads in the linear springs representing the pontoons.

High tide:

$$F = K_{FZ}\,\Delta Z = 1.5931 \cdot 10^4\ \frac{kN}{m} \cdot 1.85\ m = 2.947 \cdot 10^4\ kN$$

Low tide:

$$F = K_{FZ}\,\Delta Z = 1.5931 \cdot 10^4\ \frac{kN}{m} \cdot (-1.58\ m) = -2.517 \cdot 10^4\ kN$$

The response from tidal variations is decided by the distance between the landfall and the first pontoon. With the current pontoon configuration, the moment caused by low tide as shown in Figure 5-16 is quite moderate. The values for tidal variation is taken from Ålesund which is probably higher than for Sognefjorden, but regardless of a reduction in variation a further optimization of the pontoon distance is possible in a future project phase.

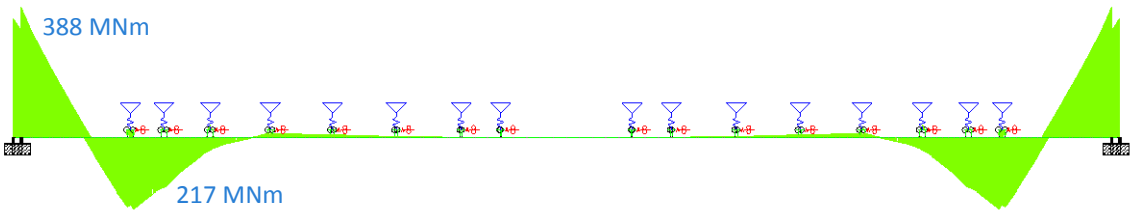

Figure 5-16, M_y from low tide

5.3.5 Current drag forces

Drag forces from the current are included in the STAAD analysis as quasi-static loads. The load case includes distributed loads on the tubes and joint loads on the pontoon nodes. Response from vortex induced vibrations and wake induced vibrations are calculated in the analytical dynamic analysis.

Figure 5-17 shows the asymmetric current load case and Figure 5-18 and Figure 5-19 show the response M_z and N_x. The asymmetric current gives significantly higher response than uniform current and mid half current, and therefore the design load combinations only include asymmetric current.

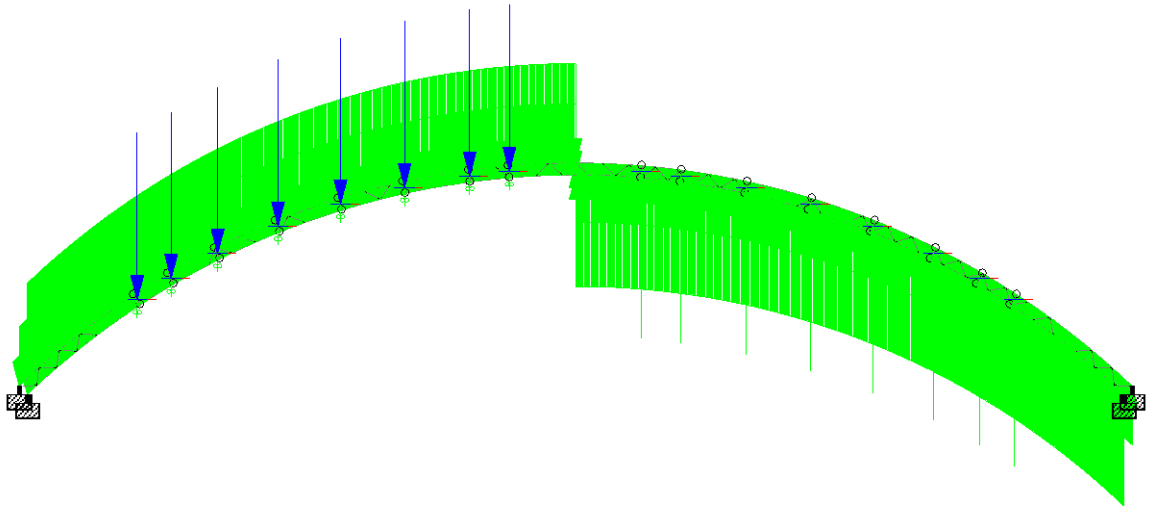

Figure 5-17: Asymmetric current load case

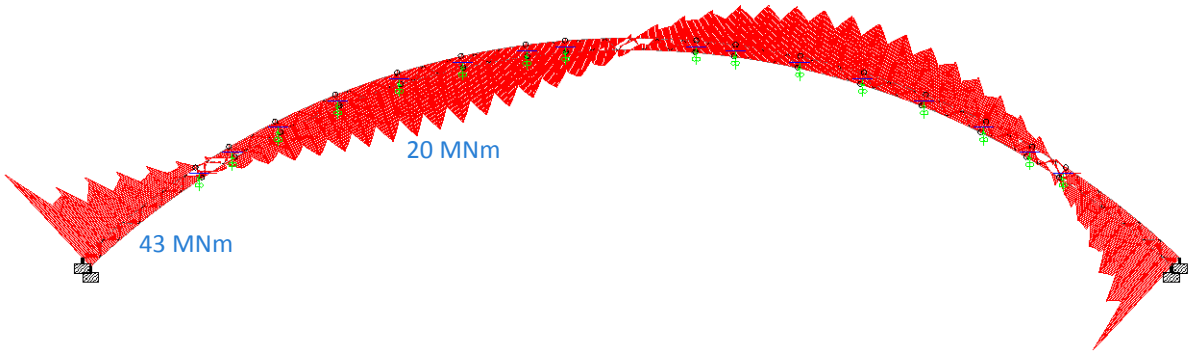

Figure 5-18: M_z from asymmetric current

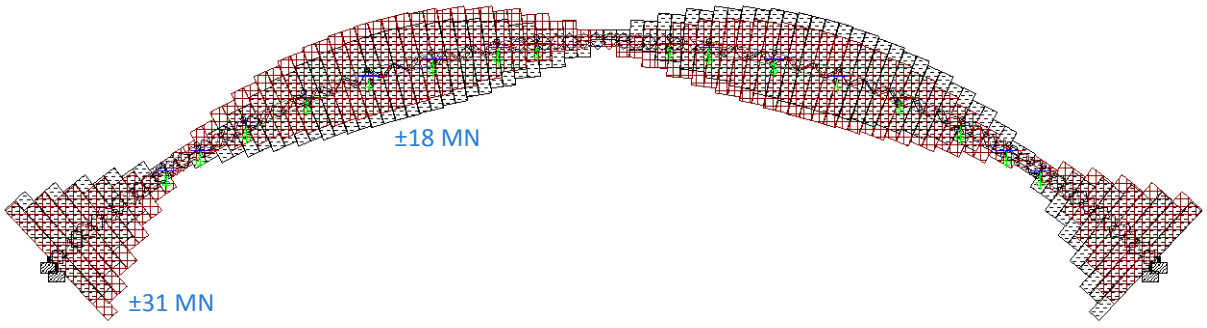

Figure 5-19: N_x from asymmetric current

5.3.6 Wave loads

The preferred method for the dynamic response analysis from wave loading have been a modal analysis performed for an Euler- Bernoulli bending beam in frequency domain Ref. (14) . The dynamic loads are the linear, and the slowly varying second order, wave loads derived by the use of potential theory. The spatial variations of the wave loading due to wave direction and from the curvature of the structure are applied by the use of a spatial correlation function, as illustrated in Figure 5-20:

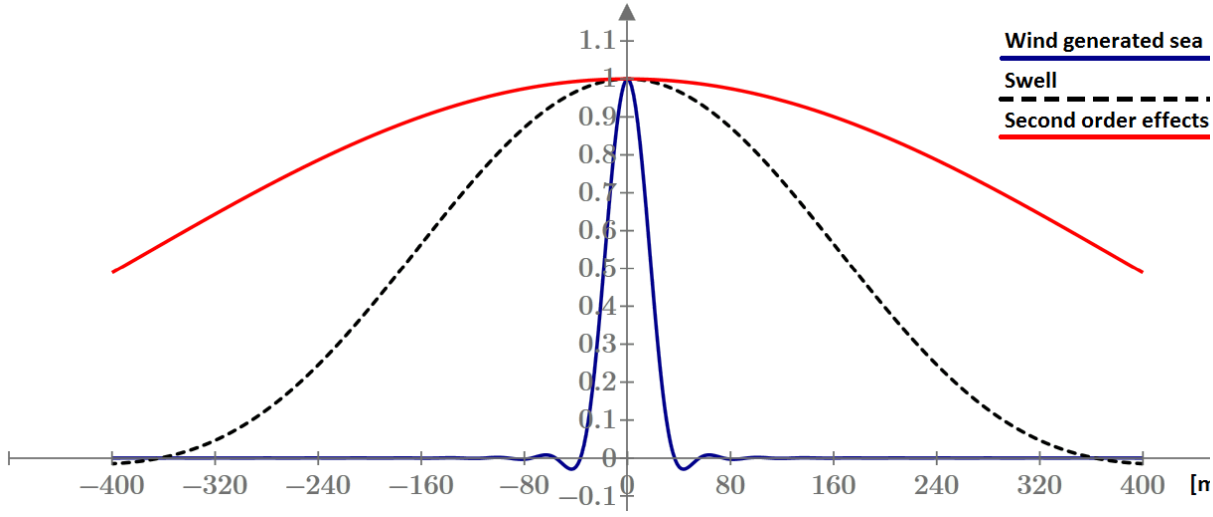

Figure 5-20 Correlation effect of different load types in space

Effects from the pontoons are assumed to be distributed along the entire span. Loads are extracted by a long wave approximation from the JONSWAP wave spectra, with on-site specific data for Wind Sea and swells. Maximum response values for each mode are extracted by statistical calculations from the response spectra. Due to variation in occurrence in time for the maximal amplitudes of difference modes a square sum method is conservative for summing the modal contributions.

The results from the analysis are presented in Figure 5-21 and Figure 5-22, where the response in meters is related to the area under the curves. As can be seen from the curves in the figures the response in roll motion is completely absent. Based on the response frequencies, on can also see that the motion is mainly response dependent. Sway response from wind generated sea are highly dominated by second order loads. The second order load effects can clearly be seen by the two peaks in sway response from wind generated waves.

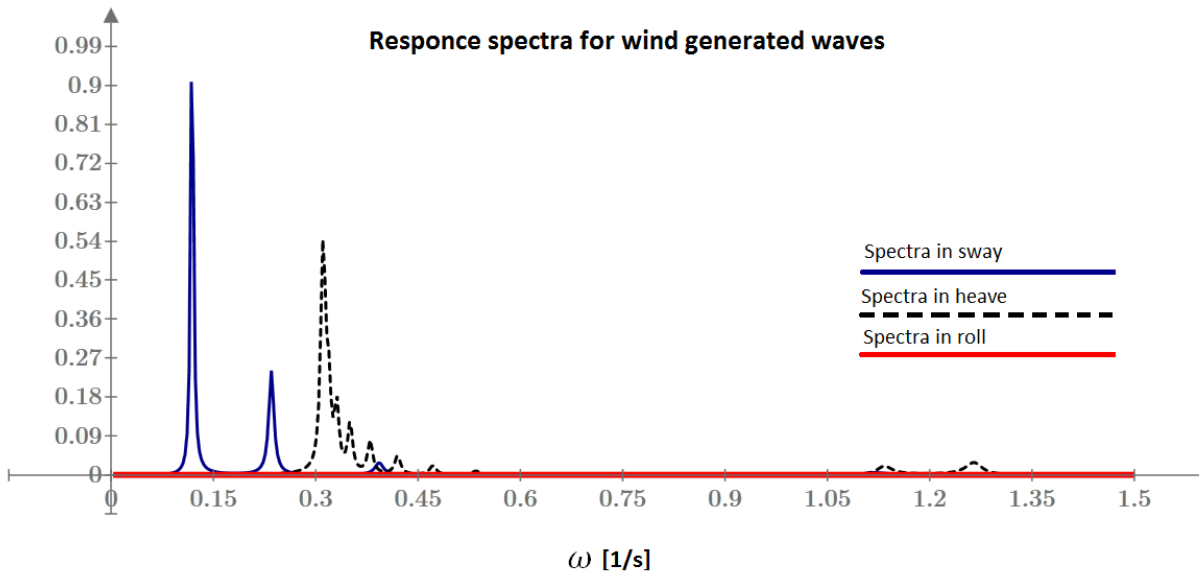

Figure 5-21: Response spectra for wind generated waves against angular frequency

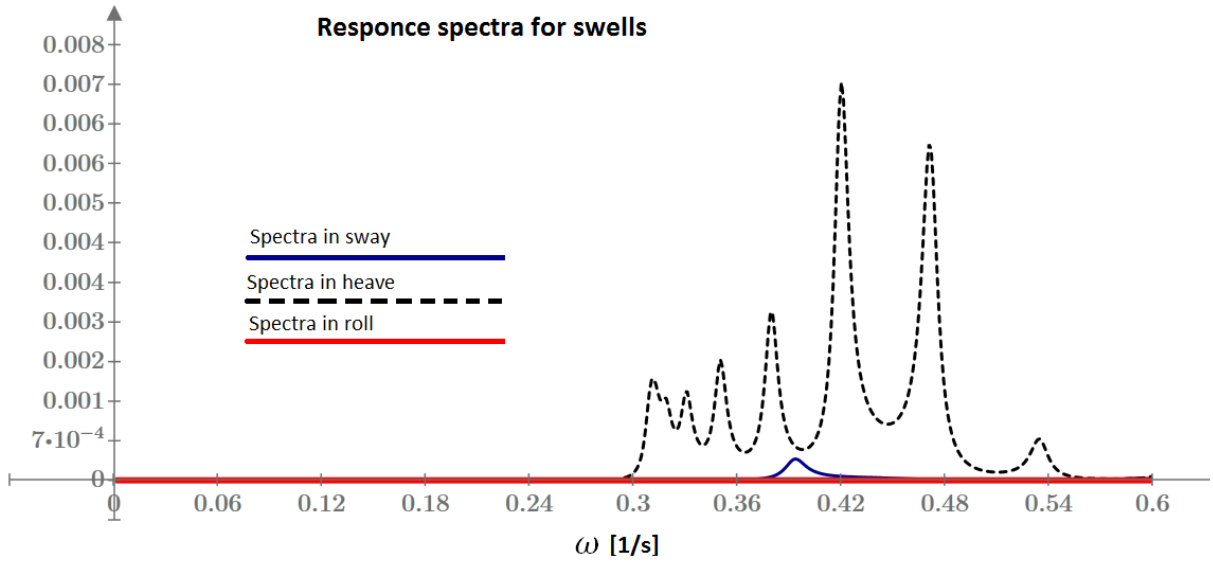

Figure 5-22: Response spectra for swell against angular frequency

By statistical means, extreme values for the response may be extracted from the spectrums in Figure 5-21 and Figure 5-22. Modal response amplitudes are retrieved in the following way:

$$\eta_{k,max}(n) = \sqrt{2 \cdot m_0(n) \log\left(\frac{t}{T_2(n)}\right)} \qquad (15)$$

Where t is the time duration of the storm which is set to three hours Ref. (8), and T_2 expressed as:

$$T_2(n) = 2\pi\sqrt{m_0(n)/m_2(n)}$$
$$m_c(n) = \int_0^\infty \omega^c \cdot S_{\eta_k}(n,\omega)d\omega \quad (16)$$

From the deflection amplitude the cross sectional forces may be calculated for each mode:

$$M_k(n) = EI_k\left(\frac{n\cdot\pi}{L}\right)^2 \cdot \eta_{k,\max}(n) \quad (17)$$

Due to a variation in time occurrence one can summarize the modal contributions using the square sum method:

$$\eta_{k,total} = \sqrt{\sum_{n=1}^{N} \eta_{k,\max}(n)^2}$$
$$M_{k,total} = \sqrt{\sum_{n=1}^{N} M_k(n)^2} \quad (18)$$

The responses from wave loading are given in Table 5-3:

Table 5-3: Response from wave analysis, 100-year return period

Response from wave analysis				
		Horizontal	**Vertical**	**Roll**
Max amplitude	Wind Sea [m], [rad]	0.321	0.277	0.039
	Swell [m], [rad]	0.008	0.426	0.036
Moment in span	Wind Sea [GNm]	1.254	0.416	0.032
	Swell [GNm]	0.708	0.529	0.015
Moment at support	Wind Sea [GNm]	2.290	0.758	0.057
	Swell [GNm]	1.292	0.965	0.028

5.3.7 Ship impact

Ship impact is applied as an impulse load with duration 0.6 s and maximum force 47 MN, see Figure 5-23.

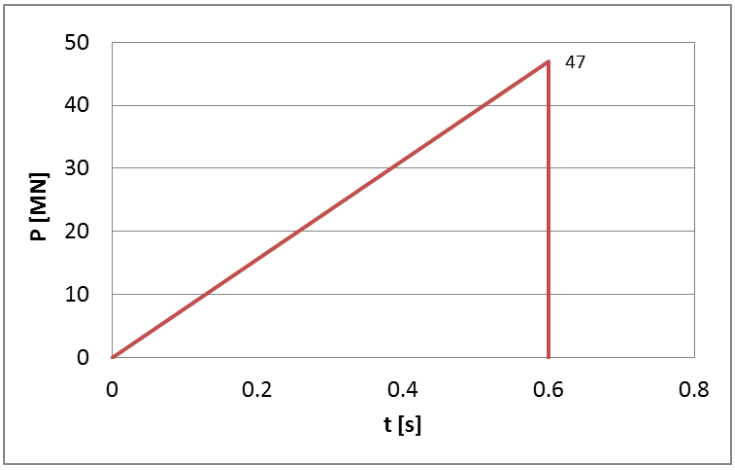

Figure 5-23: Impulse load ship impact

F shows the horizontal deflection of the tube at the pontoon as a function of time. Due to the large inertial forces, ship impact mainly give local effects.

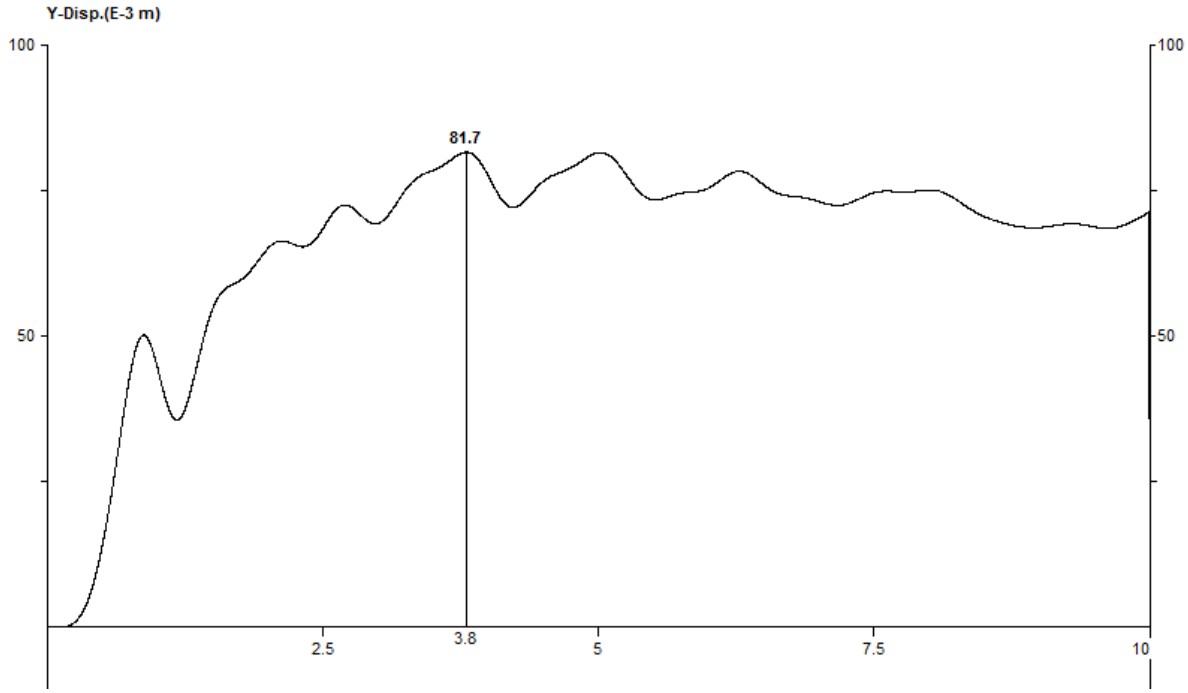

Figure 5-24:Displacement in the tube as a function of time

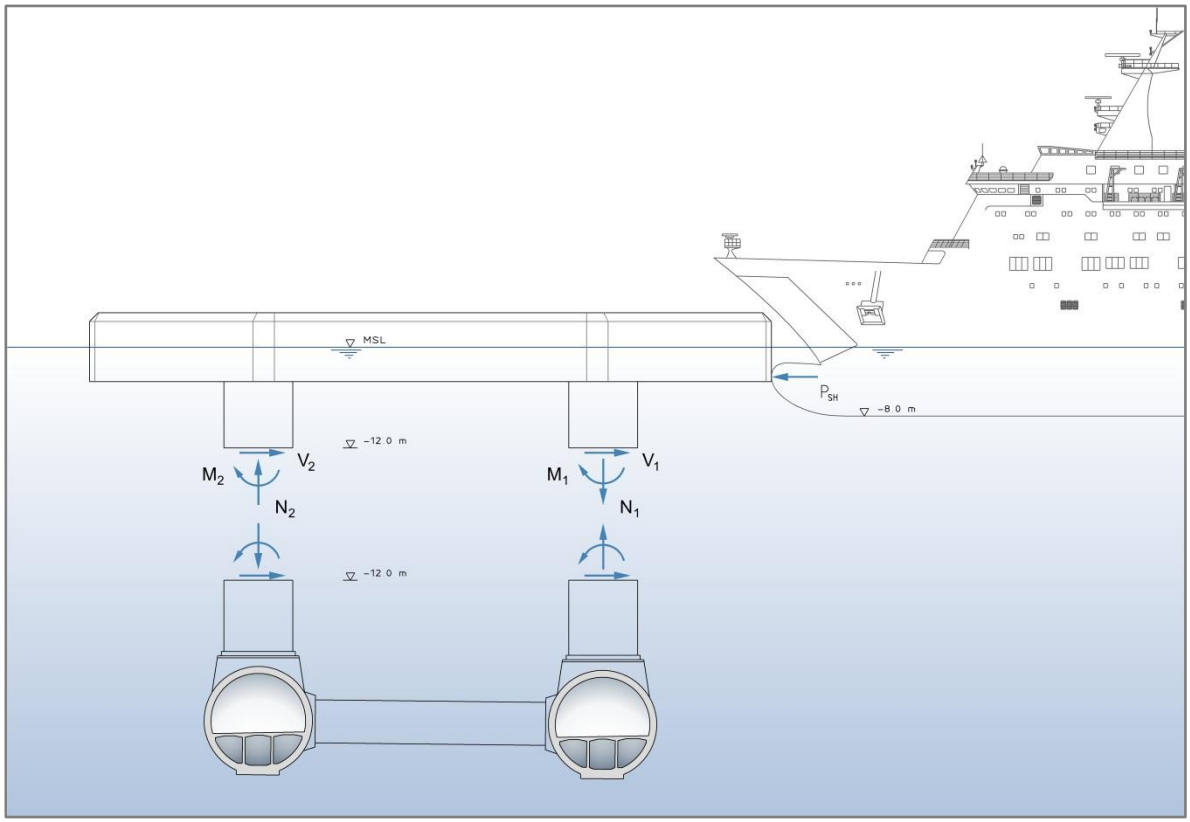

Figure 5-25: Section forces ship impact

When evaluating the results from the ship impact in STAAD and adding axial forces from wave loading the following sectional forces is chosen for dimensioning of the shafts with the ship impact mechanism:

Table 5-4: Dimensioning load case ship impact mechanism

Nx	±40	MN
Vy	30	MN
Mz	500	MNm

5.3.8 Post-tensioning

Effective prestressing force

6-31 tendons with a cross-sectional area of 4650 mm^2 have been chosen for design of the SFT. This yields an effective prestressing force per tendon of:

$$P_T = 0.9 \cdot 0.8 \cdot f_{p0.1k} \cdot A = 0.9 \cdot 0.8 \cdot 1640 \frac{N}{mm^2} \cdot 4650\ mm^2 = 5490\ kN$$

Prestressing distribution

To verify that the prestressing force remains in the tubes and does not wander into the bracings, an element of 266 m is modeled. This is approximately the length that will be casted and prestressed in dock. A prestressing force of 100000 kN is applied in the model:

Prestressing force:

$$P_x = 100000 \cdot \cos 2.844° = 99877\ kN$$

$$P_y = 100000 \cdot \sin 2.844° = 4962\ kN$$

Deflection force:

$$p_{inner} = \frac{P}{r_{inner}} = \frac{100000\ kN}{2662\ m} = 37.57\frac{kN}{m}$$

$$p_{outer} = \frac{P}{r_{outer}} = \frac{100000\ kN}{2702\ m} = 37.01\frac{kN}{m}$$

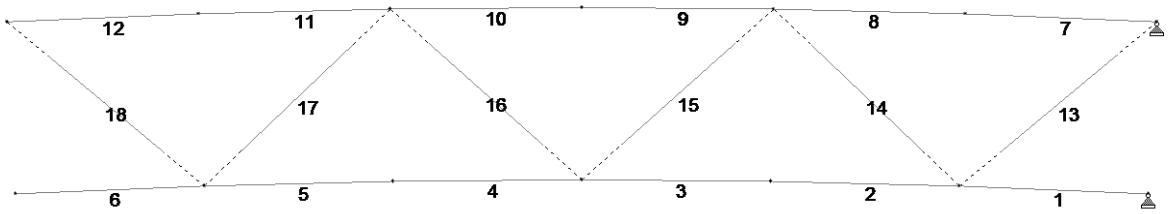

Figure 5-26: SFT element with beam numbering

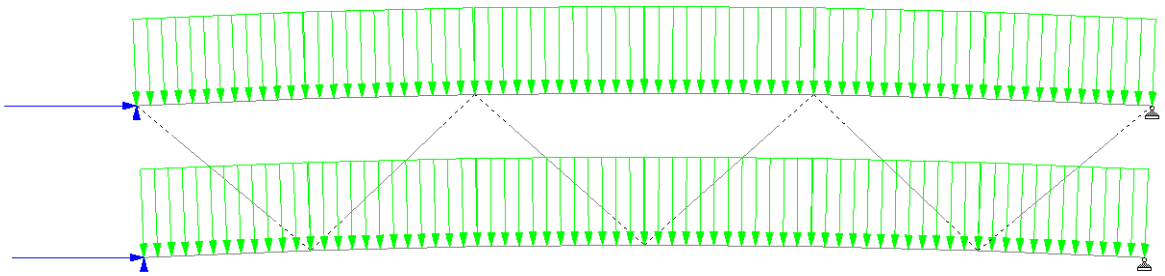

Figure 5-27: Prestressing load case

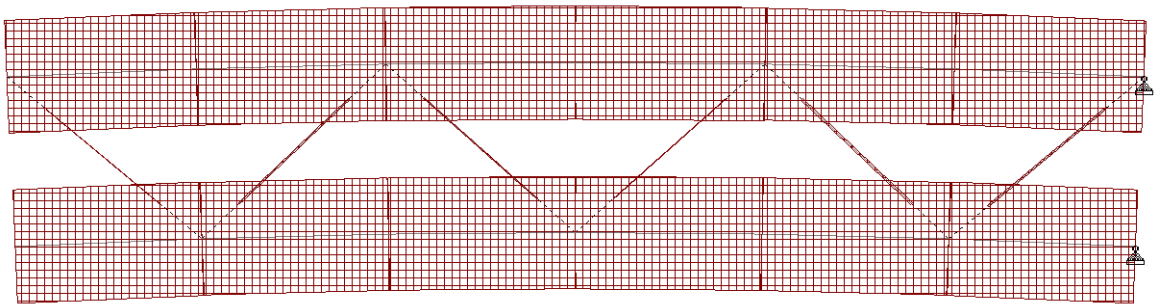

Figure 5-28: Axial force, N_x

As Table 5-5 shows, almost the entire prestressing force remains in the tubes, and an increase in prestressing tendons to compensate for this effect is omitted in the feasibility study.

Table 5-5: Effective axial force from prestressing

Beam	Fx [kN]
1	99 988
2	99 180
3	99 187
4	98 962
5	98 961
6	99 997
7	98 395
8	98 400
9	99 719
10	99 718
11	99 264
12	99 259

5.3.9 Displacement and acceleration

Acceleration

Accelerations on the SFT are fairly modest with values much lower than the values given in the euro code (15). For a storm with a 50 year return period, wave loads gives a maximum acceleration in the horizontal direction $a_{horizontal} = 0.091 m/s^2$, and $a_{vertical} = 0.20 m/s^2$ in the vertical direction. The maximal acceleration from vortex induced vibrations are $a_{VIV} = 0.007 m/s^2$.

Maximum vertical displacement

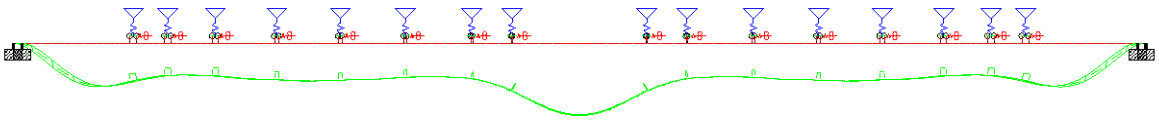

Figure 5-29: Z-displacement max self-weight

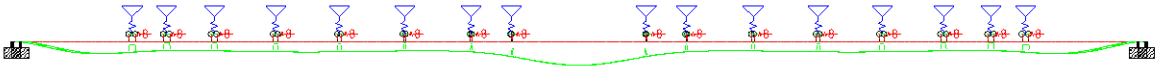

Figure 5-30: Z-displacement traffic

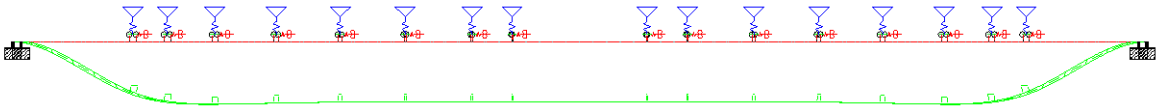

Figure 5-31: Z-displacement low tide

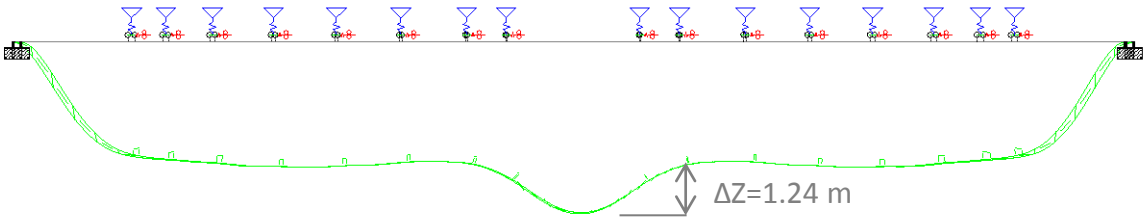

Figure 5-32: Total Z-displacement quasi-static loads, SLS

The maximum displacement from wave loads is 0.51 m and together with 1.24 m maximum relative displacement as Figure 5-32 shows, the relative displacement is 1.75 m for a span of approximately 740 m. This equals L/423, which is an acceptable level.

Horizontal displacement

The horizontal displacement is minimal compared to the bridge length and not investigated further.

5.3.10 Buckling analysis

To investigate the submerged floating tunnel's disposition for buckling a horizontal uniform distributed load of 1 kN/m (same magnitude as uniform current) was applied to both tubes. For this load, the analysis gives a buckling factor of 416, which means a load of 416 kN/m is necessary for buckling to occur. The corresponding axial pressure in each tube is:

$$N_x = p \cdot r = 416 \frac{kN}{m} \cdot 2682\ m = 1.1\ GN$$

In the dialogue phase, approximately the same buckling factor was calculated. In addition, the SFT was found not to be sensitive towards geometrical imperfections. The SFT is not vulnerable to buckling, and no further buckling analyses are performed.

5.4 Wave analysis for transportation

5.4.1 Analysis description

A 250 meter section of the tunnel has been analysed to find an approximation of the maximum loading in the diagonal braces during transportation. The section is assumed straight for simplicity. The centre of gravity for the entire cross section is assumed to be 5.3 meters above the keel of the tunnels. Temporary braces have been added to end of the 250 meter section to ensure stiffness during the transportation. The properties of the temporary braces are equal to the diagonal braces between the tunnel sections. The still water level is assumed to be 11.3 meters above the keel of the tunnels.

The wave analysis is performed utilizing Morison theory (frequency analysis) and the structure is modelled with beam elements. The Morison model drag forces are calculated with a linearization velocity of 1.8 m/s. A significant wave height, H_s, of 3 meters is assumed for the transportation phase and a design wave approach is used. Wave periods in the range from 2 to 20 seconds are checked. The characteristic maximum design wave height is calculated as follows:

$$H_{max} = 2.12\ H_s$$

A steepness criterion is included to avoid unphysically high waves for short wave periods. The wave height is limited by the following for wave periods less than 7 seconds:

$$H = 0.22T^2$$

where T is in seconds and H is in meter.

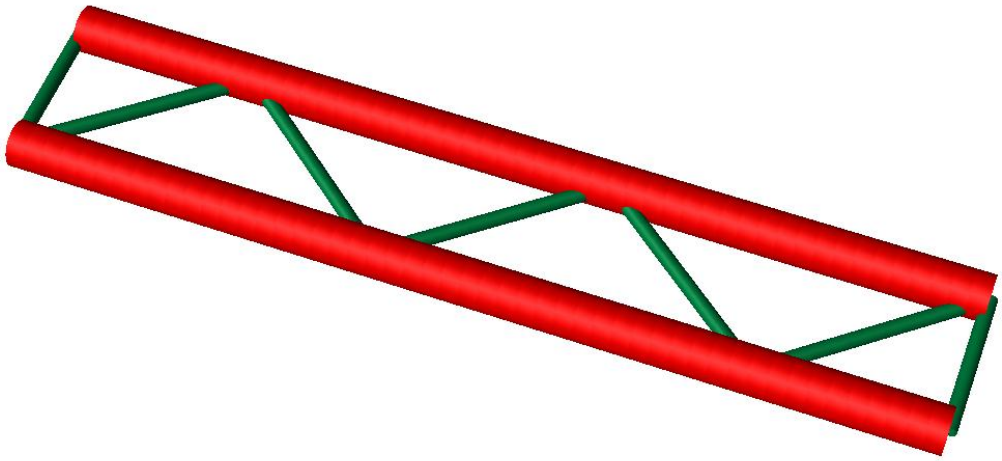

Figure 5-33: Analysis model

The structure is modelled using Genie (DNV Software) and the wave analyses are performed with HydroD/Wadam (DNV Software). The response in the braces is calculated with finite element program Sestra (DNV Software).

5.4.2 Results

The diagonal braces will be critical during the transportation phase. The estimated design moments for the diagonal braces are given in Table 5-6. The x-axis is along the beam, the y-axis is in the horizontal plane and the z-axis is in the vertical direction. The temporary braces have not been studied in detail as they could be increased in the final design.

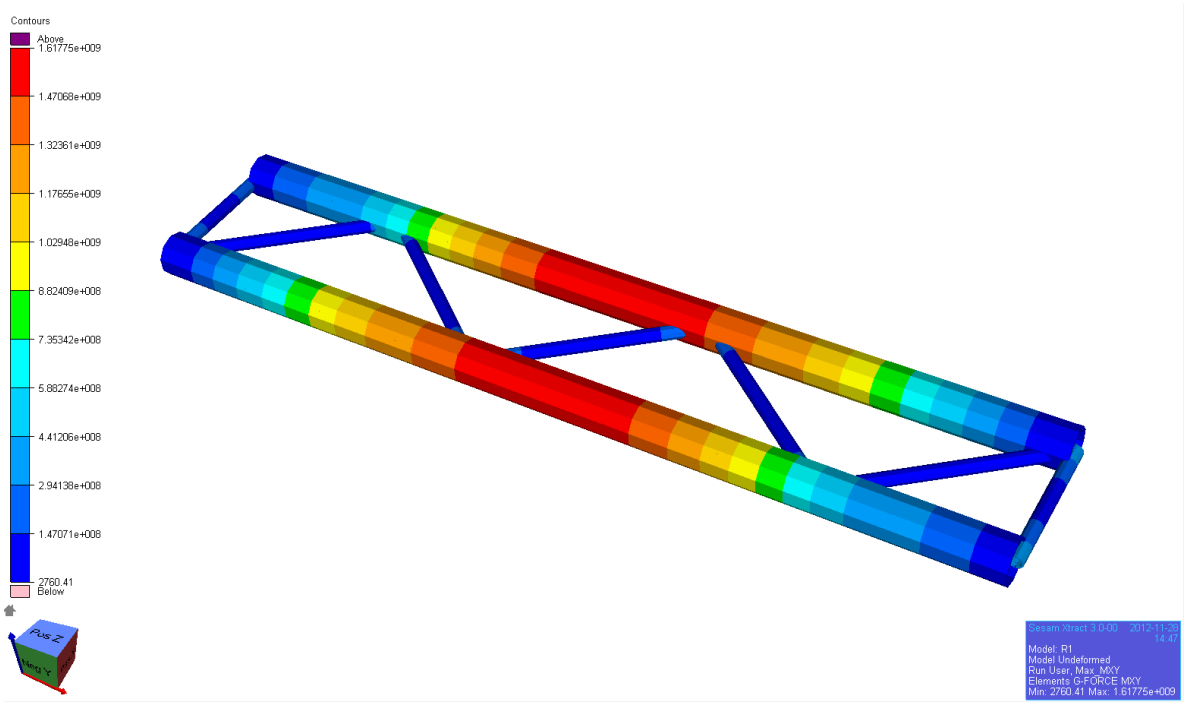

Figure 5-34: Contour plot, beam moment M

Table 5-6: Maximum beam moments for permanent diagonal braces

M_x	15	MNm
M_y	174	MNm
M_z	33	MNm

5.5 Structural design

5.5.1 General

Codes and regulations

DNV offshore standards have been used for design combinations, and these standards are in compliance with international ISO standards. The reason for choosing DNV offshore standards is to have a consistent set of standards from loads through response and to capacity.

Capacity controls have been performed with the program BD, which is a part of SVV's Miks program package. The controls are performed in accordance with the rules given in NS3473, ref. (16).

Table 5-7: Material properties

Concrete grade	B55
f_{cn} [MPa]	39.8
Reinforcement class	B500NC
f_{yk} [MPa]	500
Prestressing steel type	Y1860S7
$f_{p0.1k}$ / f_{pk} [MPa]	1640 / 1860

Detailed description of design parameters can be found in the Design Basis, ref. (17).

Utilization of prestressing tendons

To avoid plastic deformation of the prestressing tendons, and thereby a permanent weakening, a stricter requirement than the standard allows for has been introduced. A more accurate representation of the stress-strain response of a prestressing strand can be obtained using the modified Ramberg-Osgood function as shown in Figure 5-35. By comparison with the idealized stress-strain diagram from Eurocode 2, an earlier onset of plastic deformations can be found using Ramberg-Osgood. To be within the elastic area, a maximum strain requirement of 7.5 ‰ is introduced for the ultimate limit state. For the serviceability limit state applies the stress limitation of 0.8 $f_{p0.1k}$ based on characteristic loads. This corresponds to a strain of 6.7 ‰.

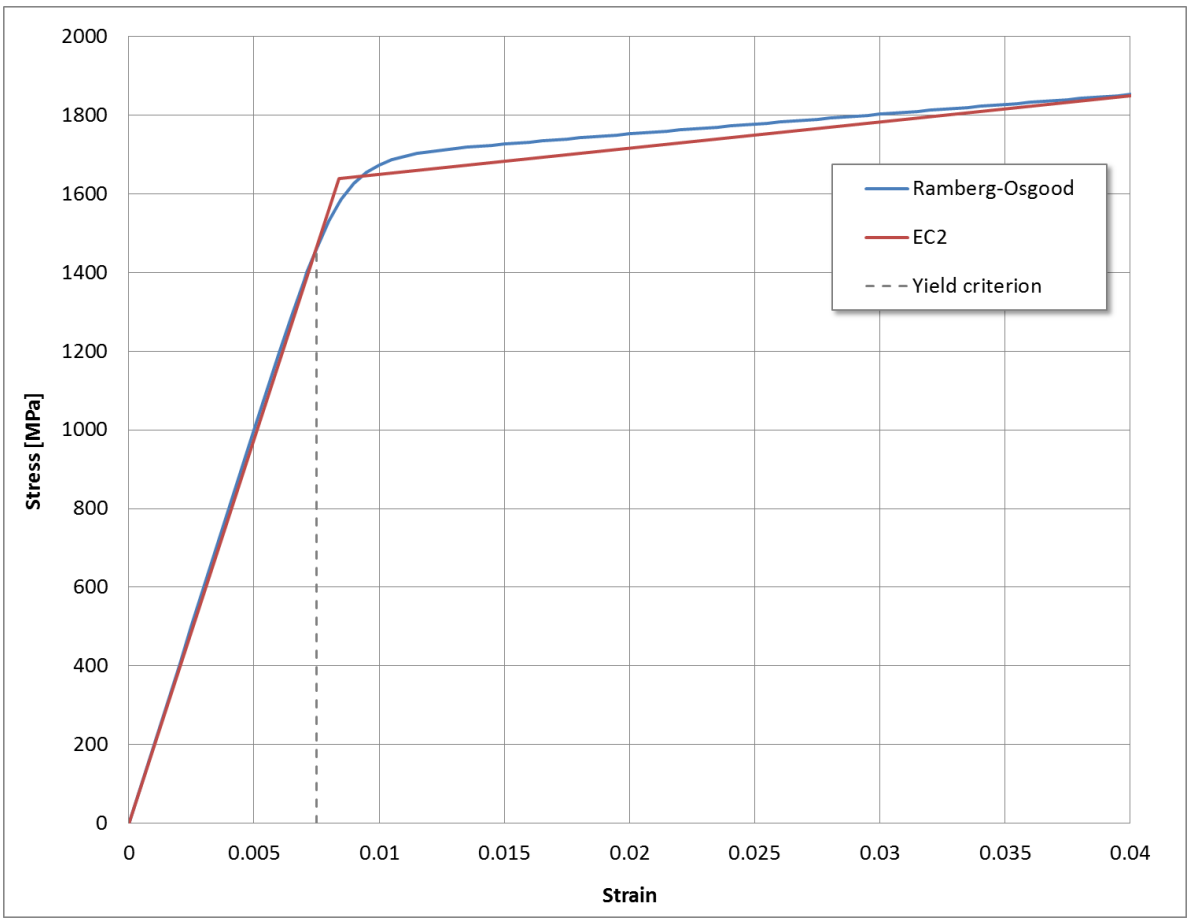

Figure 5-35: Work diagram prestressing tendons

Crack width requirement

To make certain that there is no leakage in the tubes in the serviceability limit state, the stringent requirement of an uncracked section is introduced. To investigate leakage possibilities in ULS, crack widths have also been calculated for this limit state.

5.5.2 Design combinations

In order to keep the load combinations at a manageable level, a few governing load combinations have been chosen for a capacity check.

Table 5-8: Load combinations

Load type	ULS-weight	ULS-wave	ULS-viv*	ULS-ship	SLS
Selfweight	1.3	1.0	1.0	1.0	1.0
Traffic	1.3	1.0	1.0	1.0	1.0
Environmental	0.7	1.3	1.3	0.7	1.0
Ship impact	0	0	0	1.3	0.0
Temperature	1.0	1.0	1.0	1.0	1.0
Prestressing**	0.9	0.9	0.9	0.9	1.0

* VIV is caused by current, and combined with 10 year return period for wave loads according to table F1 in DNV-OS-C101, sec.3, ref. (18).

** DNV-OS-C502, table D1, ref. (19).

Due to symmetry in several load cases, only one load combination load is chosen for each case. The loads included in design combinations are:

- Max. self-weight
- Traffic (with the joint load placed in the middle of the navigation channel)
- Asymmetric current
- Wave loads from wind sea and swell
- Loads from VIV
- Impulse load from ship impact
- Increase in temperature

5.5.3 Tube

The general cross-section is checked with the following reinforcement quantities:

Longitudinal reinforcement, both sides	2ø32c200
Hoop reinforcement, both sides	1ø25c200
Longitudinal post-tensioning tendons	52 tendons 6-31
Hoop post-tensioning tendons	1 tendon 6-19 c870

Table 5-9 to Table 5-13 shows the results from the capacity controls in BD. The strain in the post-tensioning is acceptable for all load cases and the cross-section is uncracked in SLS.

Table 5-9: Capacity control load case ULS-weight

ULS-weight						
Load [kN], [kNm]	Nx	Vy	Vz	Mx	My	Mz
	-226939	-40	876	11317	-1194204	3181
Strain	1000eps0	1000kapy	1000kapz		ε_{min} [‰]	ε_{max} [‰]
	-0.153	-0.129	0		*-0.9657*	*0.6597*
Utilization	1000eps	1000eps-u	U-eps	sig	sig-u	U-sig
Concrete	-0.918	-3.171	0.289	-19482	-28429	0.685
Reinforcement	0.611	10	0.061	97822	400000	0.245
Prestressing	7.098	18.52	0.383	1107260	1312000	0.844
Crack width	dir-w	1000eps	srk	crw		
	-1.093	0.456	0.915	0.000296		

Table 5-10: Capacity control load case ULS-wave

ULS-wave						
Load [kN], [kNm]	Nx	Vy	Vz	Mx	My	Mz
	-204036	-98	1346	8435	-1175112	2393
Strain	1000eps0	1000kapy	1000kapz		ε_{min} [‰]	ε_{max} [‰]
	-0.087	-0.137	0		*-0.9501*	*0.7761*
Utilization	1000eps	1000eps-u	U-eps	sig	sig-u	U-sig
Concrete	-0.894	-3.171	0.282	-19073	-28429	0.671
Reinforcement	0.72	10	0.072	115178	400000	0.288
Prestressing	7.206	18.52	0.389	1124178	1312000	0.857
Crack width	dir-w	1000eps	srk	crw		
	-0.734	0.544	0.92	0.000367		

Table 5-11: Capacity control load case ULS-viv

ULS-viv						
Load [kN], [kNm]	Nx	Vy	Vz	Mx	My	Mz
	-178485	-98	1056	8435	-1086715	2393
Strain	1000eps0	1000kapy	1000kapz		ε_{min} [‰]	ε_{max} [‰]
	-0.044	-0.132	0		*-0.8756*	*0.7876*
Utilization	1000eps	1000eps-u	U-eps	sig	sig-u	U-sig
Concrete	-0.821	-3.171	0.259	-17690	-28429	0.622
Reinforcement	0.733	10	0.073	117295	400000	0.293
Prestressing	7.22	18.52	0.39	1126245	1312000	0.858
Crack width	dir-w	1000eps	srk	crw		
	-0.734	0.556	0.92	0.000373		

Table 5-12: Capacity control load case ULS-ship

ULS-ship						
Load [kN], [kNm]	Nx	Vy	Vz	Mx	My	Mz
	-167827	13808	-8773	334270	-829851	-499301
Strain	1000eps0	1000kapy	1000kapz		ε_{min} [‰]	ε_{max} [‰]
	0.071	-0.129	-0.067		*-0.8448*	*0.9868*
Utilization	1000eps	1000eps-u	U-eps	sig	sig-u	U-sig
Concrete	-0.792	-3.171	0.25	-17079	-28429	0.601
Reinforcement	0.928	10	0.093	148441	400000	0.371
Prestressing	7.415	18.52	0.4	1156714	1312000	0.882
Crack width	dir-w	1000eps	srk	crw		
	-35.608	1.151	0.682	0.000565		

Table 5-13: Capacity control load case SLS

SLS						
Load [kN], [kNm]	Nx	Vy	Vz	Mx	My	Mz
	-256130	-69	858	8545	-1006073	2788
Strain	1000eps0	1000kapy	1000kapz		ε_{min} [‰]	ε_{max} [‰]
	-0.208	-0.06	0		*-0.586*	*0.17*
Utilization	1000eps	1000eps-u	U-eps	sig	sig-u	U-sig
Concrete	-0.563	-1.259	0.447	-17785	-39800	0.447
Reinforcement	0.146	2.5	0.059	29286	500000	0.059
Prestressing	6.633	6.816	0.973	1293474	1329184	0.973
Crack width	dir-w	1000eps	srk	crw	crw-l	U-crw
The cross-section is uncracked for this load case						

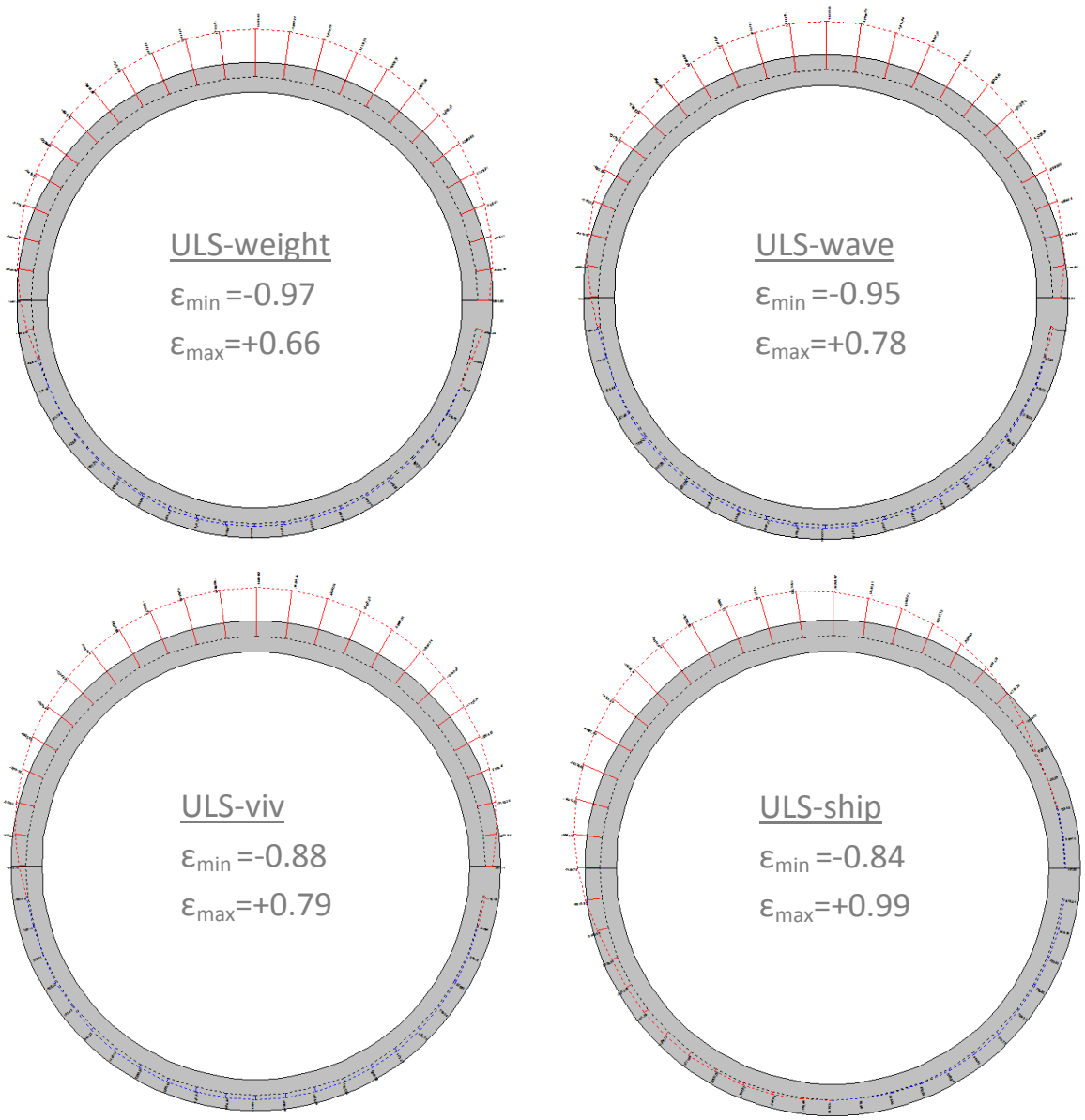

Figure 5-36: Axial force distribution, ULS load cases (Red=compression, blue=tension)

5.5.4 Bracing

Bracing utilization is governed by ship impact. Preliminary design for the bill of quantities suggests reinforcement amounts of 1.5ø32c200 on both sides with wall thickness 0.5 m. More detailed dimensioning shall be performed in a future phase when accurate wave loading for the relevant towing route is known.

5.5.5 Pontoon

Dimensioning the pontoons shall be performed in a future project phase, but they shall be compartmentalized with bulkheads. As a rough estimate for the bill of quantities, a steel weight of 3000 metric tons can be assumed.

Sliding fender

A sliding fender is suggested in the feasibility study, see Figure 5-37. The reason for adding such a fender is to protect the medium size vessels, if The Norwegian Coastal Administration wishes to do so. The friction between the fender and the pontoon can be designed to a desired collision resistance.

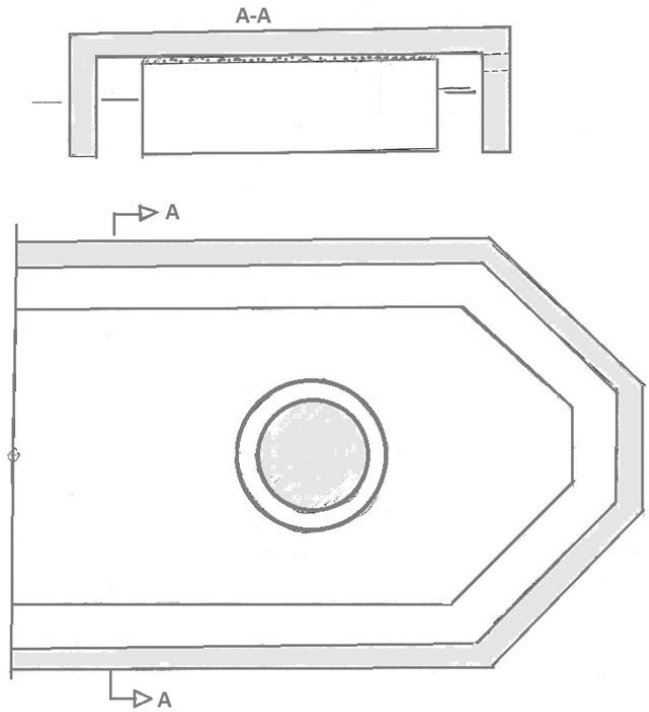

Figure 5-37: Sliding fender

5.5.6 Shaft with ship impact mechanism

Ship impact mechanism

To design an accurate ship impact mechanism, a shear failure mode has been selected. The shafts are subjected to a large variation in axial loading. To separate the effects of axial force and bending moment from the shear forces, a shear plinth is located in the middle of the shaft. The plinth only carries shear forces, and the axial tension and bending moments are carried by prestressing strands in the shaft walls. When large shear forces are imposed on the shaft due to a ship collision, a shear failure will occur in the plinth. Then the deformation that follows will yield tension in the prestressing strands and they will be clipped off against the shaft plate or fail in tension before that. Figure 5-38 show the ship impact mechanism.

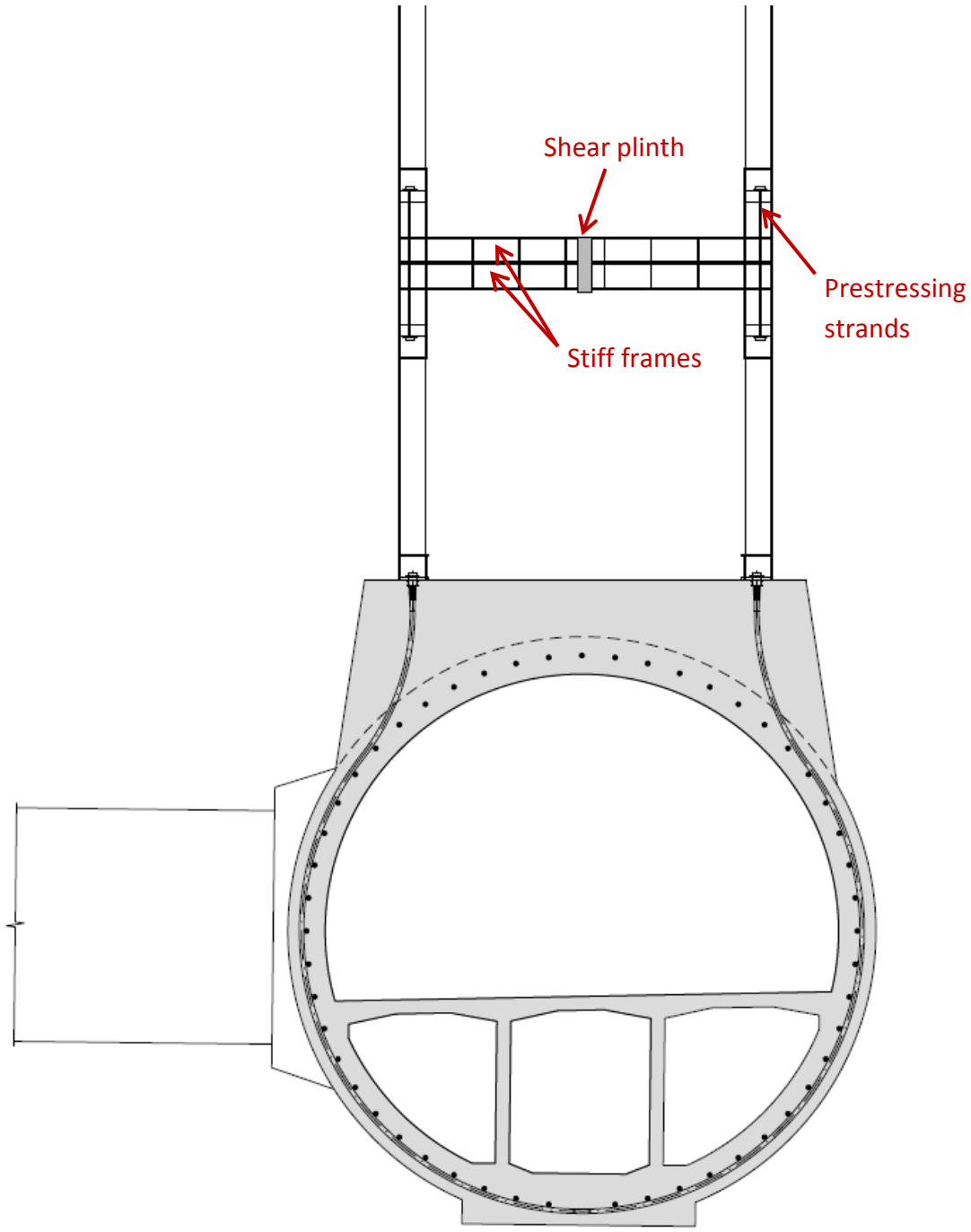

Figure 5-38: Ship impact mechanism

Shaft dimensions

Estimate of the shaft steel quantities:

$$f_{sd} = \frac{N}{A} + \frac{M}{w} = \frac{N}{2 \cdot \pi \cdot r \cdot t} + \frac{M}{\pi \cdot r^2 \cdot t}$$

$$t_{min} = \frac{1}{f_{sd} \cdot \pi} \cdot \left(\frac{N}{2 \cdot r} + \frac{M}{r^2} \right) = \frac{1}{322.7 \cdot \pi} \cdot \left(\frac{30 \cdot 10^6}{2 \cdot 4000} + \frac{500 \cdot 10^9}{4000^2} \right) = 35\ mm$$

A cross-sectional area of the shafts that is equivalent to a circular section with diameter 8000 mm and thickness 40 mm is chosen for calculation of the steel quantities.

Table 5-14: Shaft weights

Shaft weights [tonnes]	
Shaft (ø=8m, t=0.04m, L=20m)	158
Secondary stiffeners (10% of shaft weight)	16
Stiffening frames ship impact mechanism	100
Base ring beam	25
Top ring beam	25
Top deck	10
Total	334

5.5.7 Bill of quantities

A provisional bill of quantities is presented Table 5-15 comprising a material take off of main structural parts as determined by the principle structural design. The bill of quantities considers permanent structural items in-place only. Auxiliary structural elements such as temporary tunnel end caps, temporary shafts et cetera are not reflected. Note that the quantities are based on conservative load assumptions, and may be considered as a high estimate.

Table 5-15: Bill of quantities – main concrete items.

Structural item	Concrete volume [m^3]	Reinforcement [tonnes]	Post-tensioning [tonnes]
Submerged concrete tunnel	**349 144**	**78 470**	**20 961**
Traffic tubes (main hull)	284 436	59 876	20 731
Bulkhead walls	1 890	284	
Bracings	22 800	7 433	
Escape tunnels	5 880	1 411	229
Brace joints	15 742	4 723	
Shaft bases	12 908	4 195	
Element joints	5 488	549	
Landfall elements	**49 668**	**11 129**	**3 364**
Traffic tubes (main hull)	44 848	9 642	3 364
Bulkhead walls	192	29	
Bracings	2 050	668	
Brace joints	588	176	
Shaft bases	1 840	598	
Element joints	150	15	
Sum main concrete items	**398 812**	**89 598**	**24 324**

Table 5-16: Bill of quantities – main steel items.

Main steel [tonnes]	
32 permanent shafts	10 688
28 temporary shafts	2 800
16 pontoons	48 000
Sum main steel	**61 488**

6 Construction and installation

6.1 Construction

6.1.1 General

The SFT has a total length of 4083m, and will be composed by sections with varying length of about 250 to 300m. These sections will be constructed in a dry dock.

Two of these sections will become the landfall and will be fabricated, transported wet and installed first. The remaining elements will then be fabricated and towed wet to the assemble site in vicinity of the installation site, where they will be jointed together and assembled in to one continuous structure before secured and mounted to the pre-installed landfall elements.

The pontoons will be fabricated at dedicated shipyard and brought to site by heavy lift transportation vessel or be towed wet from shipyard (depending of distance between installation area and shipyard). The pontoons will be installed after the tunnel has been positioned and secured at the installation site.

6.1.2 Dry dock

The construction of the elements will be performed in a dry dock. The existing Hanøytangen Dock located at Sotra will be used as a base case for this study. This site has previously been used for construction of offshore structures and the site is therefore very well suited for this type of construction. Using the dock at Hanøytangen imposes a towing distance of some 80 Nm to the assembly site in Sognefjord. The majority of the towing route is inshore in protective waters which mostly consist of calm waters.

Another site that also might be considered to use, is the site for Lutelandet Offshore AS. This site is for the time being under development. Lutelandet is an industrial area that could be well suited for this type of construction. It has to be further developed with dry-dock and necessary facilities for concrete construction activities. The towing distance to the bridge site will in this case be 25 Nm.

The dock areas are shown in Figure 6-1 and Figure 6-2.

Figure 6-1: Hanøytangen dock area

Figure 6-2: Lutelandet dock area

Consideration should be made to which two construction sited may be of an advantage. This will reduce construction time, and may result a more competitive process which can also reduce production cost. However, for the purpose of this feasibility study the Hanøytangen site has been chosen.

Design requirements:

- Length 300m
- Breadth 130 m
- Depth 12 m

Dock gate to be opened and reinstalled within 1 week.

The dock Hanøytangen can after some modifications be tailored to meet this requirement by new western dock rock-wall and new dock-gate

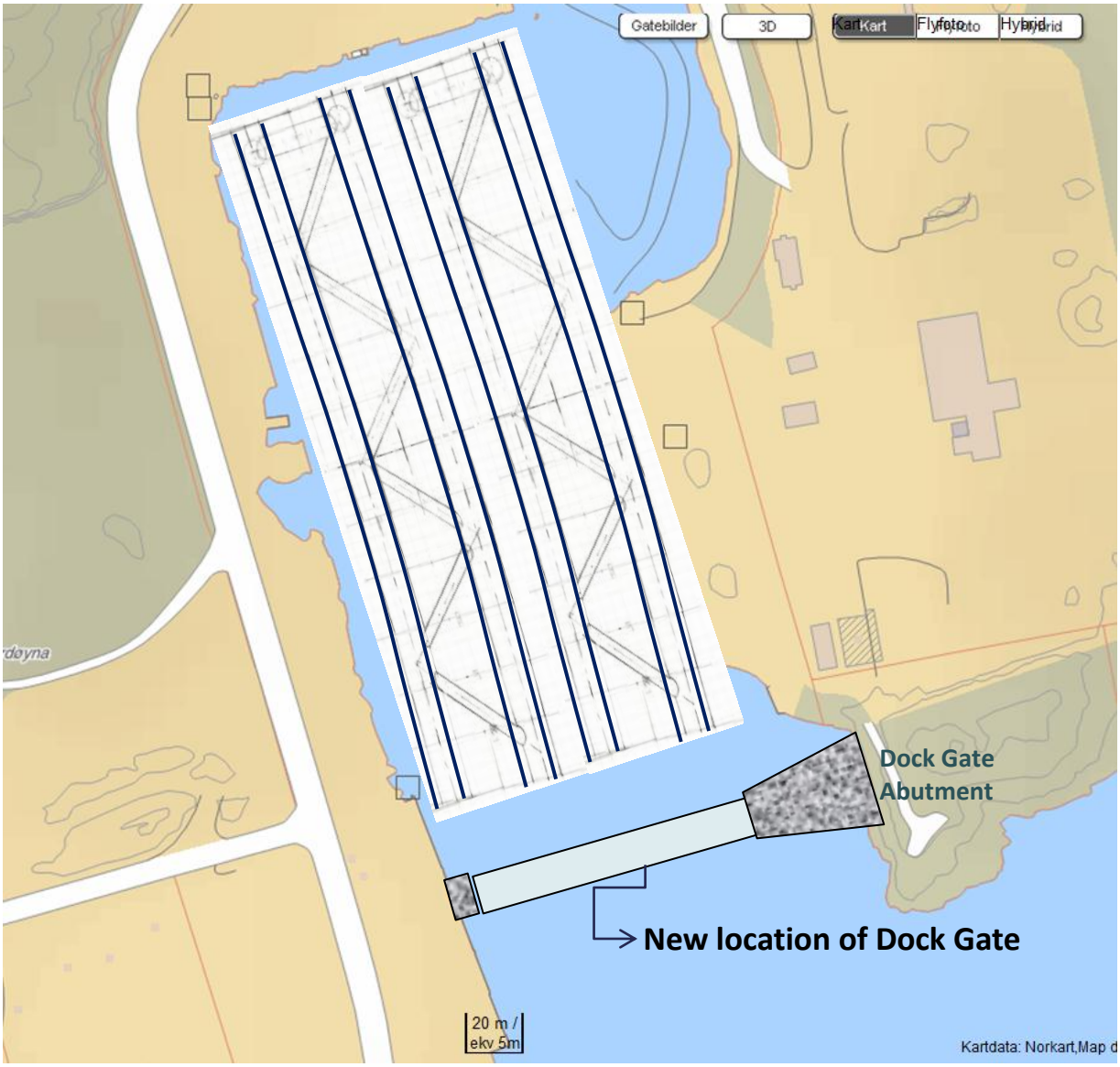

Figure 6-3: SFT elements in expanded Hanøytangen dock

The site shall have sufficient area to accommodate:

- Materials storages
- Bathing plants

- Prefabrication plants
- Warehouses
- Offices

The existing site has been used earlier for similar projects and can be upgraded to the requirements.

6.1.3 Construction of elements

Two sections will be constructed simultaneously by the use of well-known equipment and method. The sections will be fabricated with varying length of about 250 to 300m. The breadth of each section is some 55 m.

One element consists of:

- Two tubes with cross-bracings
- Two permanent shafts
- Two temporary shafts
- Total length 250 to 300 m
- Breadth 55 m

The construction will be performed by in situ poured concrete, using formwork placed on rails and in sections length of about 30m. The base of the cross section will be casted before the remaining part, hence there will be two longitudinal joints at the base, and one cross sectional joint every 30m. Prestressing in the longitudinal direction will be performed successively with an average cable length approximately 100m. This procedure is a common method for constructing of submerged tunnel sections.

6.1.4 Tow out of dock

The completed tunnel elements will be moored in the dry dock prior to flooding of the dock. When afloat the tunnel sections will be pulled by winches towards fenders and moored along quay sides of the dock to get access of tractor tugs at the stern of the tunnel sections.

4 tractor tugs of about 50 TBP will be employed for tow of tunnel sections out of dock. One tug attached to the stern and one tug attached to the bow to control orientation and movement's perpendicular to the tunnel sections. Two tugs will be connected with towing lines to the bow of the tunnel sections for motive power pulling the sections out of dock. The same tractor tugs will further be employed for towage of tunnel sections to assembly site and for berthing and positioning of tunnel sections towards previous tunnel sections for the assemble of sections. Figure 6-4 show the tug configuration.

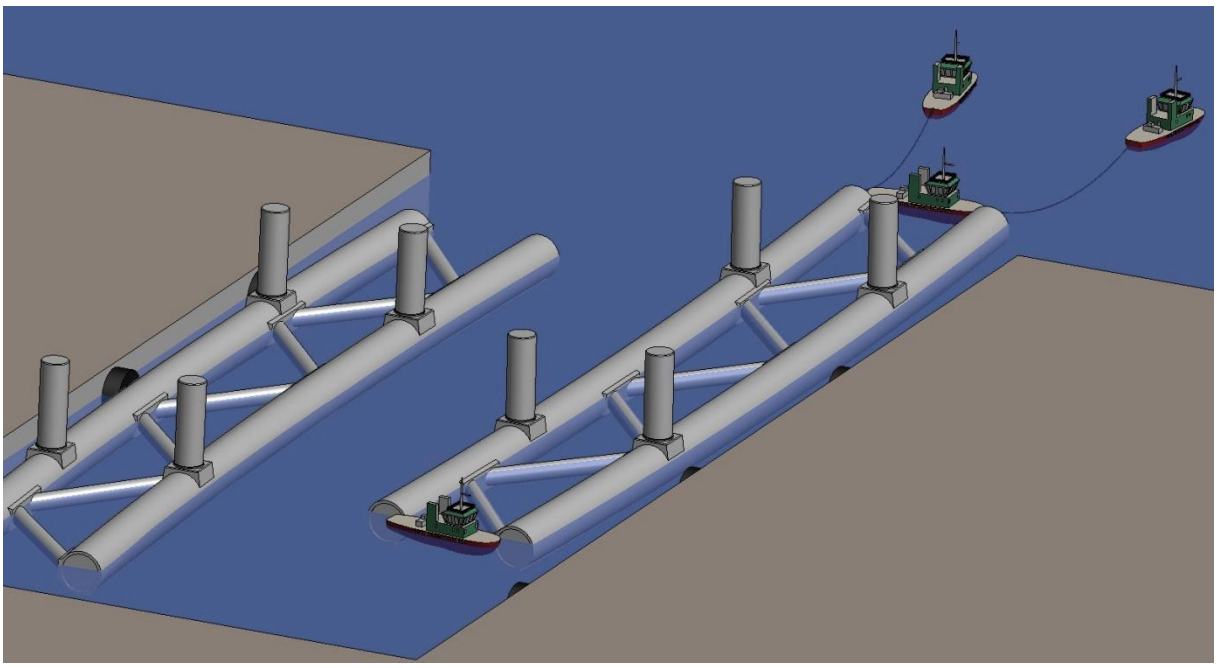

Figure 6-4: Tug configuration out of dock

6.1.5 Weight, stability and submerging tests

The weight and geometry will be thoroughly monitored trough the construction phase. In addition to a final weight and stability control is performed trough tests performed on the finished element when anchored in the flooded dock. In the stability test, amongst others, main values of the Vertical Center of Gravity (VCG), and Vertical Center of Buoyancy (VCB) and total weight will be established.

The weight consists of:

- Concrete
- Equipment
- Steel shafts
- Solid ballast
- Water ballast

The main parameter in the control is the weight of the concrete, being some 80% of the total. Contributions from the equipment and the steel shafts are small compared to the total, and also easy to estimate accurately. The solid ballast will be chosen to give robustness to the structure for unforeseen weight changes. Water ballast capabilities will be as such to take in to account the need for eccentric ballast in temporary phases. The level of water ballast may be measured very accurately, and will therefore not affect the accuracy level of the weight distribution.

Submerging test

Outside the dry dock a submerging test will be performed. The structure will be submerged to a draft some 50 % larger than the operating draft at the bridge site. The purpose of this test is to verify the tightness and detect any leakage in the structure.

Key data for a 300 m long tunnel section:

Draft	12,6 m
Displacement	85 000 tons
GM-value	0,8 m
Draft	37,6 m
Displacement	90 000 tons
GM-value	1,8 m

6.2 Tow to assembly site

The elements will be towed from the construction site in Hanøytangen to an assembly site in vicinity to the installation site at Sognefjorden.
The towing draft will be about 10 m leaving a freeboard of about 2,5 m. The tow will go mostly in sheltered areas but will also have areas exposed to open sea. The route have sheltered areas for haltering the tow in case of bad weather
The tunnel section will be towed using a fleet of one lead tug of about 150 TBP and 4 assisting tugs of some 50 TBP each.
Towing distance is about 80 Nm and the towing speed is estimated in the range of 4 - 5 knots, i. e. less than a day towage.
The weather condition chosen for the tow is the same as the design condition in Sognefjorden for the wind sea case, hence wave height about 5 m.

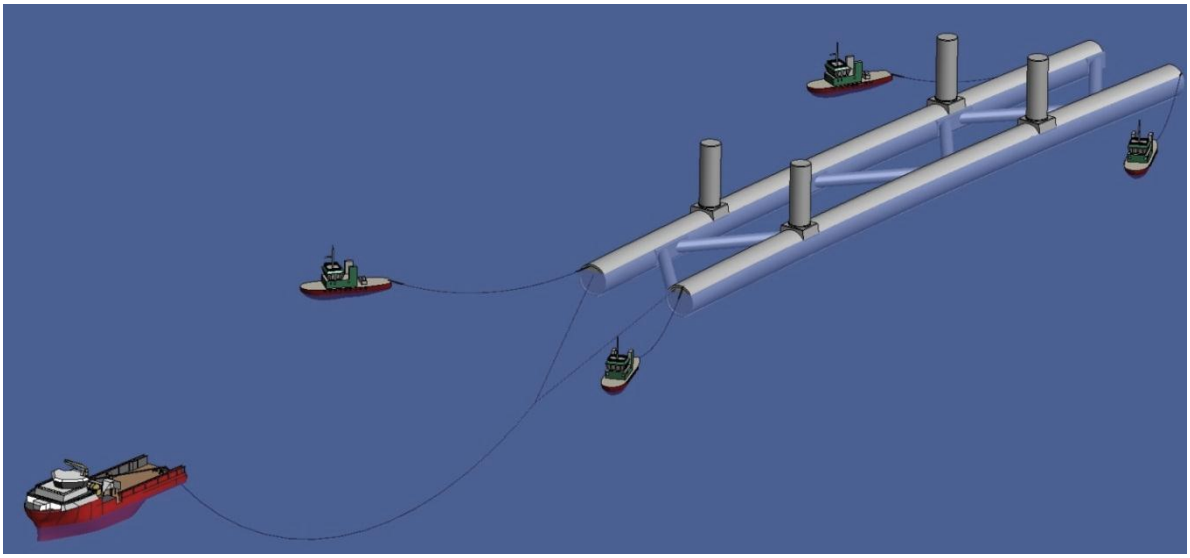

Figure 6-5: Tow to Sognefjorden

Similar towages have been made in the past with similar displacement, dimensions and towage configuration. 1 lead tug and 4 assisting tugs was employed when towage of

facility RNAD 210 for ministry of defense in UK. A concrete structure of 80 000 T displacement and 2 x 200 m pontoons with cross bracings.

Figure 6-6: Towage of RNAD facility 210

6.3 Temporary mooring at assembly site

The tunnel sections will be temporarily moored in Sognefjorden adjacent to the installation site. It is foreseen that the mooring site is on the southern side of the fjord. The sections being some 250 -300 m in length will be moored at each ends to preinstalled berthing facility. The berthing close to the shore will be towards fixed structures like jetties or dolphins, and for the berthing further from the shore this could be towards barges secured to shore by steel tubes in an A- frame configuration hinged to shore fixations. The moorings will allow for some flexibility using large fenders and mooring lines. Similar system has been used in the Coulport project with a permanent mooring by tubular steel bars some 70 m from shore.

Figure 6-7: Coulport mooring

The tunnel sections will be joined together when secured in the temporary mooring.

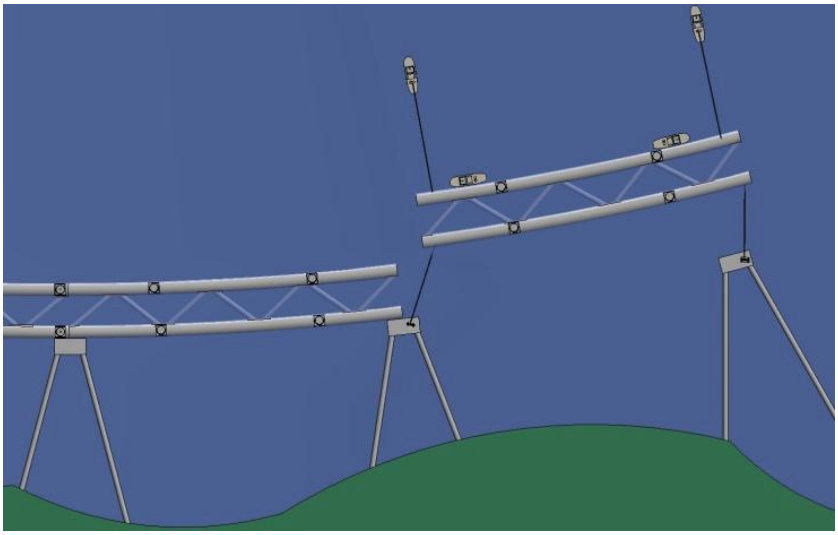

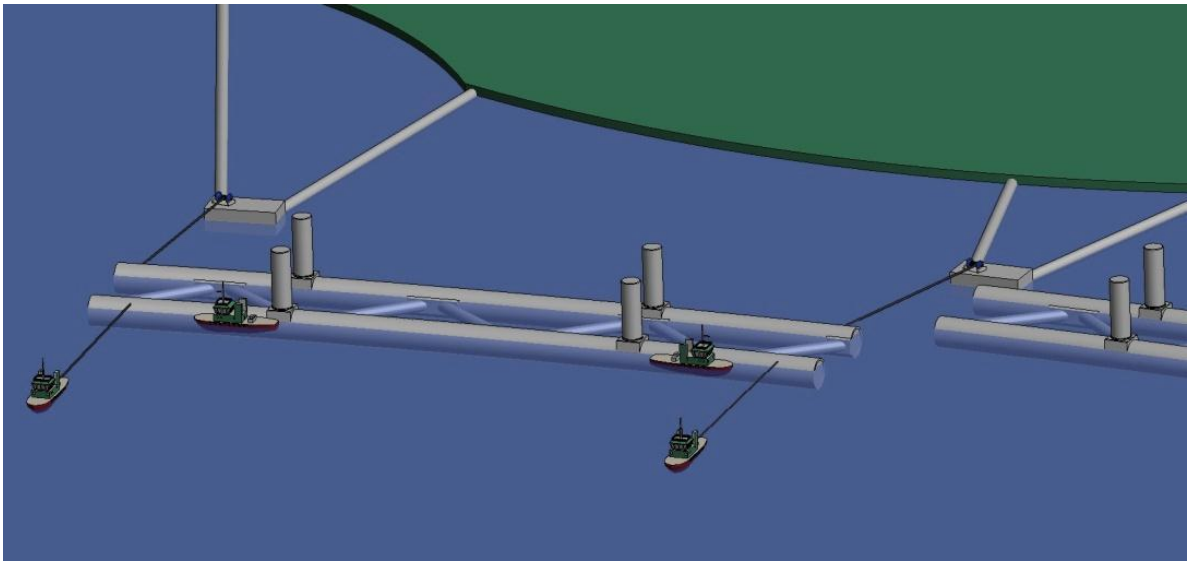

Figure 6-8: Mooring at assembly site

When 4-5 tunnel sections has been jointed to a continuously structure, here called a "string", the length is about 1300 m. Next string to be assembled outside previous assembled string until 3 rows of strings are completed and moored outside each other. Key data for one string, length of 1300 m:

Draft	12,6 m
Displacement	341 000 T
GM-value	1,0 m

The tunnel will be assembled to full length by shifting outer string and assemble to inner string until the tunnel sections is assembled to full length. The tug fleet consists of one lead tug of 200 TBP, one tail tug of 200 TBP and 4 tractor tugs of 50 TBP each. 2 winches on shore will assist pulling the string towards fenders on berthing facility.

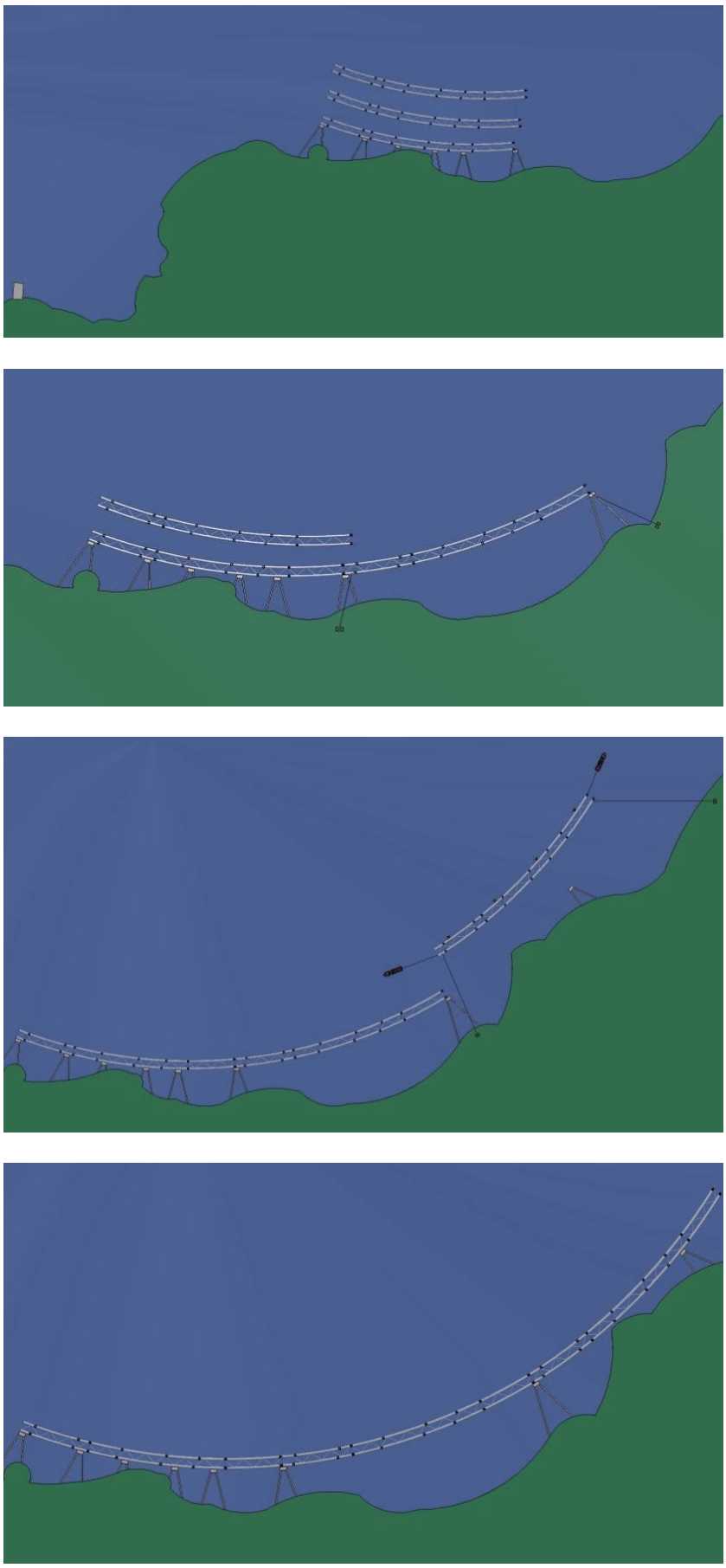

Figure 6-9: String assembly

The shifting and positioning of one string is comparable with towage and positioning of the Salhus floating bridge of 1246 m, but less weather sensitive since mainly stable current loads and not sensitive to wind load.

Figure 6-10: Towage of Salhus floating bridge in one single piece of 1 246 m

6.4 Jointing of tunnel sections

The jointing of the elements will be performed when the elements are moored to the jetties/barges.

The sequence of work is as follows:
Step 1:
Move the element towards the jointing point of the previously jointed element by the use of winches and assisted by smaller tugs. Contact to the shear keys will be achieved in this operation. In addition some smaller fenders provide will ease this operation.

Step 2:
Install temporary long anchor steel bolts on the outer tube wall on the area laying above the waterline in addition to install a contact point at the lower part of the tube. Install some water ballast at the opposite end of the element. This will give a stabilization moment of the joint. The long bolts will provide some flexibility in the first phase of the operation.

Step 3:
Install the short anchor bolts on the outer face of the tube-wall and install some jacks, at least 4, in the joint itself. The bolts shall keep the joint in locked position during the concreting of the joint. Use the jacks and tensioning of the bolts to adjust the alignment of the element. The first installed long bolts to be removed. This operation step 1 to step 3 is estimated to take about 1 day.

Step 4:
Install the cofferdam on the outside of the tube. The cofferdam consists of steel segments to be bolted and sealed to the outer face of the tube. De- watering of the space inside the cofferdam and inside the tube between the bulkheads to be performed.

Step 5:
Perform the concreting of the joint by first install formwork on the outside of the tube, then install reinforcement on the outer face, install cables in the ducts and install reinforcement on the inner-face of the tube-wall. The inner formwork shall then be installed in steps following the concreting of the joint. Access to the area shall be through a hatch in the upper level of the tube. This operation is estimated to take 2 weeks.

Step 6:
The joint will be tested by water pressure on the outside of the tube wall in the cofferdam compartment. The pressure will be 50 % higher than the operating water pressure at the site.

Environmental loadings through the operations

Load transverse the longitudinal direction:
The elements are moored to jetties/barges and the horizontal loads transvers to the element are then taken direct into the structures, similar as the mooring of large ships.

Load in the longitudinal direction.
In this phase load from swell is dominating. When the step 3 is finished the joint is designed for 1 year return period.

Jointing of strings
The strings, 3 nos each about 1300 m in length, are assembled together based on similar procedures as described above. The access to the join will be through the shafts.

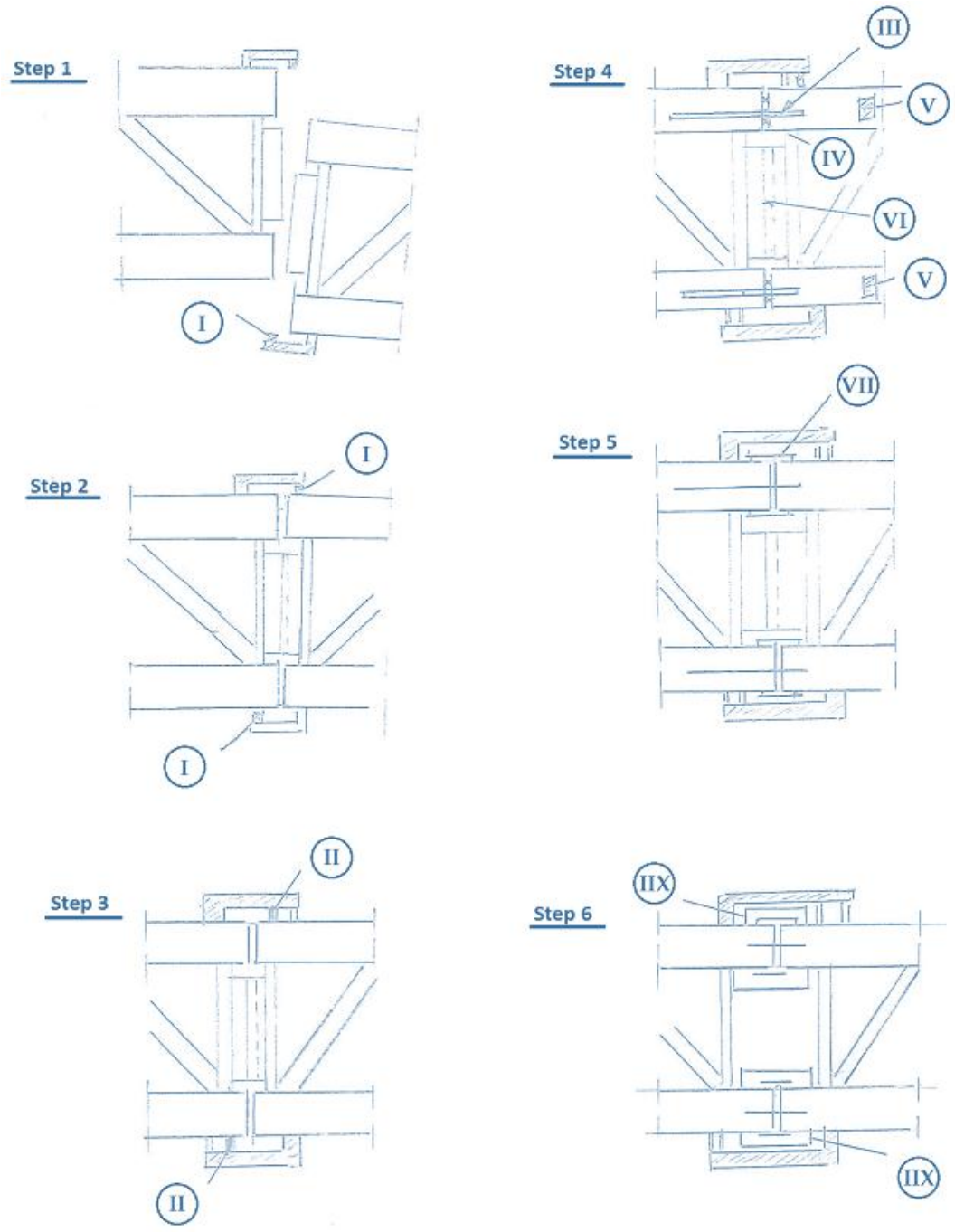

Sequences

Step 1	Approach speed; 0.1m/sek
Step 2	Docking speed; 0.05m/sek
Step 3	Install lateral support (I)
Step 4	Install upper bolts (III), activate jacks (IV), adjust ballast water (V) Horizontal shear key (VI)
Step 5	Install restoring bolts (VII)
Step 6	Install cofferdam (IIX)
Step 7	Drain cofferdam
Step 8	Concreting
Step 9	Testing
Step 10	Remove cofferdam

6.5 Landfalls

Separate landfall elements will be installed at each landfall prior to the final installation of the bridge. The landfall-element is approximately 250 m in length with 100 m inside a rock tunnel and the remaining 150 m into the fjord, as illustrated in Figure 6-11

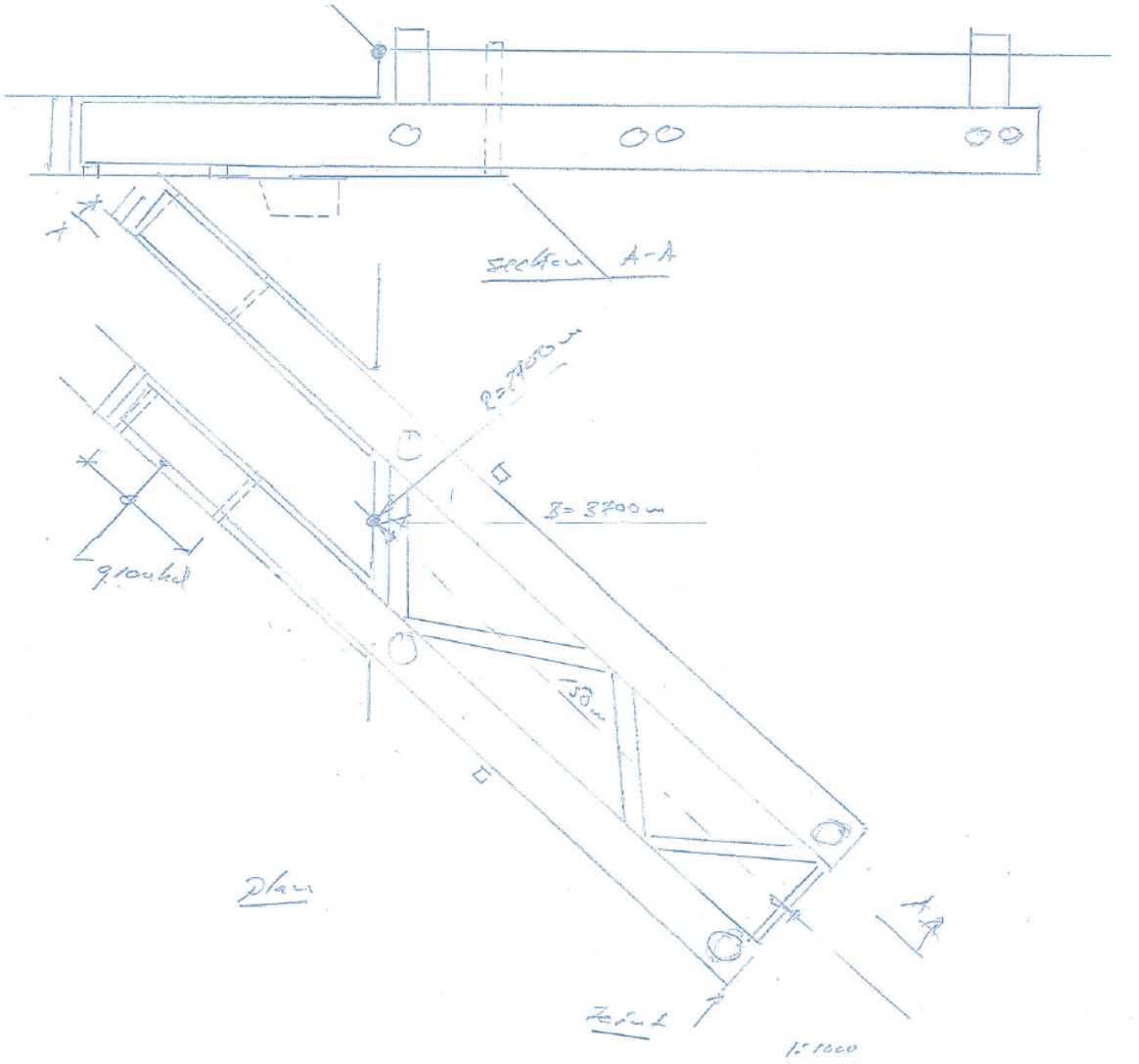

Figure 6-11: Visualization of landfall elements

The sequence of work is as follows:

- The outer face of the rock slope is blasted forming a vertical rock wall.
- The rock tunnels are driven from the landside down to a few meters, for example 5m, from the sea.
- A concrete blast wall is constructed some distance behind in the tunnels. Blasting of the last remaining rock wall at the outlet is performed. During this operation this outer part of the tunnels are water filled with a water head smaller than the outside water pressure. Blasted rock will then flow into the tunnels and be partly

trapped in a receiving excavated sump adjacent to the outlet. This operation is a common method used in the hydropower industry.

- The element is then towed to the site, submerged and moved into the tunnel. In this position the element is ballasted down to preinstalled support points and temporarily secured by activating a set of jacks placed in foundations in the tunnel. The element is now secured, the annulus between the element and the rock wall at the entrance is sealed off and the concreting work between the tunnel element and the rock wall can be performed. The blast concrete wall at the rear will then be removed providing access to the element.

- The global tensile load in the bridge is anchored some 100m behind the tunnel entrance. This is performed by concrete tensile members, anchored in a concrete block. In this way a huge rock block can be activated in anchoring the bridge. The concrete members are running horizontally at each side of the tunnel wall ending up with a shear block adjacent to the element. Similar shear blocks are incorporated on the tube. The global tensile load in one tube is about 240 MN.

- From the end of the tube elements the rock tunnel proceeds to the surface of the rock above water line. In order to make sure that no water will leak through the rock into the bridge the rock tunnel will be lined by concrete.

6.6 Installation of SFT

The tunnel will be installed as one unit. In this phase the tunnel consists of the arched tubes with bracings, the permanent shafts and temporary shafts. No pontoons are installed to the shafts in this operation.

Key data:

Length	3800 m
Displacement	1 100 000 tons
Draft	32 m
GM-value	Greater than 30 m
Shafts	Water-filled

The maximum current velocity measured by SINTEF during a 400 days period is 0,35 m/sec at 20 meter water depth and 0,77 m/sec at surface. This correspond to 6,5 MN (about 650 T) in drag force perpendicular to the tunnel.

A current velocity measurement system cross the fjord at 20 m water depth and at surface will be deployed prior to the towing operation.

A navigation system will be deployed showing map of the area and actual shape and position of the tunnel relative to the map. Motive power and direction from each individual tug will also be showed on the tow master screen.

A remote operated ballast system and a sounding system to measure ballast content to be installed in the temporary shaft at the ends of the tunnel in order to be able adjust for draft due to tidal variation when entering mating area between landfall elements and SFT.

The tow master and captains from the tug fleet will simulate maneuvering the tunnel in a simulator to learn how the tunnel behaves before starting the towing operation.

From the mooring/assembly site the tunnel will be submerged to a draft corresponding to the actual draft at the installation site.

The tunnel will be moved from the temporary mooring/assembly site to the installation site, a distance of about 3 -4 Nm. The towing will be performed by 6 main tugs of about 200 TBP each and 8 assisting tractor tugs of about 50 TBP each. The tractor tugs will be moored to the shaft of the tunnel and will almost act as thrusters to the tunnel. At the installation site additional holding and moving forces will be applied by a set of winches placed on land at both abutments.

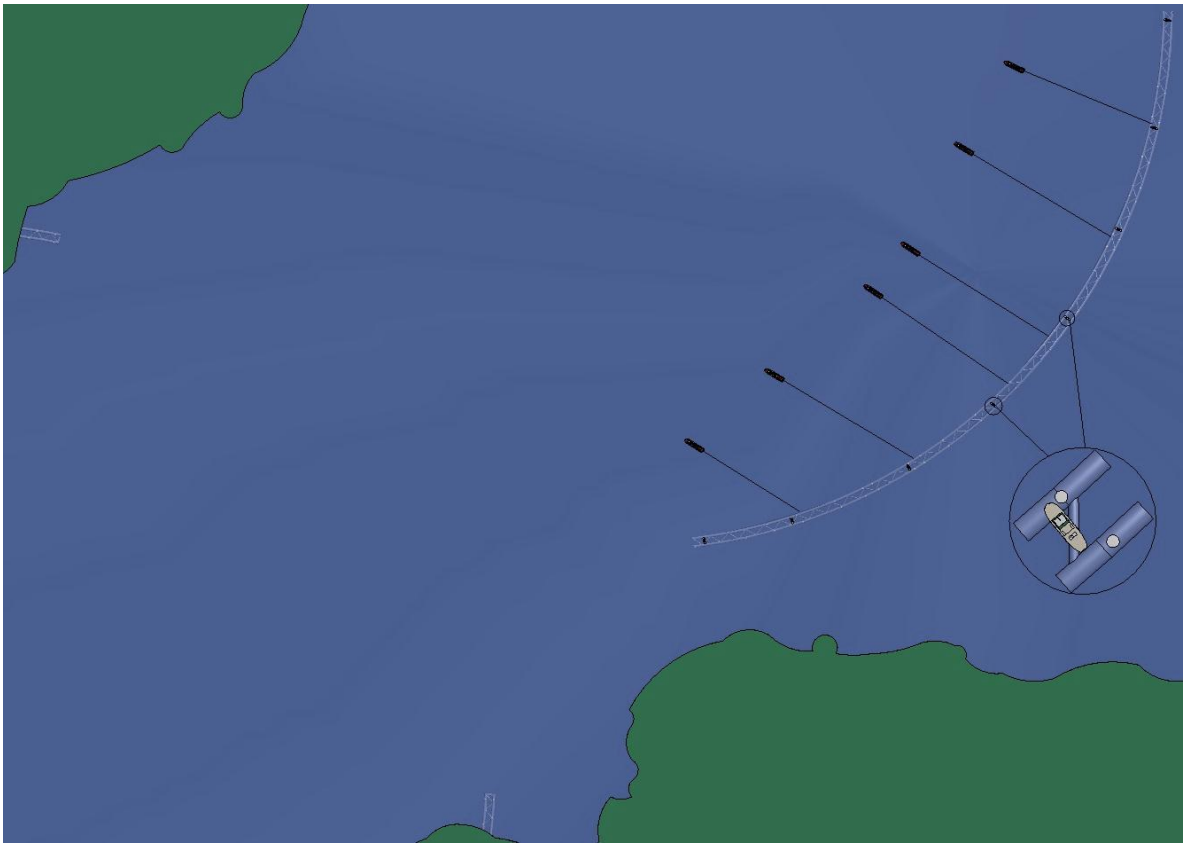

Figure 6-12: Tow configuration for installation

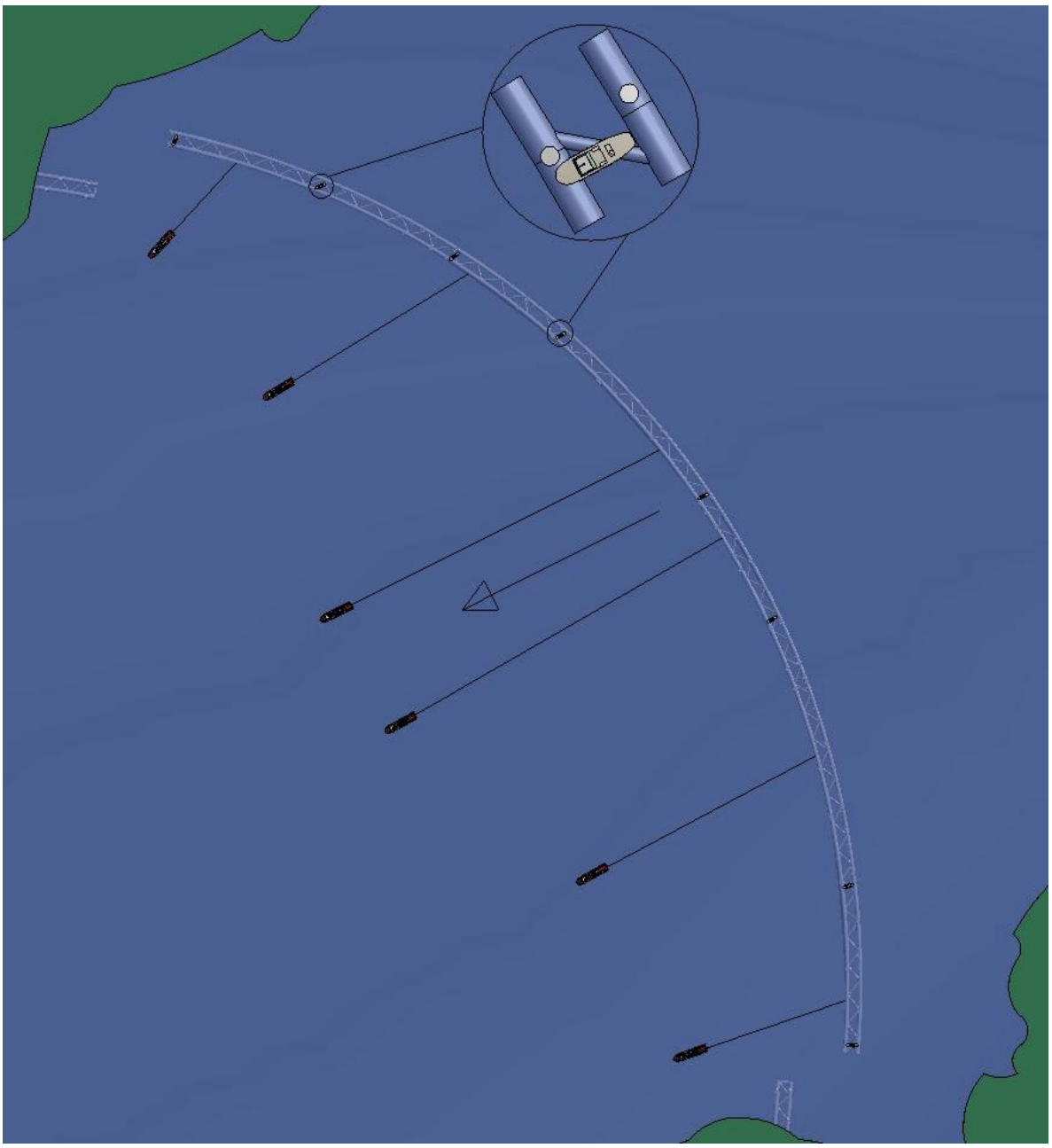

Figure 6-13: Tow configuration for installation

The tow master and his engineering team will continuously evaluate the current velocity cross the fjord and weather conditions and make the final decision how and when to proceed with the installation.

The form of the bridge has to be kept in theoretical correct within limits of +/- 2 m in the installation phase. In the installation operation any change in the tide are counteracted by water ballasting in the temporary shafts at the ends of the tunnel.

When it has been decided to proceed with the installation the sequences of work are as follows:

Step 1:

Decide to install and start operation. Approaching speed 0,2 m/sec.
The tunnel to be moved parallel to the final position, kept in correct theoretical geometrical form with the use of tugs.

Step 2:
Docking tunnel, speed 0.05 m/sec. Docking will be at Landfall 1 first and then, some seconds later at Landfall 2. Docking will be performed against steel structures, equipped with fenders, mounted on the outer face of the landfall element and steel structures on the tunnel itself. Docking force 200 tons. In this operation the tunnel is guided by a guide beam on a slab situated between the two tubes.

Step 3:
Landfall1: The locking devices shall be installed. The device is a steel type box structure to be placed between the above described steel structures and the concrete tube wall. The lateral support will secure the tunnel in transverse direction.

Step 4:
Landfall1: Installing the long anchor bolts. The bolts will perform a first securing of the tunnel to the landfalls in longitudinal direction. Perform water ballasting at the end of the tunnel to make positive weight on the landfall element. The contact area is the slab described in the step 2. This weight will provide locking in the vertical direction of the tunnel in addition to bolts through the slab.

Step 5:
Landfall1: Installing the short anchor bolts. The bolts are spread on the outside of the tube wall. Hydraulic jacks shall be installed in the jointing area. When some 20 % of the bolts are installed a check on geometry at Landfall 2 shall be performed and an adjustment of the jacks and tensioning of the bolts at Landfall 1 to be performed. During the step 5 the long bolts installed in the step 4 shall be removed.

Step 6:
Landfall1: Install the cofferdam
Landfall2: Make adjustment of the tunnel by transverse force to the locking structure as described in the step 3. The length of the tunnel is designed to be + 0 and – 2 m from theoretical length. From here on follows the same procedure as shown above for the Landfall 1.

Step 7:
Landfall1: Dewatering inside the cofferdam

Step 8:
Landfall1: Perform the concreting of the joints

Step 9:
Landfall1: Perform the water testing

Step 10:
Landfall1: Remove the cofferdam

Environmental conditions during the operations

The tugs and winches must keep the tunnel in correct position until the step 5 has been executed for both landfalls. This work is estimated to take 1 day. The securing work performed inclusive step 5 for both landfalls shall be sufficient to keep the tunnel in correct position acting as an arch without the use of tugs or winches. The work after step 5 until the concreting has been executed is estimated to take about 3 weeks.

The environmental condition for this securing work, after step5, is designed for a return period of 1 year condition. This results in 40 bolts at outer face of each tube. The work has to be very well planned in advance and training of the divers and the personal must be performed. Each jointing site, 2 nos at each landfall, shall have a complete set of divers and equipment for the operation.

6.7 Installation of pontoons

The pontoons will be installed when the bridge is securely jointed to the landfalls elements. The pontoons will be towed to the site and installed by floating crane. The pontoons are fixed to the shafts by inclined rods in the space between the shafts and recesses in the pontoons. The rods provide the weak link for vertical loads. The weak link for the horizontal loads is in the bolts fixing the shafts to the tubes.
During the installation water ballast in the tubes will be adjusted. Access to the water ballast system is through the shafts.

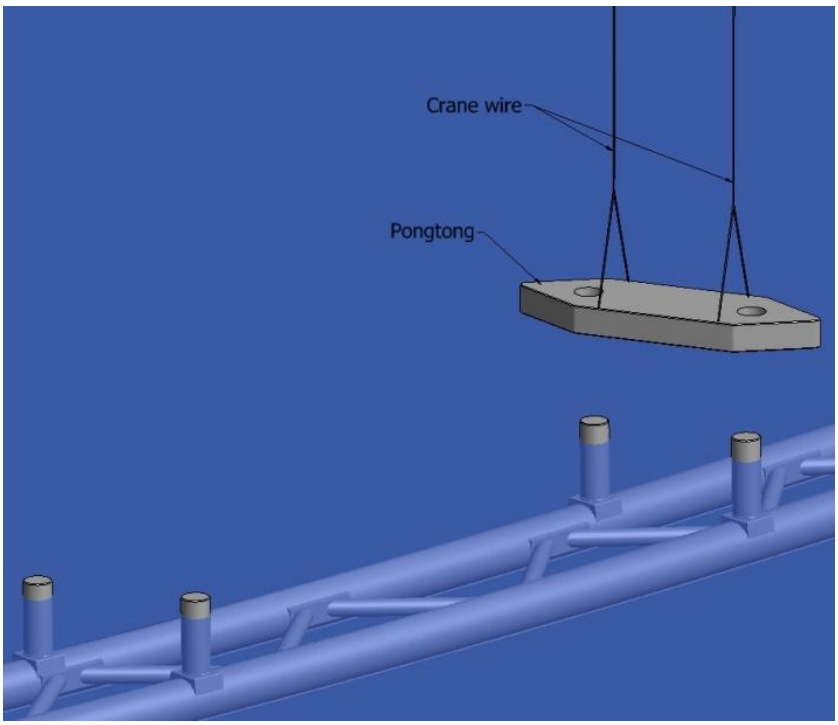

Figure 6-14: Lifting pontoons in place

Figure 6-15: Heavy lift vessel Rambiz

6.8 Construction time schedule

A project plan for the construction is performed. The plan shows detailed engineering, construction and the installation. The work prior to this, as pre-engineering is not included. The plan is based upon the Hanøytangen dock and one construction site only. If two docks are utilized the total construction time will be reduced, as shown in Figure 6-17. Evidently, fabrication of elements is on the critical path.

Prior to start the construction the dock must be upgraded. The width of the dock must be widened by blasting along the western rock wall and a new dock gate must be fabricated. The new dock gate can be constructed behind the existing dock gate. The existing dock gate will be a part of the new gate. The water depth in the dock is about 17 m, which is far more than required, some 13 m.

After the dock upgrading and the general rigging period of 8 months the construction of elements in the dry dock will start. The two landfall-elements will be constructed first. The construction time for one element is estimated to be 8 months. Two elements will be constructed simultaneously. Construction of inner walls and slab follows behind the construction of the outer wall as well as the bracings.

Prestressing will be executed when the total length has been constructed.
Mechanical outfitting is installed in the dock phase as well as the asphalting work. 4 shafts are mounted in dock, two being permanent and two being temporarily. For some elements only temporarily shafts are used.
The construction of an element is estimated to 8 months. After the dock phase the elements are moved out of the dock and water tested outside the dock gate and after testing towed to the mooring site adjacent to the bridge site. Rock tunnel work will start in parallel providing the installation of landfall-elements to be performed early in the project.

The finished elements will to be towed to the site for the jointing work.
The towing of the bridge from the jointing site to the installation site included berthing, will take some days while the concrete work of the jointing will take several days, assuming total 4 weeks. Then the pontoons on the shafts will be installed using floating cranes. Remaining work inside the tunnel will be time consuming, assuming 1 year. The total construction time is estimated to be in the order of 7 to 9 years.
Prior to start the detailed engineering, Front End Engineering and Design (FEED) and tendering must be performed. This has not been looked into at this stage.

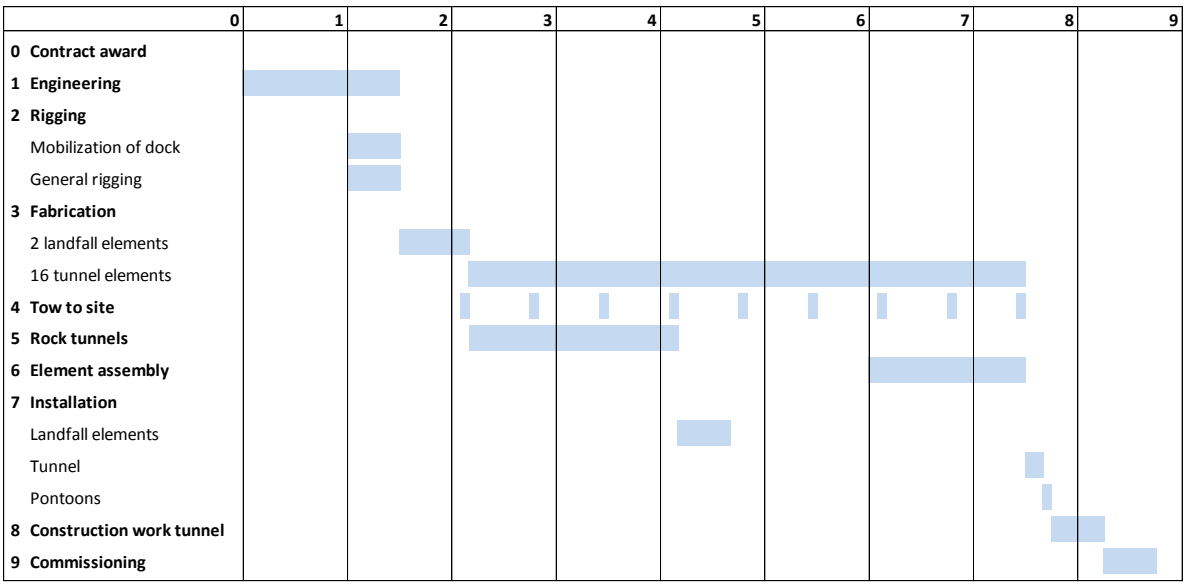

Figure 6-16: Construction schedule in years, one dock

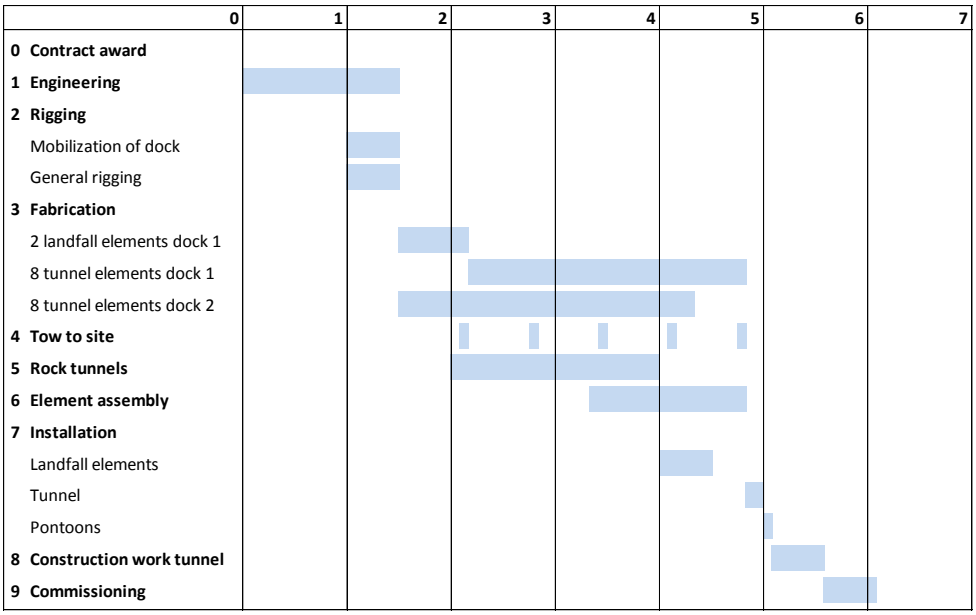

Figure 6-17: Construction schedule in years, two docks

7 Operation and maintenance

7.1 Arrangement

7.1.1 Inspection and maintenance access

The width of the traffic tubes provides space for two traffic lanes. However, only one lane will be used for ordinary traffic at a time. The spare lane provides space for emergency stops and a safe temporary working place for tunnel inspection, maintenance and repair. In the upper part of the traffic tubes above the free room profile there is space for signal boards, ducts, pipes, fans, cables etc. Permanent facilities for control, maintenance and repair may be located in the diagonals.

All structural elements shall be subject to regular inspection to see signs of incipient deterioration. Convenient access to all significant elements shall be provided. External inspection to be carried out by ROV or divers. If found appropriate, removal of marine fouling could be part of the inspection.

7.1.2 Technical rooms

Where necessary technical rooms with electrical installation, emergency power supply, telecommunications etc will be located in the diagonals.

7.2 Mechanical and instrumentation systems

7.2.1 Traffic control systems

Operation and traffic control is assumed provided from a manned central control room. The traffic control will be executed by appropriate light signals.

7.2.2 Ballast systems

The traffic tubes will be fitted with systems for ballasting/de-ballasting. Ballast chambers, 50 m long, will be located underneath the roadway slab. The systems shall keep the tubes in correct elevation and avoid overstressing of the tube or other elements. Pump rooms will be provided in each ballast chamber. The pumps will be controlled automatically by signals from sensors. The pump system will be redundant (3 x 50 %). Each pontoon will be fitted with bilge/ballast systems.

7.2.3 Bilge and drain systems

Drains shall be provided to guide all water penetrating into the tubes or brought in by the cars. Drain and bilge sumps for easy drainage shall be located at the pump rooms. All excess water shall be drained off the tunnel.

7.2.4 Ventilation

Ventilation will be provided by fans located above the free room profile. Under normal circumstances ventilation fans will be controlled automatically by signals from smoke and air quality sensors in the tubes. In the case of fire, ventilation should provide over pressure in the emergency exits and exhaust toxic gases through separate canals.

7.2.5 Instrumentation systems

The structure shall be instrumented for systematic monitoring of motions, possible overstress, toxic gases, corrosion protection systems and unplanned influx of water. Where appropriate these systems shall release immediate corrective response such as ballasting/de-ballasting without direct manual intervention.

7.2.6 Corrosion protection

The structural steel components, steel fixing plates etc. shall be provided with anodes for cathodic protection.

7.2.7 Other systems for risk mitigation

Other risk mitigation systems such as firefighting equipment, submarine warning etc, will be installed according to recognized regulations.

7.3 O&M strategy

An Operation and Maintenance Strategy (O&M Strategy) has been developed for the Sognefjorden Floating Tunnel Crossing based on past Arup global experience and shall be adjusted with Client´s practice and process.

7.3.1 Aim

The Aim of the O&M Strategy is:

- To guarantee the Integrity & Safety of the structure during Full Service Life. For components with limited service life, Replacement program shall be in place.
- To maintain satisfactory accessibility and inspectional conditions
- To perform I&M&O activities without traffic disruption
  - Any known faults shall not develop to a stage where remedial works would require disproportionate disruption of the traffic
- To perform I&M&O activities with limited traffic disruption during the repair or replacement of critical/vulnerable elements

7.3.2 Objectives

The objective of the O&M Strategy is to set out as detail as possible on this early stage of the project the strategy that will be followed by the i) I&M and ii) Operational Organization during the service time of the Tunnel. Engineering Design decisions have an impact on the requirements on materials, accessibility, Health and Safety, Environmental, inspections, maintenance, and operations.

I&M Manual

This Manual is a live document over the project design and construction stage of a project, which describes the inspection and maintenance works to be performed on every structural elements that composes the tunnel. It contains and details the I&M nature, category, frequency, scope for each of these elements.

Operation Manual

This Manual is a live document over the project design and construction stage of a project, which describes the inspection and maintenance works to be performed on every equipment elements that composes the tunnel. It contains and details the I&M nature, category, frequency, scope for each of these elements.

These Manuals will developed themselves as the project stages and construction site progresses, and as new team members/stake holders participate actively in the realization of the Sognefjorden Crossing.

8 Risk and robustness assessment

8.1 Purpose and scope of the risk evaluation

It is an indispensable requirement to the Submerged Floating Structure that the safety is at least as good as for other fjord crossings on bridge or in rock tunnel. The best endeavors are made to achieve this goal by application of well proven and recognized technical solutions, conservative design assumptions and generous design acceptance criteria. Main emphasize is given to redundancy and element reliability.

In the next phases of planning and design the viability of the structure, the marine operations, the jointing and the construction methods will be verified by hydro-elastic model test, mock up tests, operation simulations and other advanced investigations.

However, already at this early stage of design and planning safety related aspects will be a major design driver. The overall structural concept has never been used before. The dimensions, the complexity, the slenderness, the joints and the marine operations exceed previous experience. Even if each individual element and operation is found to have adequate safety, in principle a hazardous chain of events may be released unless the interaction of elements is adequately understood.

To this end the main hazards to the bridge, their possible consequences and their possible mitigating actions have been identified, ref section 8.7 below. Further, in addition to this a separate hazard identification study (HAZID) has been made, ref section 8.3 below. The HAZID is a recognized technique for identification and evaluation of significant hazards in terms of cause, consequence, possible escalation, risk reducing measures and a rating of probability and consequence. This process was completed in a work shop attended by prominent independent experts in all related technologies and in reliability analyses.

In conclusion, this HAZID did not reveal any hazard that threatens the technical feasibility of the concept. It was found to be a sound concept for further development.

8.2 Process

The risk management methodology proposed for the next phase of the design process is illustrated in Figure 8-1. It includes the essential elements for a systematic approach to risk management, namely identification, assessment, control, monitoring and review.

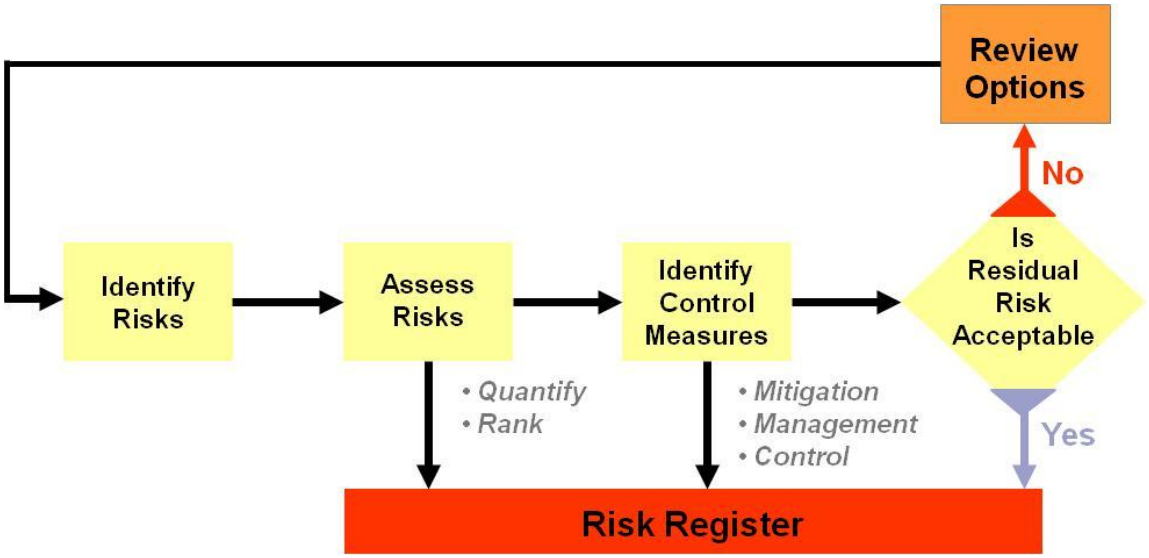

Figure 8-1: Project risk management process

8.3 Risk identification

Complementary methods will be used to generate a comprehensive list of discrete risks and uncertainties. Risk identification methods will include:

- Risk register reviews: The existing project risk register will be reviewed as will risks from other comparable projects.
- Interviews: Experts, will be asked to identify risks within their respective areas of responsibility/expertise.
- Workshops
- Continual reviews: All project team members will be encouraged to identify risks as the project evolves.

The risk record in section 8.7 and robustness record in section 8.8 below summarize the risks possibly jeopardizing the project in permanent and temporary phases. Planned risk mitigating measures and their inherent challenges are also included.

8.4 Hazid

The risk assessment of the project is supplemented by a hazid conducted by a team of experts independent of the design team.

In conclusion the hazid did not reveal any hazard that threatens the technical feasibility of the SFT concept and that it is a sound concept for further development.

Main areas for improvement are suggested:

- More information about environmental data
- Hydrodynamic parameters for high Reynolds numbers

- Structural dimensions of the SFT to be increased at the landfall
- Better definition of the mechanical systems
- Better definition of personal access for segment joining operation
- Better illustrations

These items have been considered in the final stages of the conceptual design.

8.5 Redundancy and reliability

Structural redundancy and reliability of the crossing are essential to its functionality and safety of its users. Qualitative methods will be used to analyze and rank the concept. The proposed methods include:

- Expert analysis
- Failure Mode, Effects Analysis
- Hazard & Operability (HAZID) analysis.

The use of these methods will; (i) capture the experience and knowledge present within the team; (ii) provide insight in the cause and effect of failure of individual system components: and (iii) provide a good starting point for quantitative analysis methods that can be applied at a later stage as part of a RAMS analysis.

8.6 Safety

A demonstrable high level of operational safety of the crossing is paramount to its acceptance and long term success. For that reason a detailed safety analysis will form part of the basis for the selection of the preferred concept. The integral safety of the crossing can be subdivided into a number of aspects including:

- Structural safety
- Fire safety
- Security
- Traffic safety
- Tunnel safety
- Nautical safety
- Dangerous goods

Related to the inherent safety characteristics of the crossing are the accessibility to emergency services and their available means. In order to qualify the degree of safety of the different concepts deterministic scenario analyses are proposed.

8.7 Risk record

In the following is recorded risks possibly jeopardising the project during construction / installation and in the operation phase together with possible measures to avoid the risks.

The challenges in counteracting the risks have been divided in four levels of complexity indicated by colours in the tables below:

Risk not relevant or counteracted by simple or trivial measures	
Risk to be eliminated by recognised measures	
Risks eliminated by measures investigated by advanced theoretical or experimental analyses	
Risk not likely to be avoided by reasonable measures	

The concept is not exposed to risks of complexity red as such concepts are not recommended for further studies.

8.7.1 Risk of damage during the construction phase

Table 8-1 shows the risks of damage during the construction phase that was identified in the hazid.

Table 8-1: Risk register for damage during the construction phase

Risk	Risk mitigation
Grounding during element or element assembly transport	Comprehensive bathymetric survey of the entire route swept by elements or assembly of elements. The area to include tolerances for deviation from planned routing. Credible obstacles to be removed before towing.
Failure / maloperation of bilge and ballast systems	Provide redundant systems (3x50%). High quality equipment. Stringent operation procedures. Skilled operators.
Failure / maloperation of winch and cable systems	Provide redundant systems (3x50%). High quality equipment. Stringent operation procedures. Skilled operators. Force and movement monitoring.

Risk	Risk mitigation
Failure / maloperation of tugs	Use new tugs in good condition. Redundant systems. Stringent operation procedures based on comprehensive analyses and conservative acceptance criteria. Due considerations to possible fluctuating current directions. Skilled operators trained in simulator. Force and movement monitoring. Stringent systems for organisation and communication.
Hydroelastic motions VIV and galloping of free floating traffic tubes	Free floating elements will be exposed to VIV. But the tubes are flexible and the complete bridge should be designed to survive the pertinent motions which are moderate.
Connection between elements during assembly stage	Optimisation of design and construction of joints and temporary connections. Design and methods to be documented by comprehensive analyses, stringent work procedures and mock up tests
Static overstressing traffic tubes	Probability is low provided correct operation of tugs and winches
Inaccurate alignment and dimension deviations of tube and landfall joint. Motions of joint after grouting and before proper pre-stressing	Adequate and redundant system of winches and tugs to guide the tube in place. Final positioning supported by male/female dowels. Stringent operation procedures. Complete operation within a defined weather window
Leaks, influx of water and possibly sinking of tube or pontoon	Proper design and construction of all structural elements. Adequate capacity redundant bilge and ballast systems. Stringent operation procedures. Leak monitoring.
Operation delays into bad weather season	Proper time planning with reasonable float. Quality and redundance of all equipment and systems to avoid breakdown, Identify sheltered bays for protection of bridge elements during an unexpected storm. Design the structure and its elements for a winter storm as an accidental load case.
Marine operations, structural response and methods for correct positioning of the end sections of the tunnel	Comprehensive geological and geotechnical investigations. Optimisation of sections with respect to stiffness and strength Detailed operation planning
Lack of environmental data, Waves, current, wind	Environmental data acquisition and treatment

8.7.2 Risk of damage during the operation phase

Table 8-2 shows the risks of damage during the operation phase that was identified in the hazid.

Table 8-2: Register for risk of damage during operation phase

Risk	Risk mitigation
Traffic tube ramming by ship	Ensure adequate keel clearance
Overload of SFT pontoons	The pontoons will be designed with so low strength that a failure will not impair or cause leak in the traffic tube. The traffic tube will be designed to avoid any impair by loss of the net buoyancy of anyone pontoon. It will be given so high strength that it will not be impaired by common environmental loads or impact of small ships
Traffic tunnel ramming by submarine	Low probability. If probability increase in future provide transponders for acoustic warning
Dropped objects, dragging chain or wire	Low probability of objects larger than a current ship anchor. May be designed for. If sawing the traffic tube by dragging chain might be a possibility the top of the tube may be protected by a steel plate.
Fire	The traffic tubes will be made of concrete of adequate durability during a design fire. Escape ways and safe havens will be provided. Ventilation system designed for accidental fire. Fire fighting systems to be provided. Possibly restrictions on cargo.
Explosion	The traffic tubes will be hoop reinforced to take the internal overpressure from a deflagration.. Transportation of explosives which might release a detonation should be considered forbidden.
Warfare, sabotage and terrorism	The tunnel is provided with more escape possibilities than other long bridges. It is also provided with pumps to counteract a reasonable influx of water. In general the risk is not higher than for other bridges i.e. accepted by society
Loss of oxygen supply	Provision of ventilation systems and sensors and signals for automatic refusal of cars entering a toxic area. Transportation of toxic gases to be limited.

Risk	Risk mitigation
Failure or maloperation of bilge and ballast systems	The bridge shall have systems for trimming and adjustment of the effective weight. Pipelines from the bridge to sea shall be lifted above highest external water level. Systems shall be reliable and redundant and be operated by skilled professionals only. The bridge shall be designed for an accidental load case assuming malfunction at a specified probability level
Failure or maloperation of weight control	A reliable weight control system should be operated. Overload should be designed for as an accidental load
Water filling of pontoon	The pontoons will be divided by watertight bulkheads Floatability and stability will be checked with 1-2 compartments filled. There will be installed bilge systems with adequate capacity. There will be fendring of the collision zone and there will be no direct connections from any compartment directly to sea.
Leakage into the traffic tube	Instrumentation to monitor possible water influx. Redundant bilge and ballast systems of adequate capacity to dewater the tunnel and to stop influx of water from the rock tunnel. Seepage of water at joints etc to be sealed by epoxy injection. Design to survive partial water filling.
Partial overstress of traffic tube and pontoons	Structural elements constructed on land is assumed to have adequate strength by virtue of appropriate load cases, materials, design, construction and quality systems. Overstress risk during transportation joining, submergence and other operations in floating conditions is avoided by analyses of dynamic behaviour and forces. Safe positioning and execution of critical operations must be ensured by proper planning and well documented procedures.
Fatigue and unstable failure	Pre-stress concrete sections to avoid opening and closing of submerged cracks. If so, concrete structures are not considered vulnerable to fatigue

Risk	Risk mitigation
Corrosion	Design to avoid corrosion by recognised methods i.e. Cathodic protection (anodes or impressed current), steel coating, corrosion allowance, flame spread alumina. Regular thickness measurements and inspection and maintenance of protection systems
Concrete deterioration	Concrete deterioration is avoided by proper choice of binders, additives and aggregates to achieve a low water permeability. Fly ash and silica are important ingredients. Concrete in the splash zone to be paid particular attention. Epoxy membrane if found necessary. Regular inspection to see chloride penetration and possibly electrochemical investigations
Earthquakes	The seismic activity with a return period of 10 000 years on the western coast is moderate i.e. abt. 3 m/sec^2. This may be designed for.
Land slide generated waves	The structure may be designed for a land slide as specified by SINTEF
Inner subsea waves	Theoretical and experimental investigations indicate inner waves not to be a significant risk
Unwanted hydroelasic behaviour: Vortex shedding, galloping etc.	Physical and numeric modelling for investigations of hydrodynamic parameters. The dimensions of tunnel to be chosen to avoid cross flow vibrations.
Lack of environmental data	Environmental data acquisition and treatment
Dynamic response from simultaneous wave and current	Model tests by Veritec have indicated excessive response by simultaneous slow drift effect of waves and current. It is considered likely that this effect is caused by unintended slow current fluctuations in the testing. However this possible effect should be further investigated.
Extreme tides caused by combination of astronomical tide, current, wind, low pressure and greenhouse effect	Adjust the platform level by ballasting
Need to exchange elements	Accessability, redundance

Risk	Risk mitigation
Uncertain soil or bedrock conditions and landfall degradation	Comprehensive geological and geotechnical investigations. Appropriate choice of landfall site. Adequate landfall design. Rock injection to improve strength and water influx.

8.8 Robustness

Robustness is evaluated as requested in the Rammer for gjennomføring av dialog og etterfølgende konkurranse, Particular bidding rules cl. 7.3.C.

"Robustness" may be interpreted as:

1) In the operation phase: Ability of existing structures to withstand exposure going beyond the actions directly designed for.
2) In the design phase: Ability of a design concept to be adapted to a wide range of applications.

In Table 8-3 the robustness of the SFT has been evaluated based on both of the two interpretations.

Table 8-3: Evaluation of robustness

Change in design assumptions	Consequences of changed design assumptions
Impairment or delay of operation caused by external impact	**Ship collision**: Top of traffic tubes below keel depth. Pontoons provided with weak link, the pontoon may be knocked off without impairing the traffic tube. The structure designed to survive loss of one pontoon. **Ship anchor:** A ship anchor cannot hook up on a structure composed of smooth large diameter cylinders such as the arched SFT **Wind**: Submerged structure not exposed to wind **Current and waves**: The structure is in deep water and the exposure to waves and current is minimal. Thus, the structure is overdesigned and may withstand more hostile conditions even if introduced in the operation phase. In the design phase the concept may be adapted to withstand all credible conditions in Norwegian fjords.
Loss of buoyancy caused by structural deficiencies	In the design phase the structure may be given redundant bilge and ballast system of whichever capacity wanted. If requirements will be sharpened in the operation phase more pumps may be installed.

Change in design assumptions	Consequences of changed design assumptions
Changed requirements to the ship lane; location, width height and depth	**Location**: In the design phase the ship lane may be located wherever wanted. As the pontoon system is designed to be adequate also with one pontoon lost, the ship lane may be changed even in the operating phase. **Width**: In the design phase the width may be increased significantly beyond the specified 400 m. **Height**: No limitations. **Depth**: The largest ships calling at Norwegian fjords have moderate draft. Requirements to more than 20 m depth are very unlikely, but an increase down to 30-40 m may easily be coped with.
Changed traffic volume or requirements to design or application of the roadway	There are two traffic lanes each direction giving a capacity ADT of 15 000, which is abundant. If both lanes in one direction is blocked moderately sized cars may be transferred to the tube with traffic in the opposite direction. In the design phase the arrangement of the traffic tubes may easily be changed, if necessary by increasing the tube diameter.
Changes in subsea geological or geotechnical conditions	The SFT shall be continued into a rock tunnel If, based on comprehensive investigations, the bedrock is not found to be sound a change in location should be considered. Such alternative location might give a longer tunnel, but this is foreseen to cause technical problems.
Applicability for crossings other than Sognefjorden	The specified bridge location is considered to be among the most demanding in fjords beyond the reach of ocean waves. Thus the concept could be used for all inner fjords. For sites further out in the fjords or skerries, the application of this concept requires in depth further site specific investigations.

9 Suitability for other crossings

The feasibility for use of the current concept as described for Sognefjorden for other crossings is here evaluated. The influence of several design parameters on the design is explained.

9.1 Design parameters

9.1.1 Length of crossing

The length of the crossing is a key parameter, and is of importance in most of the design drivers. Several important key parameters are driven by the length:

- SFT stiffness
- Slenderness of the structure
- Natural frequencies
- Structural capacity

This goes primarily on the sway direction. In heave, the stiffness in driven by the pontoon waterline stiffness and the distance between the pontoons.

The stiffness in sway can be adjusted by change of cross section dimension and/or change the distance between the tubes for different span lengths.

9.1.2 Current, wave and wind condition

Current

Current is the main driver for the present design. In-line vortex induced vibrations caused by current gives the load effects of the largest magnitudes. Cross flow VIV gives higher amplitudes, and must hence be avoided. The response model for VIV motions are shown in Figure 9-1, as taken from DNV-RP-F105.

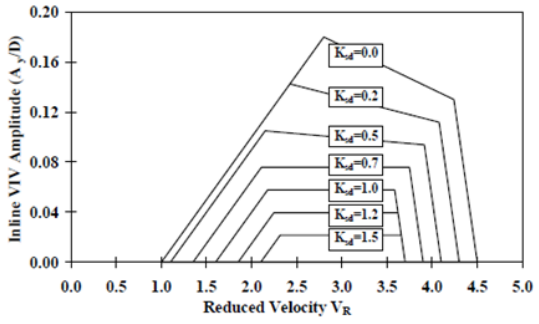

Figure 4-1
Illustration of the in-line VIV Response Amplitude versus V_R and K_S

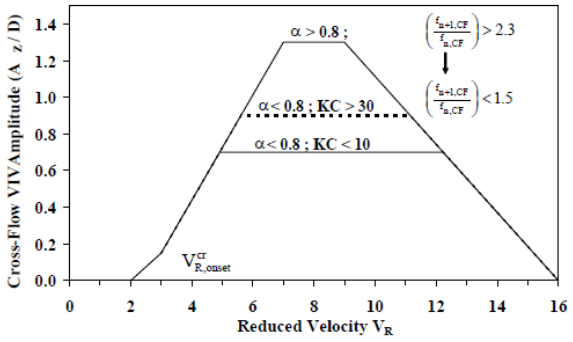

Figure 4-4
Basic cross-flow response model

Figure 9-1: VIV response amplitudes for in-line and cross-flow motions

It is shown that in-line VIV starts with reduced velocity equal 1, and cross flow starts with reduced velocity equal 2. The main importance is to come out with a natural frequency for

the first mode in heave to avoid cross flow motions. The study for Sognefjorden shows that IL VIV can be handled by structural strengthening locally towards the landfalls.

Tuning of natural frequencies by geometry change and pontoon distance is then the option to change the reduced current velocity by adjusting the natural frequencies to avoid CF VIV.

Exact current measurement at the crossing site and at different depths is hence important to have control of the VIV onset reduced velocity.

Wave

In the design for the Sognefjorden crossing, wave responses are of a small magnitude compared to the load effects from current. However, for other crossings wave effects may be dimensioning. For a more unsheltered location, the amount of swell going in to the bridge site may be of larger magnitude, and hence an important parameter in the design. Wave drift motions may also be of importance with more severe sea state.

Wind

Wind loads are not of importance for the concept, as the exposed wind area is negligible compared to the wave and current load effects.

9.1.3 Ship passage

The concept is flexible with respect to ship passage location. The pontoons can be rearranged to fit fairways. The present concept has a 400 m sail opening with corresponding depth of 20 m, which should be suitable for most fjord crossings. A depth above 20 m is possible if required. No limitation is given by the height of the sail opening.

The “weak link” design for the pontoon connection to the tunnel makes the tunnel redundant to severe ship impact loads. The tunnel itself is not damaged in a collision event, and the structural integrity will be intact, even if one of the pontoons becomes detached during a collision.

9.1.4 Road traffic

The traffic loads are negligible compared to the environmental loads. The present design for Sognefjorden allows for two lanes in each direction. Maintenance in one of the tunnels is thereby possible by routing traffic in each direction in one of the tunnels. For shorter and shallower spans, one single tunnel may be an alternative if the amount of traffic does not require two lanes in each direction.

9.1.5 Geological site conditions

The geological conditions at the landfalls are of importance. The SFT requires a stiff connection at the landfalls, where both axial forces and bending moment is transferred

into the rocks. It is also a requirement that the geological conditions is such that a tunnel can be driven in the rock from both sides to a level of -20 to -30 m below sea level.

The bathymetry of the landfall sites is of importance. A steep sloped landfall site will require less amount of preparation in order to have a “clean” entry for the tunnel and tunnel forces into the rock.

The seabed conditions in the fjord itself are not relevant for this concept, as the SFT is anchored in the ends and not dependent of sea bed anchoring.

9.2 Feasibility compared to other E39 crossings

The use of the proposed concept for other crossings at the “Ferjefri E39” project is evaluated. No specific data on environmental condition has been made available for the remaining crossings, so the use of the concept is based on same conditions as Sognefjorden, but with the actual length and depth. No detailed calculations are made to verify the evaluations for the remaining crossing sites.

The different crossings with associated depth and length are summarized in Figure 9-2. The length varies from 1.6 km to 7.5 km, and the depth varies from 200 to 1300 m.

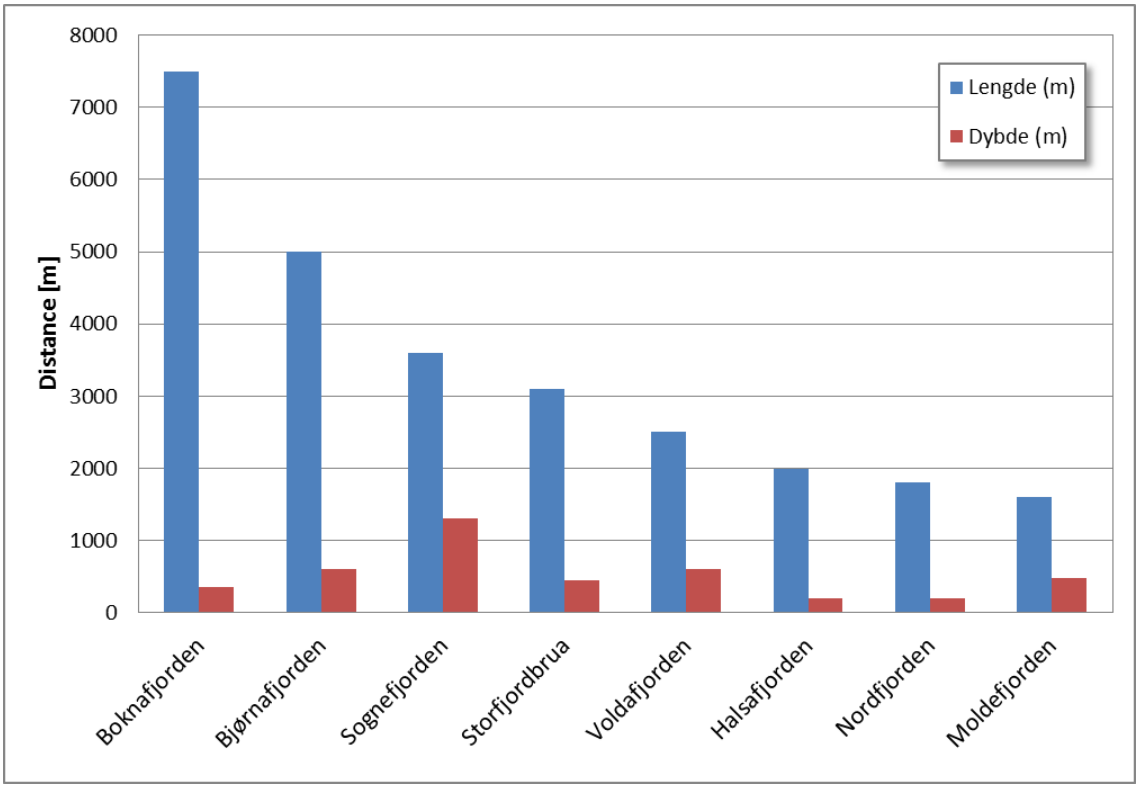

Figure 9-2: Length and water depth at the different crossings for ferry free E39

The concept with submerged tunnel is feasible for all of the crossing sites, but some variations may be introduced compared to the Sognefjorden SFT to make a more

reasonable structure with respect to the span length and water depth. This goes primarily on use of side anchorage to the sea bed for the more shallow water crossings (< 500 m), single pipe for the shorter crossings and a combination of these.

The concept for Sognefjorden SFT is in Table 9-1: Feasibility for the E39 crossings evaluated on basis of the above.

Table 9-1: Feasibility for the E39 crossings

Crossing	Length [m]	Depth [m]	Feasible concept	Suggested variation	Reason for variation
Boknafjorden	7500	360	No	Straight tube with anchorage to sea bed	Large length and shallow water of crossing
Bjørnafjorden	5000	600	Yes	None*	Length of crossing
Sognefjorden	3600	1300	Yes	-	-
Storfjordbrua	3100	450	Yes	None*	
Voldafjorden	2500	600	Yes	None*	
Halsafjorden	2000	200	Yes	Single straight tube with anchorage to sea bed. Single tube arch with end anchorage.	Relative small length and shallow water
Nordfjorden	1800	200	Yes	Single straight tube with anchorage to sea bed. Single tube arch with end anchorage.	Relative small length and shallow water
Moldefjorden	1600	480	Yes	Single straight tube with anchorage to sea bed. Single tube arch with end anchorage.	Relative small length and shallow water

*None: The SFT as proposed for Sognefjorden is considered as the most relevant concept. Adjustment to the cross sectional data, distance between tubes and pontoons, alignment etc. is however expected in order to optimize the structure.

The length of the Boknafjorden crossing makes the proposed alternative unfeasible. Side anchorage to the sea bed is here necessary in order to control the horizontal forces and

movement in the tunnel. A configuration with a single or double straight tube combined with sea bed anchorage is considered as most relevant here.

For Bjørnafjorden, Voldafjorden and Storfjorden, the proposed alternative is feasible as described for Sognefjorden. Relatively long span and deep water makes the end anchorage together with a double tube arched construction the most relevant configuration of the SFT.

Nordfjorden, Moldefjorden and Halsafjorden are relative short crossings, combined with shallow water. The proposed solution for Sognefjorden is feasible for these crossings, but a single straight tube with anchorage to the sea bed is here considered the most relevant solution. A single tube arch with end anchorage as for Sognefjorden may also be an option for these crossings.

10 Recommendations for further work

The feasibility study has resulted in a submerged floating tunnel concept that is proven to be a viable and technically feasible crossing solution. The developed concept is moreover found to be robust and fairly flexible with respect to the envisaged boundary conditions that form the basis for the study. Yet, the study has identified certain areas of uncertainty, in particular related to the prediction of dynamic load responses, which in the current design has been compensated by conservative assumptions or design strategies. Addressing these aspects is deemed to greatly improve the basis for future crossing studies.

With the scope to eliminate governing uncertainties pertaining to the initial design, recommendations for further work is advised and briefly outlined in the following.

10.1 Proposed activities

10.1.1 Analysis programs

During the current feasibility study a set of calculation schemes for 1st and 2nd order responses have been developed by the Reinertsen Olav Olsen Group (RE-OO). These have been applied on previous tests performed at Marintek, and some deviations are seen that need further clarification.

The proposal is to go further into the tests, and outline the raw data to see if the post processing of test data can be improved. Also, the program developed by Marintek under expert group on dynamics in 1996 is to be considered, however this is valid only for single tube. The activity also includes needed modification of existing Mathcad based analysis programs for 1st and 2nd order responses.

10.1.2 Viscous damping estimate

For the 2nd order slowly varying response damping is a governing parameter. A vital contribution here comes from the truss structure between the two pipes. The idea is to come up with a theoretical model for estimating viscous damping.

The estimate is to be based on existing experimental data together with previous calculations on viscous damping. This includes establishment of damping model for the double pipe tunnel, evaluation of major contributions, scale effects for evaluating test results, effect of current and the contribution from viscous damping as related to other contributions.

10.1.3 Prepare 2D-tests on VIV and galloping

In the current feasibility study VIV response characteristics for the double tube are based on DNV-RP-F105 (2006) as valid for single pipelines for subsea application. Minor work exists on multiple pipe behavior. The idea is now to come up with a test program for further investigation.

The problem around grouped pipes also exists within oil and gas free spanning pipelines and the idea is now to incorporate oil companies like Statoil, ConocoPhillips, BP and Shell in a joint venture project on VIV and galloping. We have been in contact with Statoil and they have expressed positive interest. Reinertsen has also been awarded grants from Norwegian Research Council for the testing of the concept of artificial seabed, and the plan is also to coordinate with these experiments. The idea is also to include DNV to follow their process of implementing test results into design guideline, like was done for Ormen Lange VIV tests.

The present activity covers the planning of tests as well as the coordination with participants. In order to better define the parameters for testing response prediction by existing knowledge is carried out. Experience from the Ormen Lange VIV tests will be taken in here.

It is foreseen section tests in towing tank in scale close to 1:20 / 1:30 similar to previous section tests on single tube. The model section includes truss between the two major pipes, thus viscous damping may also be studied.

Preparation of tender documents to actual vendors on testing is included.

10.1.4 2D-model testing

This activity comprises follow-up of the tests and needed coordination with company performing the testing.

The output from tests is taken into the tunnel design for VIV and galloping to see that we are on conservative side in the design of the double pipe tunnel. In case of participation from oil companies the test results will be implemented into a DNV type of guideline for multiple pipes VIV and Galloping.

RE-OO asked Marintek about costs for performing tests in the towing tank. It is estimated two weeks duration for the tests on the double pipe tunnel, including some different centre line distances between the pipes and also different surface roughness.

The envisaged 2D test can be carried out for approx. NOK 300 000 including 2 weeks in towing tank and model fabrication. Follow-on is estimated to around 200 man hours. Subsea pipeline testing for oil companies comes in addition. Coordination may reduce cost

for the tunnel test somewhat, but not much. The essence of coordination with oil business is primarily to get a larger test sample as basis for guideline.

Marintek have indicated capacity for testing over the summer 2013.

10.1.5 Test program for environmental data acquisition

In the present generic feasibility study current is proven to be the governing environmental load parameter. Rough current simulations and thus conservative characteristic current design data has encumbered the accuracy in prediction of current-induced load effects. In more detailed studies for future, specific crossings accurate simulations of current velocities, direction and variation with water depth will be decisive. Realistic 3D current representation will require seasonal current measurements using sets of acoustic Doppler current profilers. These measurements should be supplemented by current meters for mapping of lateral current variations. A test program for current measurements should be worked out in preparation for starting data acquisition in early planning stage.

Normally adequate wave characteristics are obtained through numeric simulations (e.g. StWave). For validation of the wave analyses, in particular wave refractions, buoy measurements at site will at some stage be required. The test program should also consider collecting of statistical data on tidal variation as well as measurement of stratification, variation of water density and temperature.

The activity should include planning of test program and specification of out-put requirements.

11 References

1. **Norwegian Public Roads Administration.** *Håndbok 185 Bruprosjektering Eurokodeutgave. Edition Nov.* 2011.

2. —. *Håndbok 185 Bruprosjektering Eurokodeutgave – 6.13 Rørbruer.* Dec. 2011.

3. **Blevins, Robert D.** *Flow-Induced Vibration.* Malabar, Florida : Krieger Publishing Company, 2001.

4. **Zdravkovich.** *Flow Around Circular Cylinders, Fundamentals, vol. 1.* s.l. : Oxford University Press, 1997.

5. **SINTEF.** *Mulighetsstudie for kryssing av Sognefjorden Opedal-Lavik Estimat på bølger og strøm.* 2011.

6. **Det Norske Veritas.** *DNV-RP-F105.* 2006.

7. *Experimental investigation of flow-induced vibration interference between two cylinders.* **Assi, G.R.S., et al., et al.** s.l. : Journal of Fluids and Structures, 2006, Vol. 22.

8. **Det Norske Veritas.** *DNV-RP-C205.* 2010.

9. **Faltinsen, O. M.** *Sea Loads on Ships and Offshore Structures* . s.l. : Cambridge University Press, 1990.

10. **Standard Norge.** *NORSOK standard N-003, Action and action effects.* 2007.

11. **Ramboll.** *Risk assessment Part I – Frequency analysis. Report R-rap-001-1, revison 3b.* 05.09.2012.

12. *Maneuvering of two Interacting Ships in Calm Water', Proc. PRADS2010, the 11th International Symposium on Practical Design of Ships and other Floating Structures.* **Xiang, X. og Faltinsen, O. M.** Rio de Janeiro, Brazil : s.n., 2010.

13. **Standard Norge.** *NS-EN 1992-1-1, Design of Concrete Structures – Part 1-1: General Rules and Rules for Buildings,.* 2008.

14. **Dr. Techn. Olav Olsen.** *Hydrodynamic wave responce method.* Oslo : s.n., 2012.

15. **Euro Code.** *Endringsblad A1, Grunnlag forr prosjektering av konstruksjoner.*

16. **Standard Norge.** *NS3473, Concrete structures, Design and detailing rules.* 2003.

17. **Group, Reinertsen Olav Olsen.** *Design Basis.*

18. **Det Norske Veritas.** *DNV-OS-C101, Design of offshore steel structures, General (LRFD method).* 2011.

19. —. *DNV-OS-C502, Offshore concrete structures.* 2012.